



U.S. Department
of Transportation
**Federal Railroad
Administration**

Investigation of the Effects of Tie Pad Stiffness on the Impact Loading of Concrete Ties in the Northeast Corridor

Office of Research
and Development
Washington, DC 20590

DOT/FRA/ORD-83/05

April 1983
Final Report

This document is available to the
U.S. public through the National
Technical Information Service,
Springfield, Virginia 22161.

NOTICE

The United States Government does not endorse products or manufacturers. Trade or manufacturers' names appear herein solely because they are considered essential to the object of this report.

NOTICE

This document is disseminated under the sponsorship of the Department of Transportation in the interest of information exchange. The United States Government assumes no liability for its contents or use thereof.

1. Report No. FRA/ORD-83/05		2. Government Accession No.		3. Recipient's Catalog No.	
4. Title and Subtitle Investigation of the Effects of Tie Pad Stiffness on the Impact Loading of Concrete Ties in the Northeast Corridor				5. Report Date April 1983	
				6. Performing Organization Code Battelle	
7. Author(s) F. E. Dean, H. D. Harrison, R. H. Prause and J. M. Tuten				8. Performing Organization Report No.	
9. Performing Organization Name and Address Battelle's Columbus Laboratories 505 King Avenue Columbus, Ohio 43201				10. Work Unit No. (TRAIS)	
				11. Contract or Grant No. DOT-FR-9162	
12. Sponsoring Agency Name and Address U. S. Department of Transportation Federal Railroad Administration Office of Research and Development Washington, DC 20590				13. Type of Report and Period Covered Final Report March 1981- January 1982	
				14. Sponsoring Agency Code RRD-10	
15. Supplementary Notes					
16. Abstract This investigation was conducted in response to the discovery in June 1980, that rail seat bending cracks had developed in many concrete ties which had been in service on the Amtrak Northeast Corridor track for periods of a few months. The study was initiated by the Federal Railroad Administration to investigate the cause of the cracks and to identify a solution which would arrest further crack development while minimizing the retrofitting of components. The study was conducted in three phases: a. Existing load and tie strain data were examined over a large frequency bandwidth (0-1200 Hz) to determine whether impact loads could be identified at levels above that known to cause tie cracking. Such high-frequency impacts were found on a small percentage of high-speed passenger train wheels. These impacts were caused by wheel tread irregularities. b. Laboratory impact tests verified that major reductions in tie pad stiffness could significantly reduce the tie bending moments resulting from impact loads. c. Field measurements of impact loads and tie bending moments were conducted in a test zone where more flexible tie pads were substituted. The tests verified that flexible tie pads which are adaptable to the current fastener system could reduce the occurrence of bending strains which can crack ties. However, it was shown that the elimination of tie cracking will require both a more flexible pad and a program to eliminate the wheel conditions causing the highest impact loads on Northeast Corridor passenger trains.					
17. Key Words Impact loading, Concrete ties, Concrete tie fasteners, Tie pads			18. Distribution Statement Document is available to the U.S. Public through the National Technical Information Service, Springfield, VA 22161		
19. Security Classif. (of this report) Unclassified		20. Security Classif. (of this page) Unclassified		21. No. of Pages 82	22. Price

METRIC EQUIVALENTS OF ENGLISH UNITS USED IN THIS REPORT

<u>Multiply the English Unit</u>	by	<u>To obtain the Metric Unit</u>
Basic Units:		
Foot (ft)	0.3048	Meter (m)
Inch (in)	25.4	Millimeter (mm)
Pound (force) (lb)	4.4482	Newton (N)
Degrees Fahrenheit (°F)	$5/9 (F - 32)$	Degrees Celcius (C)
Combined Units		
Kip = 1000 lb (kip)	0.3048	Kilonewton (kN)
Foot-Pound (ft-lb)	1.3358	Joule = Watt-Sec. (J)
Pound/Inch (lb/in)	1.751	Newton/millimeter (N/mm)
Strain ($\mu\text{in/in}$)	1	Strain ($\mu\text{m/m}$)

TABLE OF CONTENTS

	<u>Page No.</u>
PREFACE	vii
EXECUTIVE SUMMARY	viii
1.0 INTRODUCTION	1
2.0 BACKGROUND	3
3.0 ANALYSIS OF DYNAMIC LOADS AND TIE BENDING MOMENTS FROM JUNE 1980 TESTS	8
3.1 Test Layout	8
3.2 Data Processing	8
3.3 Statistical Results	10
3.4 Summary	14
4.0 LABORATORY STUDY TO DETERMINE THE EFFECTS OF TIE PAD STIFFNESS ON THE ATTENUATION OF IMPACT STRAIN IN CONCRETE TIES.	16
4.1 Introduction.	16
4.2 Test Procedures	16
4.3 Test Results.	20
4.4 Destructive Tie Tests	32
5.0 TRACK MEASUREMENTS TO VERIFY THE EFFECTS OF PAD STIFFNESS ON IMPACT	34
5.1 Introduction.	34
5.2 Pad Selection	34
5.3 Test Layout	35
5.4 Test Procedure.	35
5.5 Instrumentation	35
5.6 Test Results.	38
6.0 SUMMARY OF RESULTS	57
6.1 Background.	57
6.2 Reevaluation of June 1980 Test Data	57
6.3 Laboratory Tests of the Effects of Tie Pad Stiffness on Impact Attenuation	58
6.4 Field Tests to Determine the Effects of Tie Pad Stiffness on Impact Attenuation	59
7.0 CONCLUSIONS AND RECOMMENDATIONS.	61
REFERENCES.	62
APPENDIX A. INSTRUMENTATION AND DATA PROCESSING.	A-1
APPENDIX B. RECOMMENDATIONS FOR PERFORMANCE AND CHARACTERISTIC TESTS OF CONCRETE TIE PADS	B-1

LIST OF FIGURES

	<u>Page No.</u>
FIGURE 2-1. Typical Advanced Rail Seat Bending Crack.	3
FIGURE 2-2. Percentage of Cracked Rail Seats in Special Test Zone of Concrete Ties at Aberdeen, MD., Milepost 68.48	5
FIGURE 2-3. Condition of Flexible Pad Removed From Track After 10 Months	6
FIGURE 3-1. Aberdeen Concrete Tie Test Site, Milepost 68.7 - 68.9, Track No. 4	9
FIGURE 3-2. Frequency Spectrum of Rail Seat Bending Signal from Tie 31 at Aberdeen	11
FIGURE 3-3. Time History of Rail Seat Bending Strain Filtered at Different Bandwidths of Frequency.	12
FIGURE 3-4. Rail Seat Bending Moment vs. Frequency of Occurrence for Data Filtered at 300 and 1200 HZ	13
FIGURE 3-5. Vertical Wheel/Rail Load vs. Frequency of Occurrence, June 1980 Measurements on Nec Track at Aberdeen, MD	15
FIGURE 4-1. Impact Loading Fixture.	17
FIGURE 4-2. Measurement of Rail Seat Bending Moment by Tie Strain Coupon.	19
FIGURE 4-3. Frequency Spectra of Rail Seat Bending Strain from Track and Laboratory Measurements.	21
FIGURE 4-4. Typical Time Histories of Tie Strain from Track and Laboratory Measurements	22
FIGURE 4-5. Effect of Tie Pad Substitutions on Impact Strain at Tie Rail Seat.	24
FIGURE 4-6. Typical Load-Deflection Plots from Tie Pad Stiffness Measurements.	25
FIGURE 4-7. Tie Bending vs. Drop Height for Tests up to Maximum Simulated Track Input	30
FIGURE 4-8. Tie Crack Development vs. Impact Hammer Drop Height	33
FIGURE 5-1. Layout of Instrumented Zone	36

LIST OF FIGURES

(Continued)

	<u>Page No.</u>
FIGURE 5-2. Instrumented Track Zone and Transducers	37
FIGURE 5-3. Placement of Deflection and Acceleration Transducers.	39
FIGURE 5-4. Exceedance Levels of Tie Bending Moment and Vertical Load for Northeast Corridor Passenger Traffic Above 70 MPH on Each of Three Tie Pads.	40
FIGURE 5-5. Effect of Tie Pad Stiffness on Rail Seat Bending Moment and Vertical Load, All Freight Traffic	42
FIGURE 5-6. Tie Bending Strain Data for Amfleet and Conventional Cars - Arrangement by Pad Type	44
FIGURE 5-7. Tie Bending Strain Data for Amfleet and Conventional Passenger Cars - Arrangement by Car Type.	45
FIGURE 5-8. Vertical Wheel/Rail Loads for Amfleet and Conventional Passenger Cars - Arrangement by Pad Type	46
FIGURE 5-9. Vertical Wheel/Rail Loads from Amfleet and Conventional Passenger Cars - Arrangement by Car Type	47
FIGURE 5-10. Effect of Speed on Vertical Loads of Conventional Cars.	48
FIGURE 5-11. Measurements of "Peak-to-Peak" Vertical Clip Deflections on a High-Speed, One-Degree Curve of the Northeast Corridor Track at Aberdeen, MD.	50
FIGURE 5-12. Rail-to-Tie Acceleration Transfer Functions for the Three Test Pads	51
FIGURE 5-13. Rail Seat Bending Strain From Crack-Producing Impact, Conventional Passenger Train, 5-mm Flexible Pad, Tie No. 5	53
FIGURE 5-14. Examples of Vertical Load and Tie Bending Moment Records for a Conventional Passenger Train.	54
FIGURE 5-15. Wheel Conditions Identified by Track Loading Measurements.	55
FIGURE 5-16. Measurement of Wheel Tread Profile and Radial Eccentricity	56

LIST OF FIGURES

(Continued)

	<u>Page No.</u>
FIGURE A-1. Strain Gage Circuits to Measure Lateral and Vertical Wheel/Rail Loads	A-2
FIGURE A-2. Rail Loading Fixture Used for Modulus Tests and Rail Circuit Calibration.	A-3
FIGURE A-3. Vertical Wheel/Rail Load Circuit Calibration.	A-4
FIGURE A-4. Lateral Wheel/Rail Load Circuit Calibration	A-6
FIGURE A-5. Strain Gage Coupon for Installation on Concrete Ties. .	A-8
FIGURE A-6. Fixture for In-Situ Calibration of Tie Bending Strain	A-9
FIGURE A-7. Placements of Strain Gages, Accelerometers and Displacement Transducers.	A-10
FIGURE A-8. Schematic of Wayside Data Acquisition System.	A-12
FIGURE A-9. Schematic of Signal Path from Transducer to Digital Storage and Printout.	A-13

LIST OF TABLES

TABLE 4-1. Tie Pad Stiffness and Impact Attenuation Rates From Basic Tests	26
TABLE 4-2. Tie Pad Stiffness and Impact Attenuation Rates From Additional Tests.	28

PREFACE

This is the final report of an investigation conducted to determine the potential for using flexible tie pads to attenuate impact loads in concrete ties installed on the Northeast Corridor railroad track. Battelle's Columbus Laboratories conducted the study under Contract DOT-FR-9162, "Tie and Fastener Verification Studies," which is sponsored by the Federal Railroad Administration (FRA) with the assistance of the National Railroad Passenger Corporation (Amtrak).

The successful completion of this study resulted from the work of many people. As the Contracting Officer's Technical Representative, Mr. Howard G. Moody of the FRA participated actively in all planning phases and coordinated activities among Battelle, the FRA, Amtrak and several pad manufacturers. Other key participants included Mr. Ted R. Ferragut of the FRA Office of Intercity Programs, Mr. Dan Jerman of Amtrak, Mr. Dennis Wilcox of Amtrak and Mr. Gregory Mester of Deleuw, Cather/Parsons. Battelle researchers and technicians who conducted the field and laboratory tests and data evaluations included Dale Dawley, Edward Hiltner, Dale Plunkett, Kenneth Schueller, Tony So, Paul Southerland and Matthew Zelinski. The contributions of all these people are greatly appreciated by the authors.

EXECUTIVE SUMMARY

In June 1980, "hairline" bending cracks were discovered under the rail seats of concrete ties in the Northeast Corridor (NEC) track at Aberdeen, Md. The ties had been put in service in December 1978. Other spot inspections found cracks in ties which had been in service only a few months. While there was no evidence of structural failure, the cracks were a cause for concern because the ties had been designed to the latest strength specification of Amtrak. An investigation was conducted to identify the cause and to recommend corrections which would arrest the development of new cracks and the further growth of existing cracks. This program was carried out in three phases:

a. Existing dynamic loads and tie strain data from the June 1980 tests were processed over a wide-frequency bandwidth (0 - 1200 Hz) to determine whether high-amplitude impacts were occurring at frequencies higher than those previously believed to encompass dynamic track loading (0 - 300 Hz). This evaluation verified the existence of high-frequency, high-amplitude impact loads resulting from irregularities on a small percentage of high-speed passenger train wheels.

b. Laboratory impact loading tests were conducted with a one-tie test arrangement to determine the effects of tie pad stiffness on the attenuation of impact loads. The tests showed that major reductions in tie pad stiffness could reduce the impact bending strains to levels which would not cause cracking. However, the elimination of such events would require a pad too thick to be accommodated by the current NEC fastener clips. Within the practical range of pad thickness (6.5 mm), the best flexible pads attenuated impact bending strain by about 25 percent relative to that produced with the current rigid plastic pad.

c. To verify the results of the laboratory tests, field measurements were conducted on the Northeast Corridor track at Aberdeen, Md. A 5-tie zone was instrumented to measure wheel/rail loads and tie-bending moments. Pads were substituted over a 50-tie segment which included the instrumented zone. For each of two flexible pads and for the current rigid pad, data were collected over a 5-day period. The field tests proved that flexible pads which are adaptable to the current fastener clips can significantly reduce the occurrence of cracking-level tie bending moments. However, the most flexible pad used in the tests series experienced a few impacts with the potential to crack a tie. The elimination of cracking will require both a flexible tie pad and a program to correct wheel tread conditions before they become large enough to cause cracks.

As an aid to the timely maintenance of serious wheel tread conditions, it is recommended that a wheel impact detector system be installed on track. This system would be connected to existing communication lines and would permit the assessment of tread conditions on passenger train wheels before they produce cracking-level impact loads.

INVESTIGATION OF THE EFFECTS OF TIE PAD
STIFFNESS ON THE IMPACT LOADING OF
CONCRETE TIES IN THE NORTHEAST CORRIDOR

1.0 INTRODUCTION

The reconstruction of the Northeast Corridor (NEC) track includes 400 track-miles of prestressed concrete ties. As part of a field measurement program conducted at Aberdeen, Md., during June 1980, Battelle examined a selection of these ties which had been put in service during December 1978. Many of the ties had developed "hairline" cracks under the rail seats. In no case was there any evidence of structural failure of the ties. However, the cracks created concern because:

- a. The ties (Sante Fe/San Vel RT7SS-2) had been designed under Amtrak specifications which incorporated the latest bending strength requirements of the American Railway Engineering Association [1]. Thus, the ties were expected to sustain all anticipated loads without cracking.
- b. The cracks were of the same type which had eventually led to failure (loss of bending strength) in earlier designs of lower strength ties.

The FRA contracted with Battelle to investigate the cause of the cracks and to identify a solution which would arrest further crack development while minimizing the retrofiting of components. The investigation was carried out in three phases:

- a. Existing data on vertical loads and tie bending moments from the Northeast Corridor track were evaluated to determine whether processing over a large bandwidth of frequency would reveal high response levels. This study [2] identified the probable cause of the cracks as impact loads resulting from irregularities on a small percentage of high-speed passenger train wheels.
- b. Impact loading tests were conducted with a one-tie laboratory test arrangement to determine the effects of tie pad stiffness on the attenuation of bending strain [3]. The tests revealed that major reductions in tie pad stiffness could reduce the bending strains below the level which causes cracks.
- c. To verify the results of the laboratory tests, new field measurements using pads of varying stiffness were conducted on the NEC track at Aberdeen, Md. Pads were substituted in a test zone to obtain loads and strain data over a 5-day period for each pad. The field tests provided proof that flexible pads which are adaptable to the current fastener system can significantly reduce the occurrence of strains which can crack ties. However, the

elimination of tie cracking will require both a more flexible pad and a program to eliminate the wheel tread conditions causing the highest impact loads on Northeast Corridor passenger trains.

This final report of the investigation reviews the discovery of the tie cracks and subsequent static bending strength tests, summarizes the evaluation of existing data and the laboratory impact tests, describes the field measurement program, and evaluates the field data. Recommendations are made for a program of tie pad substitutions and improved wheel maintenance which could eliminate the premature cracking of NEC concrete ties and reduce the rate of growth of existing cracks.

2.0 BACKGROUND

In June 1980, a Battelle field measurements group installed a test site on Northeast Corridor concrete tie track at Aberdeen, Md. As part of a general characterization of the track and its traffic,* a crack inspection was conducted on a sampling of nearby ties. Fifteen cribs were cleared of ballast to expose 60 tie faces. Forty-eight of the 60 rail seat faces contained hair-line cracks [4]. The smallest cracks were visible only when sprayed with alcohol and extended only about one-half inch onto the smooth cast faces of the ties. However, many of the cracks extended up to the lower prestressed strands, and a few extended above the top prestressed layer where they branched out towards the corners of the rail, as shown in Figure 2-1.



FIGURE 2-1. TYPICAL RAIL SEAT BENDING CRACK

Other inspections produced cracking rates which varied with the amount of tie service and range of vehicle speeds. In the area between Edgewood and Elkton, Md., three inspections produced:

- a. No faces cracked among 15 inspected on ties newly installed by the track laying system, prior to traffic
- b. 3 faces cracked among 20 inspected on ties loaded only by the construction ballast train

*This field test was part of the Tie and Fastener Correlation Study, sponsored by the FRA under Contract DOT-FR-8164.

- c. 5 faces cracked among 60 inspected on ties loaded by two weeks of traffic (speed limit 110 mph).

Two locations on the Boston Division of the NEC were inspected with the following results:

- a. No faces cracked among 100 inspected where the speed limit is 50 - 80 mph.
- b. 19 faces cracked among 76 inspected where the speed limit is 90 - 95 mph.

No specific causes for the crack development could be identified. The possibility existed that the cracks might have been caused by damage during installation rather than by train loads. To isolate the possible effects of train loads and to obtain an indication of the effects of tie pad stiffness, Amtrak installed a special test zone of 60 new ties in September 1980. Thirty ties were fitted with a moderately flexible pad and 30 were fitted with the standard, rigid EVA pad. The ties were inspected 3 times in the next 9 months, during which about 15 million gross tons were moved on this track.

The results presented in Figure 2-2 show that both 30-tie zones accumulated significant percentages of cracks during the 9-month period. In the flexible pad zone, the rate of crack development initially lagged and then exceeded the rate in the rigid pad zone. This was caused by deterioration of the flexible pad. The surfaces of this pad were molded with rectangular ridges to increase flexibility. Sample pads removed in July 1980 contained worn ridges and spots of heavy abrasion, as shown in Figure 2-3.

Among 60 ties removed from track to make room for the test zone, 50 contained cracks. To assess the effects of the cracks on static bending strength, the tie manufacturer conducted tests on a selection of the removed ties, which included the following conditions:

- a. small, minor cracks -- extending up to the bottom layer of prestress strands
- b. medium cracks -- extending between the bottom and top layers
- c. bad, severe cracks -- extending from the top layer upward

The test produced the following mean bending moments in each category [5]:

	<u>MEAN BENDING MOMENT (IN-KIPS) AT:</u>		
<u>NO. RAIL SEATS TESTED</u>	<u>BOND LOSS</u>	<u>ULTIMATE STRENGTH</u>	
SMALL/MINOR CRACKS	7	712	729
MEDIUM CRACKS	5	643	706
BAD/SEVERE CRACKS	12	513	615

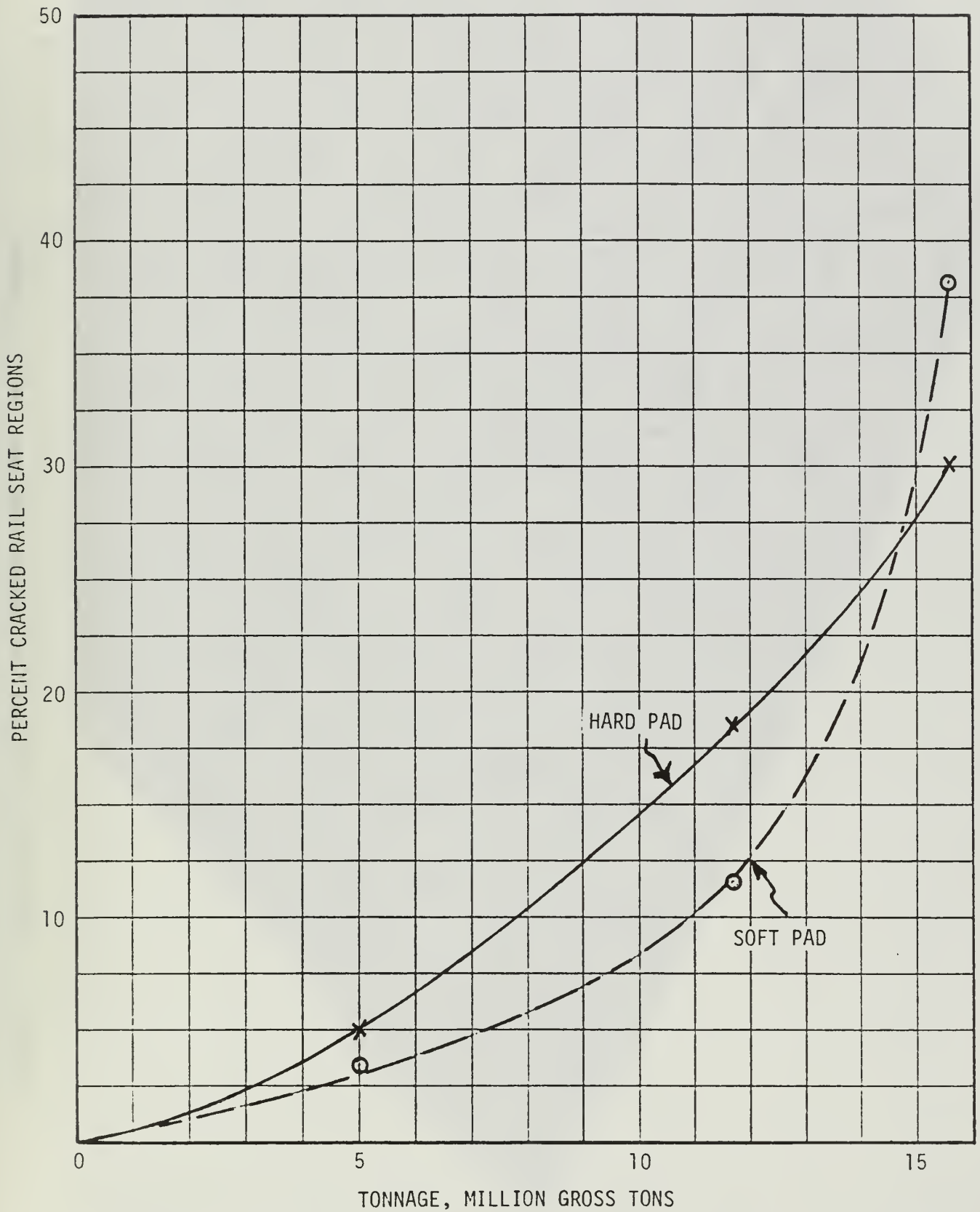


FIGURE 2-2. PERCENTAGE OF CRACKED RAIL SEATS IN A SPECIAL TEST ZONE OF CONCRETE TIES AT ABERDEEN, MD., MILEPOST 68.48

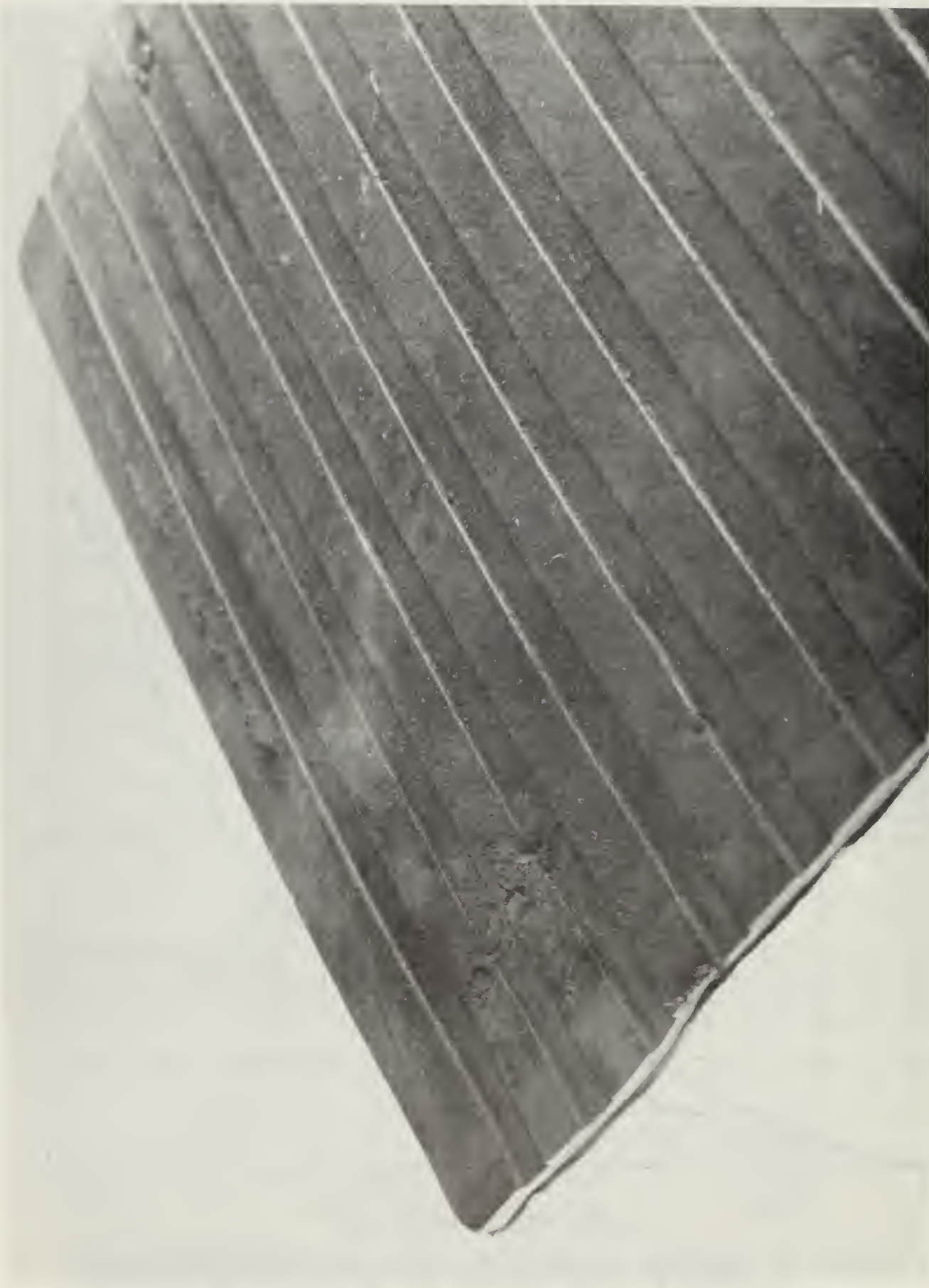


FIGURE 2-3. CONDITION OF FLEXIBLE PAD REMOVED FROM TRACK AFTER 10 MONTHS

Among the 12 rail seats tested in the last category, one tie fell below the American Railway Engineering Association (AREA) requirement for ultimate strength of new ties. This tie produced an ultimate bending moment of 478 in-kips, versus the AREA requirement of 525 in-kips. The mean bending moments in the table show a drop in ultimate strength of 16 percent due to crack progression from small/minor to bad/severe. These ties were in service for 21 months.

The tie inspections and bending strength tests clearly indicated the need for an investigation to determine the cause of tie cracking and to recommend corrective action. The three phases of the investigation are described in the following sections.

3.0 ANALYSIS OF DYNAMIC LOADS AND TIE BENDING MOMENTS FROM JUNE 1980 TESTS

Dynamic wheel/rail loads and tie bending moments were first measured on the track at Aberdeen, Md., during June 1980. The data were initially processed to capture all dynamic responses occurring within the frequency range of 0 - 300 Hz. Tie bending moments were not found at magnitudes sufficient to cause cracks. However, an examination of the data over a bandwidth of 1200 Hz showed that the effects of high-frequency impact loading had not been fully described by the initial processing. The determination of the required range of processing frequency and the resulting verification of cracking-level tie bending moments are described in this section.

3.1 Test Layout

Figure 3-1 shows the layout of the dynamic measurements site. Rail seat and tie center bending moments were measured on 7 ties. Vertical and lateral loads were measured at a single location. Data from approximately 10,000 freight axles and 4,000 passenger axles were recorded during an 8-day test period. Descriptions of the transducers and the data acquisition and processing systems are provided in Appendix A.

Strain gage coupons attached to the ties were calibrated in terms of the statically applied bending moment required to produce the strain in the linear (non-crack) region. This permitted a direct comparison of dynamic tie strain levels with a "cracking threshold," defined as the mean value (375 inch-kips) of bending moments which have produced first cracking in static bending tests [6] of ties designed to current AREA and Amtrak specifications. As shown later, this statically determined threshold was approximately duplicated in laboratory impact loading tests. This demonstrates that the bending moments required to initiate cracks are approximately equal whether they are produced by static or impact loading.

3.2 Data Processing

After initial storage on analog tape, the time histories of tie bending moment and wheel/rail load were processed to capture the peaks from each wheel pass. The initial processing included:

- a. analog filtering to attenuate responses occurring at frequencies above 300 Hz. The rate of attenuation above this limit was 24 dB per octave.
- b. analog peak detection of the filtered signal to select the peak response from each wheel pass
- c. conversion of the captured peaks to digital values which were stored on cassette tape.

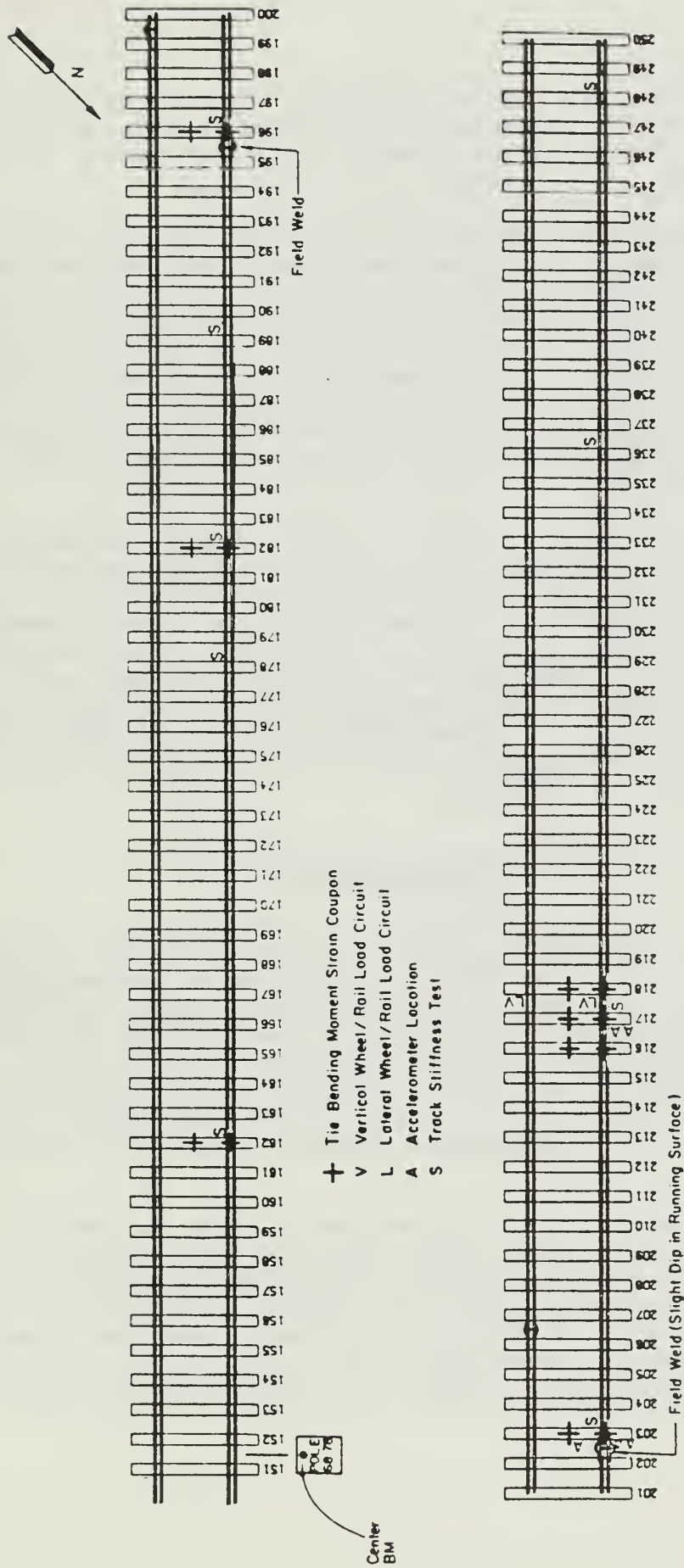


FIGURE 3-1. ABERDEEN CONCRETE TIE TEST SITE, MILEPOST 68.7 - 68.9, TRACK NO. 4

The peak values for each train pass were tabulated to permit on-site inspection. Data from the digital cassettes were processed at Battelle to obtain statistical summaries from groupings according to type of traffic, train speed, and location on track.

A 300-Hz filter bandwidth was chosen initially because previous experience had shown that this bandwidth was adequate for track measurements under normal freight service. However, the NEC track carries a unique combination of freight and passenger traffic, and much of the passenger traffic travels above 70 mph. A closer examination of the original data, particularly for the high-speed passenger traffic, showed that tie response was highly oscillatory under most wheels. The tie bending response occurred mainly at the rail seat; there was comparatively little bending moment at the tie center. Spectral analysis of a rail seat bending moment signal, Figure 3-2, identified natural frequencies of the tie at 125, 385, and 640 Hz.

The need for data processing over a wider frequency bandwidth was clearly indicated. This involved a tradeoff: as the filter bandwidth was increased, the system noise and the uncertainty associated with a given signal amplitude also increased. Figure 3-3 shows the rail seat bending moment time history from a single impact processed at four different filter bandwidths: 300, 800, 1200 and 2000 Hz. The amplitude of the bending moment pulse increases with each increase in bandwidth. The 1200-Hz filter was chosen because it provided 93 percent of the amplitude obtained with 2000-Hz filtering while reducing the system noise to about half the level of 40 kip-inch encountered at 2000 Hz.

3.3 Statistical Results

Plots of rail seat bending moment vs. percent frequency of occurrence were compiled from data processed with 300- and 1200-Hz filter bandwidths. In Figure 3-4, the results are shown separately for three types of traffic: passenger traffic above 70 mph, passenger traffic below 70 mph, and freight traffic, most of which passed the site at speeds between 40 and 60 mph. At frequencies of occurrence below 1 percent, the data for each type of traffic show substantial increases in strain level due to the expansion of frequency bandwidth. A vertical line indicates the previously discussed cracking threshold.

The right side of Figure 3-4 shows that less than 0.1 percent (1/1000) of the high-speed passenger wheels produced bending moments above the mean of levels which have produced cracks in static bending tests. For the low-speed passenger and freight traffic, this bending moment level is reached at even lower frequencies of occurrence. With these frequencies, however, a potentially cracking bending moment level occurs at an average tie location about once every 1.8 days. This estimate is based upon the following total axle counts per day:

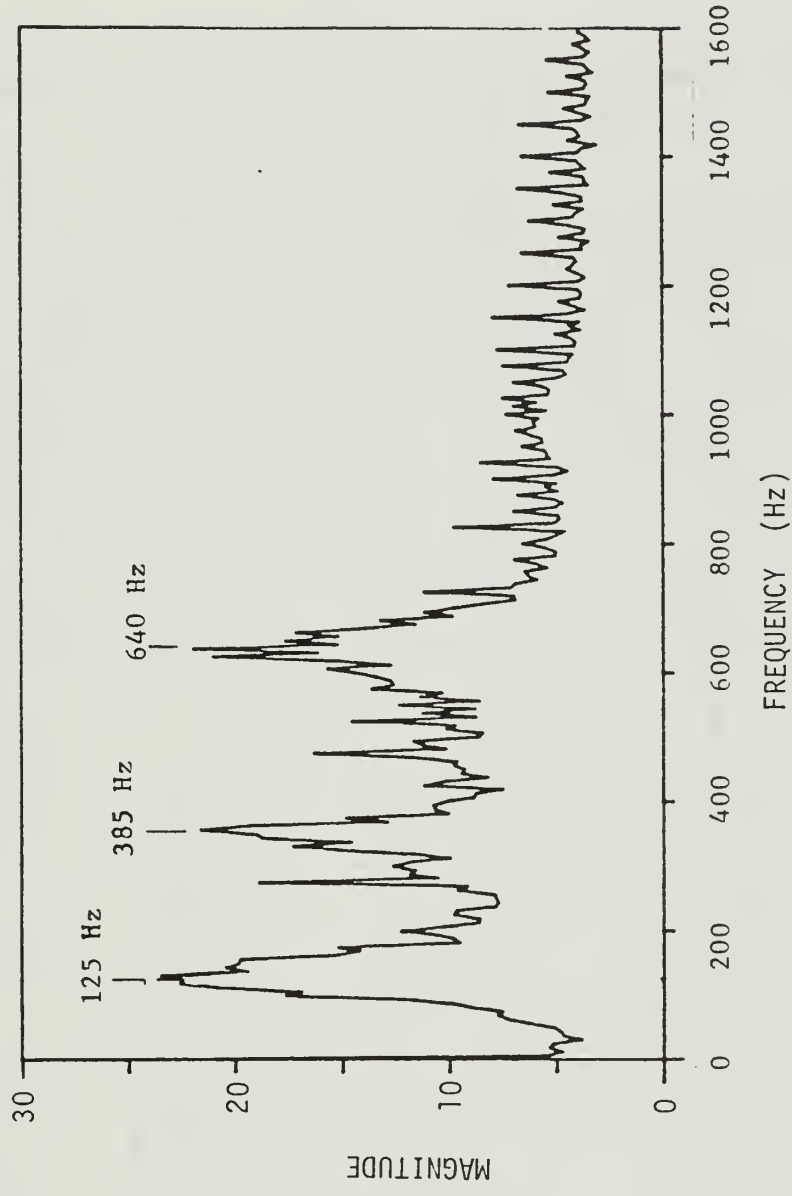


FIGURE 3-2. FREQUENCY SPECTRUM OF RAIL SEAT BENDING SIGNAL FROM TIE 31 AT ABERDEEN
 RUN 14-1, 77 MPH

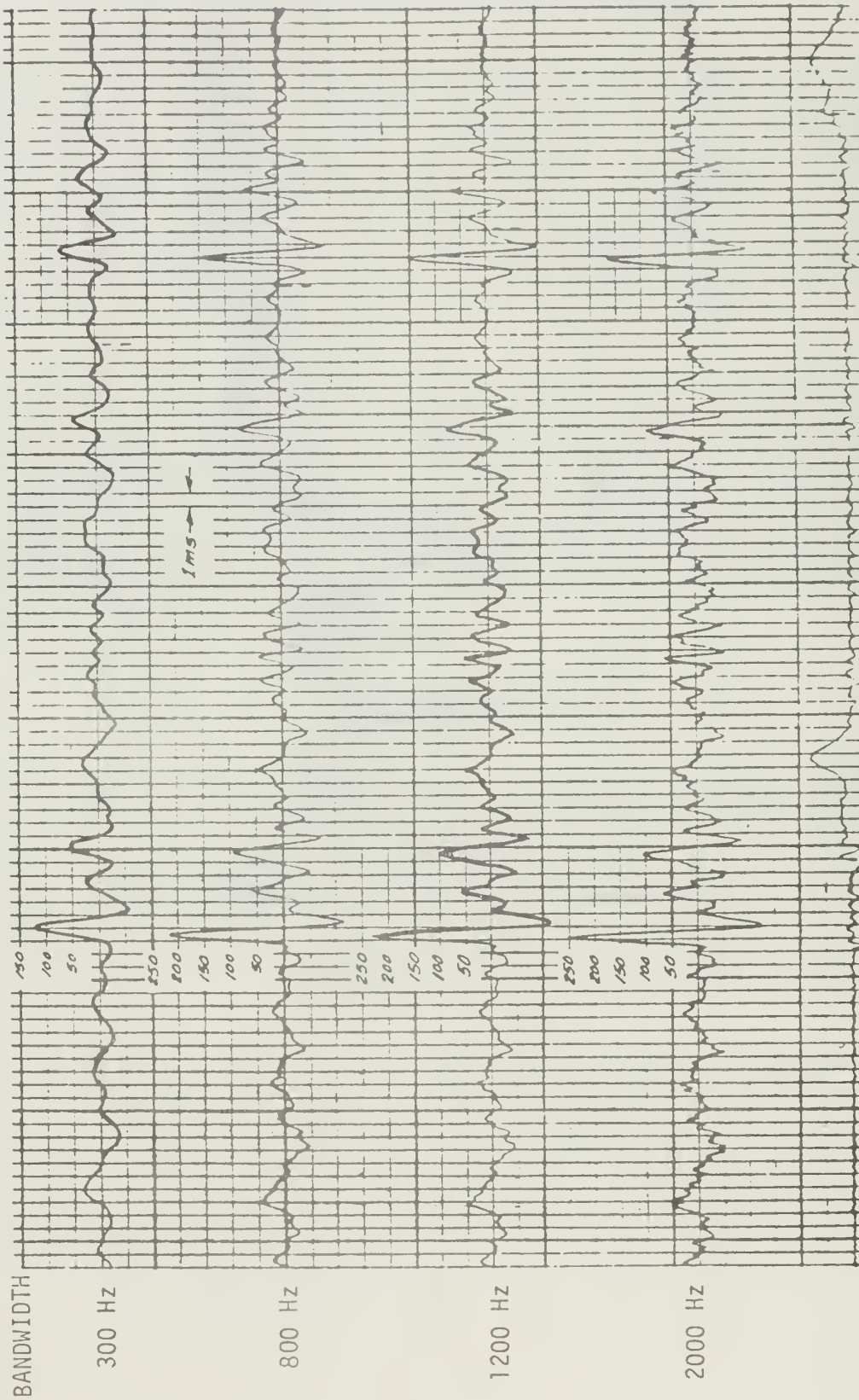


FIGURE 3-3. TIME HISTORY OF RAIL SEAT BENDING STRAIN FILTERED AT DIFFERENT BANDWIDTHS OF FREQUENCY

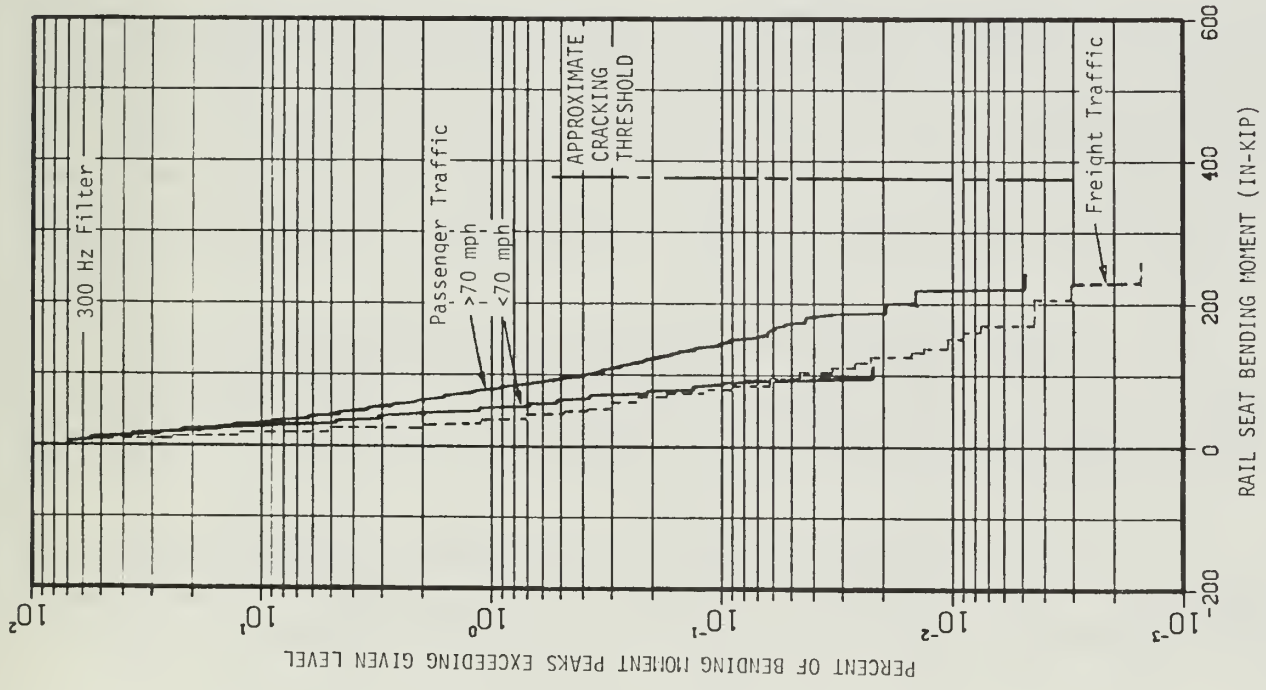
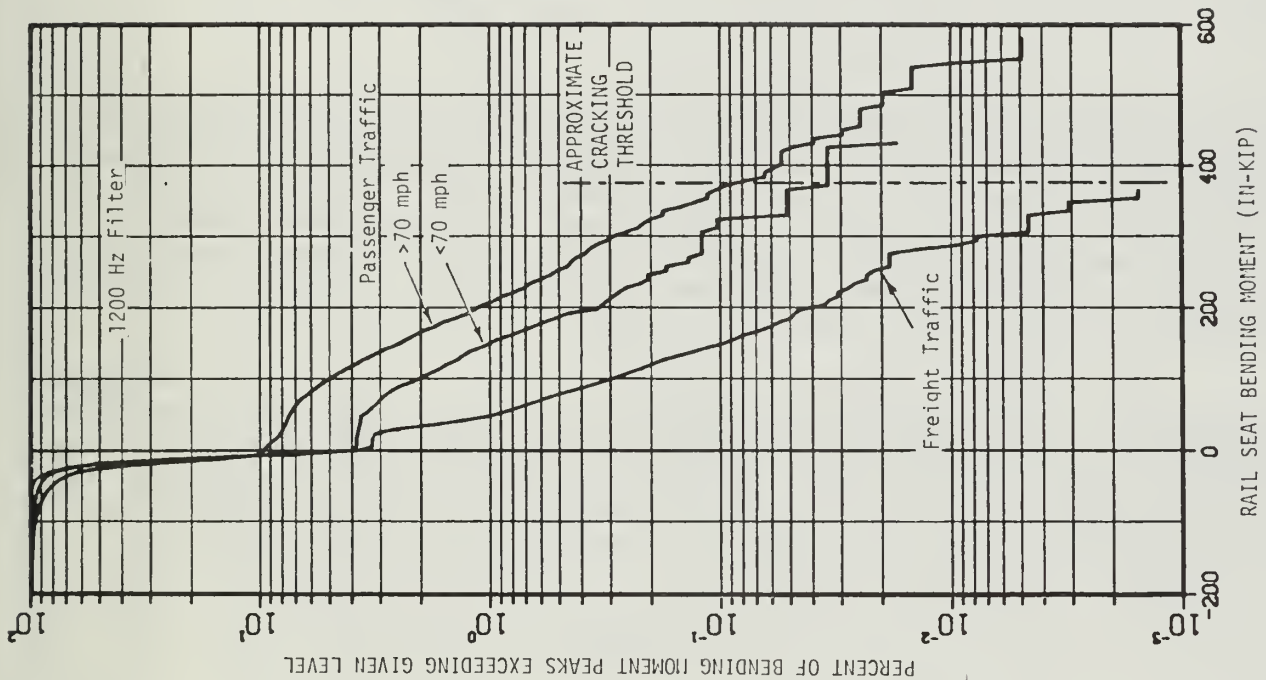


FIGURE 3-4. RAIL SEAT BENDING MOMENT VS. FREQUENCY OF OCCURRENCE FOR DATA FILTERED AT 300 AND 1200 HZ

- | | |
|----------------------|--------------------|
| a. Passenger traffic | 700 axles per day |
| 1) Above 70 mph | 540 axles per day |
| 2) Below 70 mph | 160 axles per day |
| b. Freight traffic | 1500 axles per day |

The curves in the right-hand plot of Figure 3-4 (data filtered at 1200 Hz) contain "kinks" between 25 and 75 inch-kips. The kinks result from a peculiarity of the analog peak detection applied to this data set. The peak detection system was biased to select the negative peak where two approximately equal positive and negative peaks occurred. This was common in the low-amplitude events but did not occur in the range of bending moment amplitudes where cracks are of concern. The kinks do not appear in the data filtered at 300 Hz because only positive peak detection was applied to this data set.

Major effects of wheel impacts can be seen in the vertical wheel/rail loads data. Figure 3-5 shows cumulative distributions of wheel/rail load for the three types of traffic discussed previously. The full scale range of the analog-to-digital conversion was 82 kips. Between 0.1 and 0.2 percent of the peak loads from high-speed passenger traffic exceeded this level, which is approximately 4 times the average static passenger wheel load of 20 kips.

3.4 Summary

This evaluation of dynamic loads and tie bending moment data identified the principal source of rail seat bending cracks as the high-frequency, high-amplitude impact loading caused by wheel irregularities. Bending moments above the cracking threshold were produced by less than 1 in 1000 of the high-speed passenger axles and by much lower percentages of low-speed passenger and freight traffic. Because these impacts are random events, the occurrence and the lengths of cracks comprise a random distribution of events ranging from no cracks to cracks of 6 inches or longer. On an average, each tie would experience one impact load with the potential to initiate a crack every 1.8 days.

It should be emphasized that these data were collected on well-maintained track without rail surface irregularities or visible geometry errors. The occurrence of severe cracked ties at rail joints and battered welds indicates that cracking level strains can be produced at track anomalies by the passage of normal or near-normal wheels.

This determination of the cause of cracking led immediately to an investigation of the degree of strain attenuation which might be obtained by a reduction in the stiffness of the tie pad. This investigation is described in the next section.

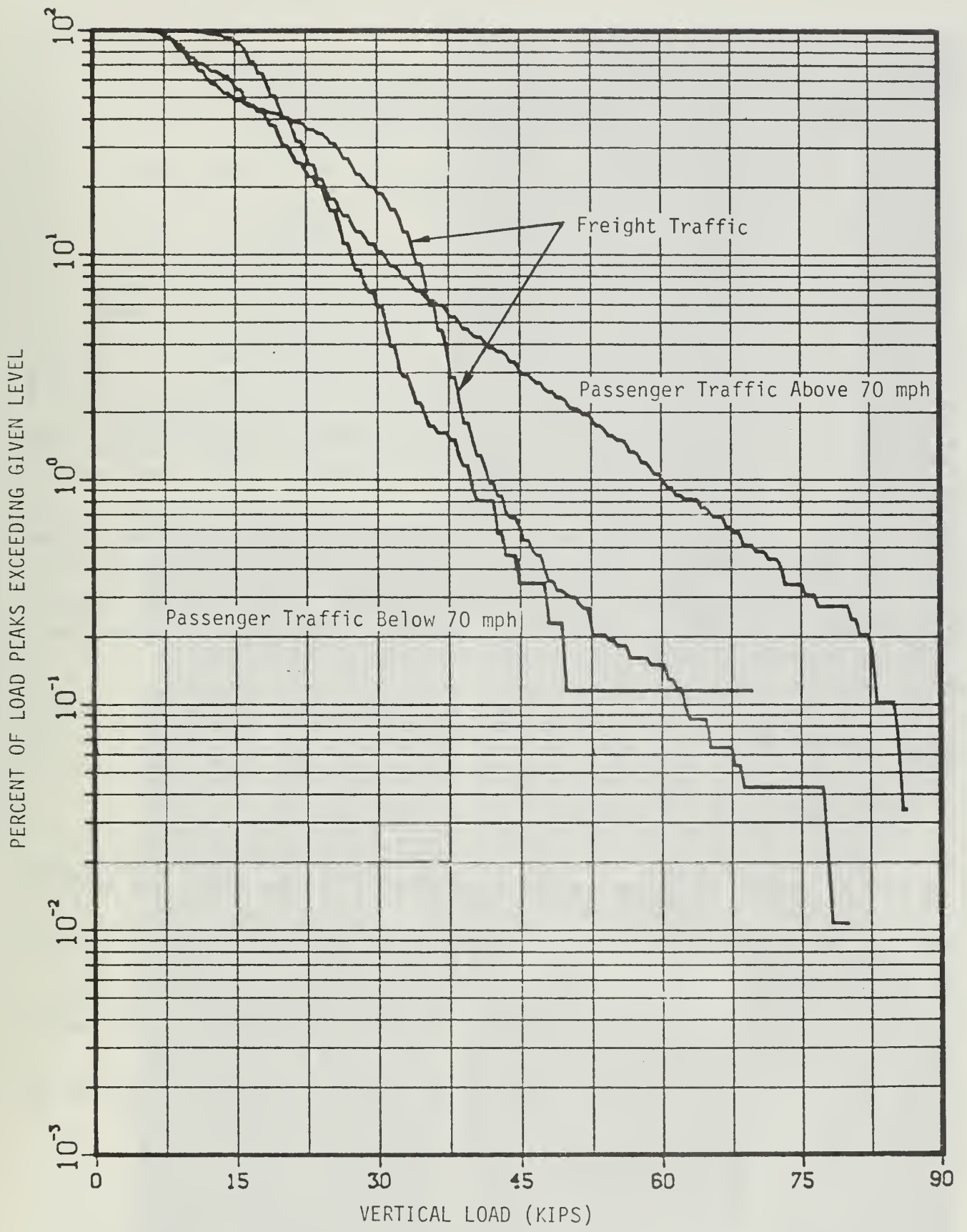


FIGURE 3-5. VERTICAL WHEEL/RAIL LOAD vs. FREQUENCY OF OCCURRENCE, JUNE 1980 MEASUREMENTS ON NEC TRACK AT ABERDEEN, MD.

4.0 LABORATORY STUDY TO DETERMINE THE EFFECTS
OF TIE PAD STIFFNESS ON THE ATTENUATION
OF IMPACT STRAIN IN CONCRETE TIES

4.1 Introduction

One possible solution to the tie cracking problem consists of replacing the current tie pad with a more flexible pad which could better attenuate impact loads. This offers the potential of reducing the impact loading from anomalies in the rail running surface (engine burns, battered welds, joints) as well as from the irregularities of train wheels. To assess the potential effects of pad substitutions, and to select pads for field tests, a method was required by which impact loads could be reproduced in a controlled manner. For this purpose, Battelle designed and constructed an impact loading fixture and conducted tests with a "single-tie" laboratory specimen. The test procedures and results are summarized here; a more complete description is provided in [3].

The major objective of these tests was to identify a level of tie pad stiffness which would prevent the initiation of tie cracks when the ties were subjected to the highest levels of impact energy measured in track. This objective was accomplished within the limitations of the "single-tie" laboratory setup. The effects of recommended pad substitutions were then verified by the field measurements program described later in this report.

4.2 Test Procedures

Impact Loading Fixture

A schematic of the dynamic loading arrangement is illustrated in the inset of Figure 4-1. To obtain the greatest possible range of impact amplitude and frequency content, provision was made for:

- a. Static loading in parallel with the impact loading
- b. Variation of impact hammer impedance by substitution of a shim between the hammer head and hammer and, if required, variation of the shape of the hammer head
- c. Variation of the support condition under the tie, by changing the spacing of Neoprene support strips
- d. A hammer weight range of 0 to 400 pounds
- e. Drop heights from 0 to 56 inches.

The physical arrangement of the drop fixture is shown in the photo of Figure 4-1. The two vertical tubes provide static load, guide the drop hammer

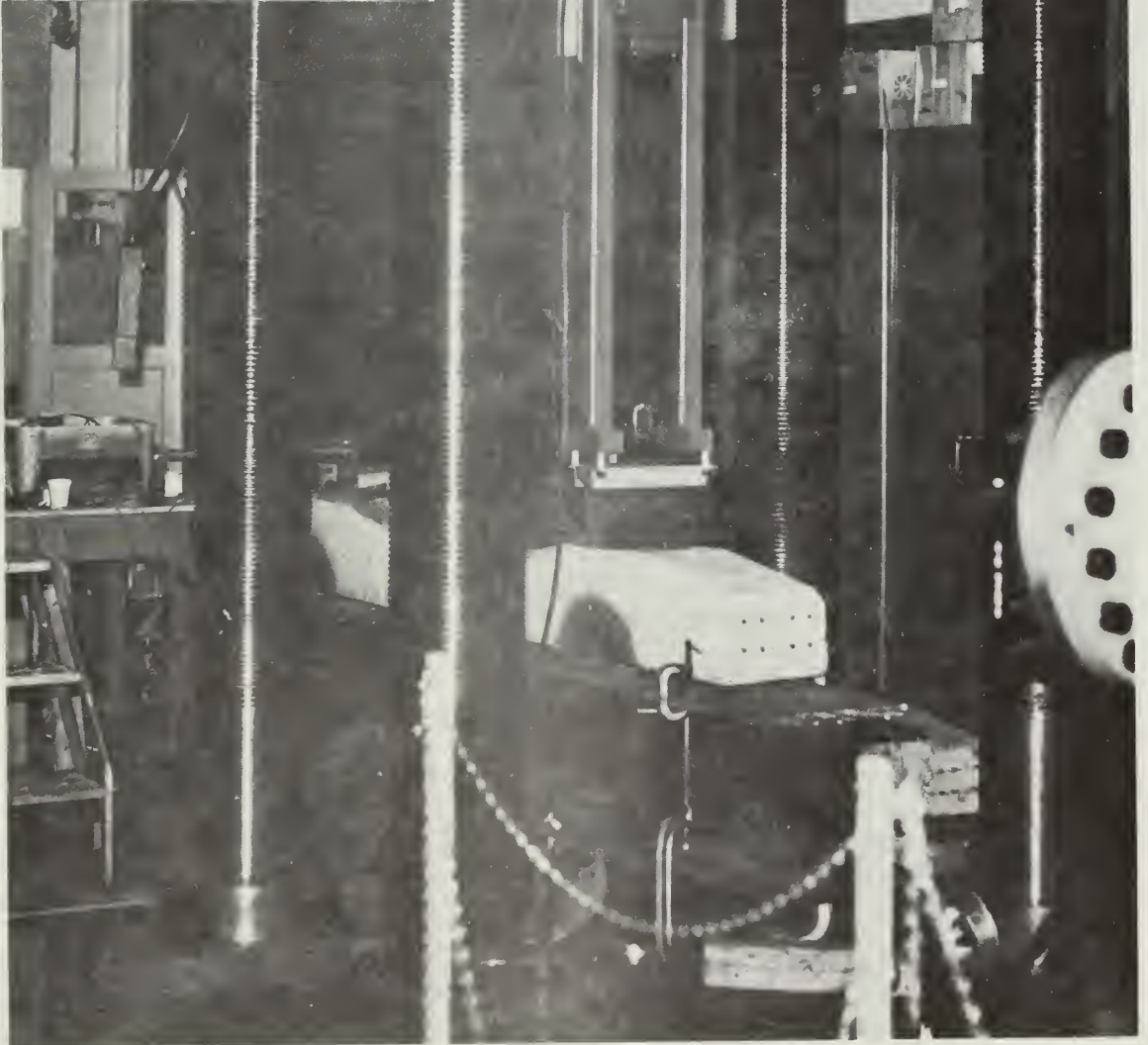
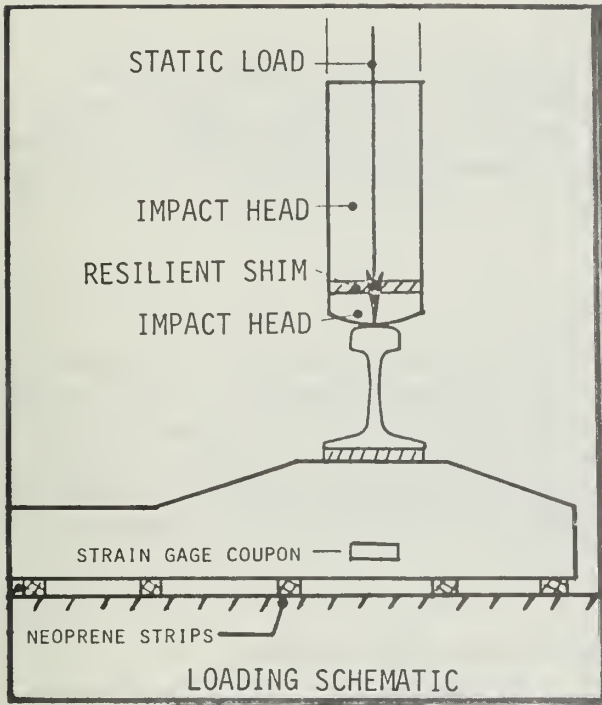


FIGURE 4-1. IMPACT LOADING FIXTURE

and permit the positioning of a frame which seats the drop hammer at any selected height. An electric hoist is suspended at the top of the frame and spring-mounted to prevent overload of the hoist chain as the hammer is seated. A quick-release mechanism releases the drop hammer from its seat in the frame.

Bending Moment Measurement

For both field and lab measurements, tie bending moment was measured by strain gage coupons placed as shown at the top of Figure 4-2. Each coupon consists of two active gages mounted longitudinally along the coupon axis and two "floater" gages, mounted transversely and mechanically isolated from the test specimen. The four gages form a complete resistance bridge, as shown at the bottom of Figure 4-2. The floater gages provide temperature compensation.

Bending Moment Calibration

Bending moment calibration was performed on two ties by application of static bending moment to the rail seat area of the tie. The loading arrangement normally used in track was duplicated as shown at the top of Figure 4-2. The pad load is assumed to be replaced by two discrete forces located by an effective moment arm. This moment arm was determined during an earlier calibration program in which loads applied through 2-inch rubber strips and through pads were compared.

The calibration permits the output voltage of the strain gage bridge to be expressed in terms of the static bending moment which produces this output voltage in the linearly elastic (non-crack) range. The same bridge sensitivity was maintained after cracking to show relative strain magnitudes.

Because the static calibrations were very consistent with the first two instrumented ties, the third tie was calibrated by adjusting the peak of the strain coupon output voltage to match that produced on the first two ties at 14-inch drop height (350 inch-kips). A later setup of the fixture in a new location produced higher strain response (375-kips) with the same sensitivity. This was due in part to a stiffening of the EVA pad as a result of the impact tests and in part because the third gage displayed some drift during all of its tests.

Crack Identification

An opaque epoxy coating was applied to the first trial tie, a previously instrumented CC244C. After crack initiation had been identified from a sudden drop in strain amplitude, a hairline crack was discovered in the epoxy on the face opposite the gage. A crack could not be found on the gage side. This led to a search for a coating which would more quickly reveal crack initiation. The final result consisted of Stresscoat undercoat and resin designed for use at temperatures as low as 65 degrees F. (The temperature

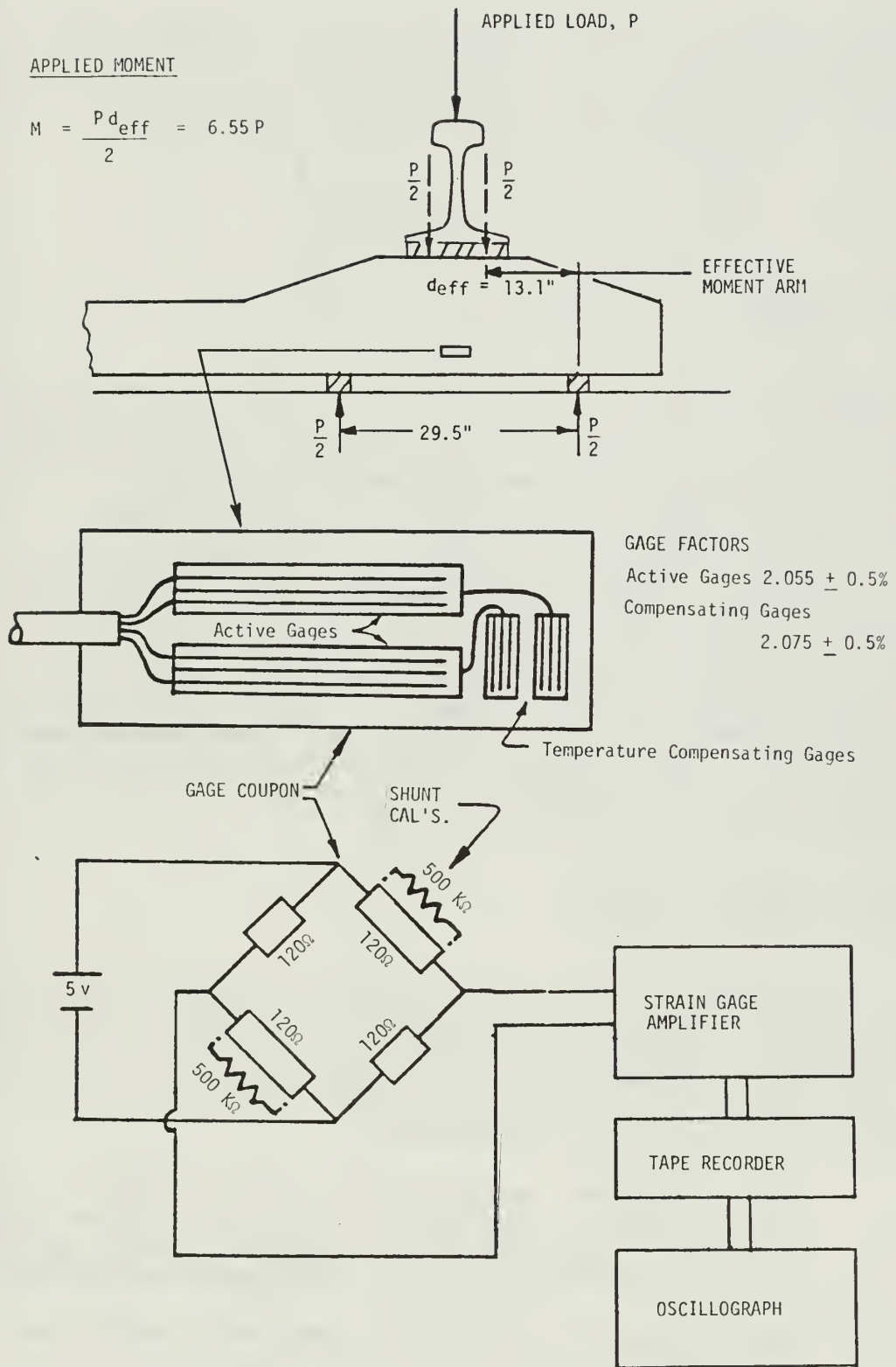


FIGURE 4-2. MEASUREMENT OF RAIL SEAT BENDING MOMENT BY TIE STRAIN COUPON

of the fatigue lab is held continuously at 70°F.) On Stresscoated tie faces, crack initiation could be identified earlier than on the epoxy coating or on untreated faces. While this procedure is not consistent with the method used to identify cracks on ties in track, it was deemed important to find cracks at the lowest strain level at which they occurred.

4.3 Test Results

Spectral Analysis

Spectral analysis of the tie dynamic response was performed early in the program by placing an accelerometer at each of 11 points on the tie surface and capturing the vibration produced by three blows with the drop hammer. These acceleration spectra were used to identify the relative magnitudes of acceleration occurring at the first three bending frequencies.

Figure 4-3 compares spectral analyses from impacts measured in the field and laboratory. The field data show major contributions to the bending moment magnitude from the first three bending modes of the tie. In the laboratory data, the first bending mode is essentially absent while the second and third modes dominate. This difference can be attributed to the single-sided loading of the laboratory arrangement, which contrasts with the two-wheel loading of the tie in track. However, the approximate duplication of the second and third bending modes in the laboratory setup indicates that the tie suspension in either case represents a beam which is very loosely coupled to its support; that is, a "free-free" beam.

Variation of Impact Parameters

A series of tests were conducted with the current Northeast Corridor pad (EVA) and a previously instrumented CC244C tie, which has approximately the same stiffness and weight distribution as the RT 7SS-2 tie used on the NEC. The impact parameters that were varied during the series included the drop height, hammer head shim stiffness, static load, and the spacing of the tie support strips. These tests revealed that:

- a. Strain amplitudes near the static breaking strength of the tie were produced at a drop height of 14 inches with the 115-pound drop hammer. Since drop height could be increased up to 56 inches, an adequate reserve of impact energy was available.
- b. The time duration of the first impact pulse could be most closely simulated with minimum static load and a flexible hammer head shim. A section of Duraflex pad was used as the final shim. For all future tests, the static load was restricted to that sufficient to restrain the fixture (about 3,000 pounds.) Time histories of track and laboratory impact strains are compared in Figure 4-4. The two records agree closely in the duration of the

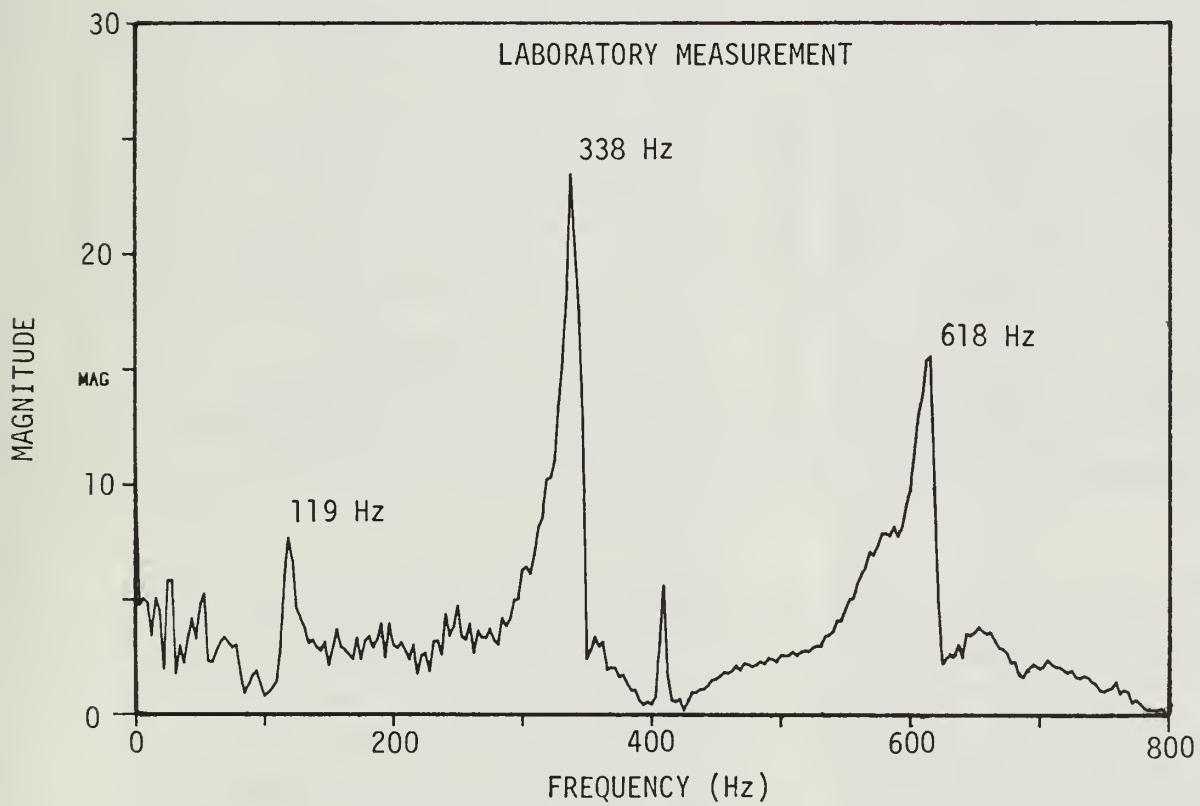
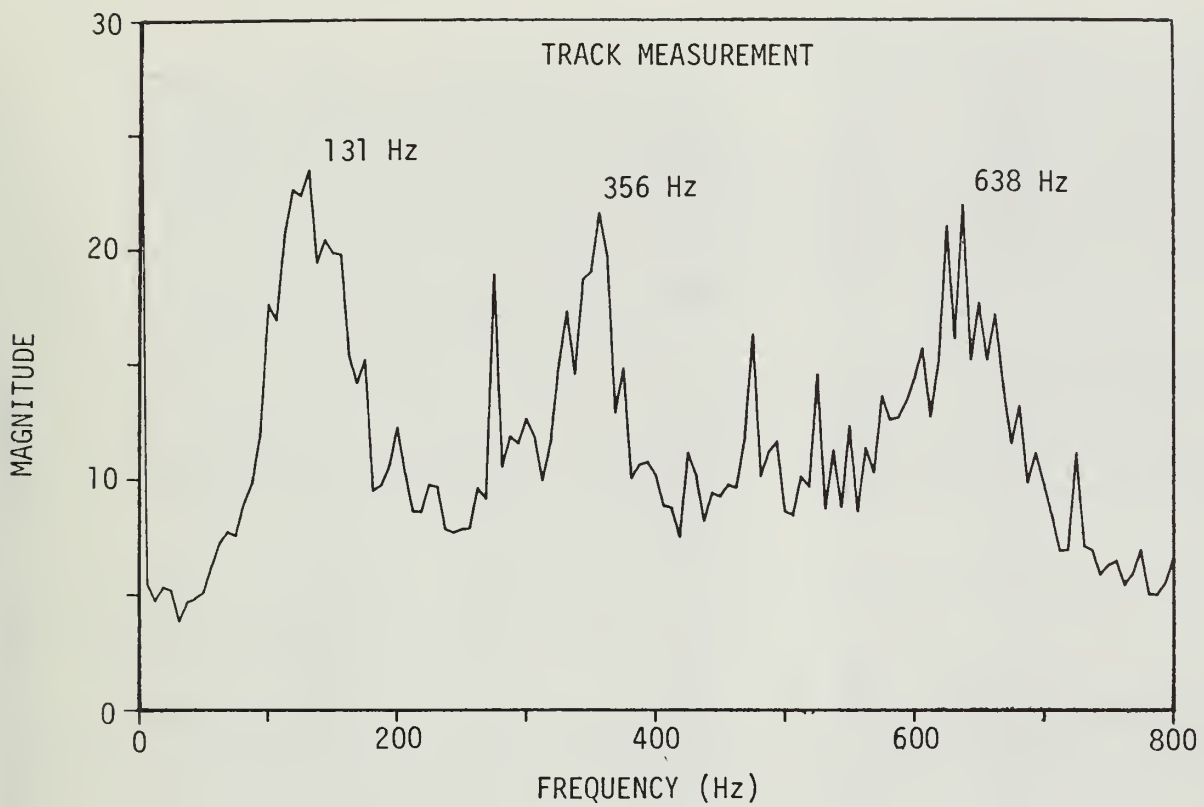
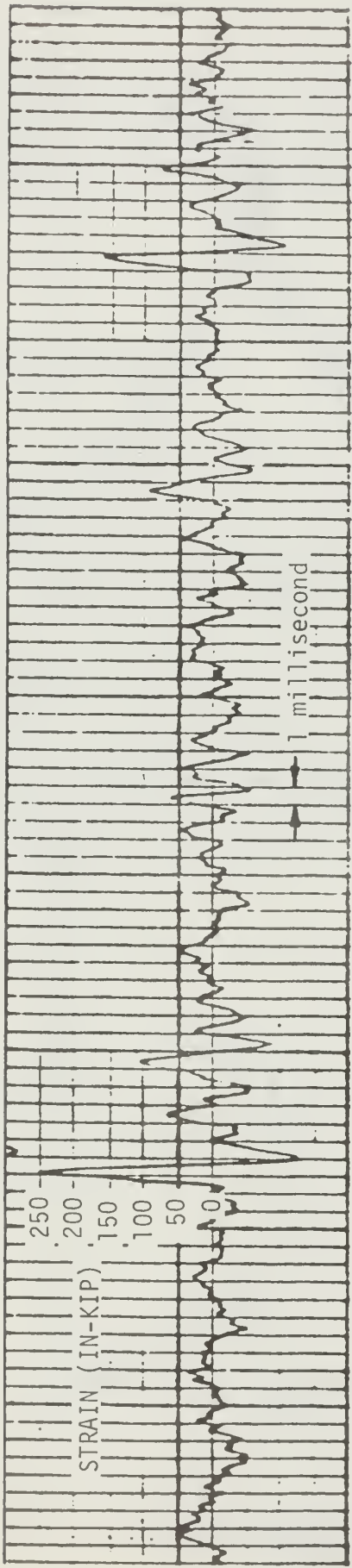
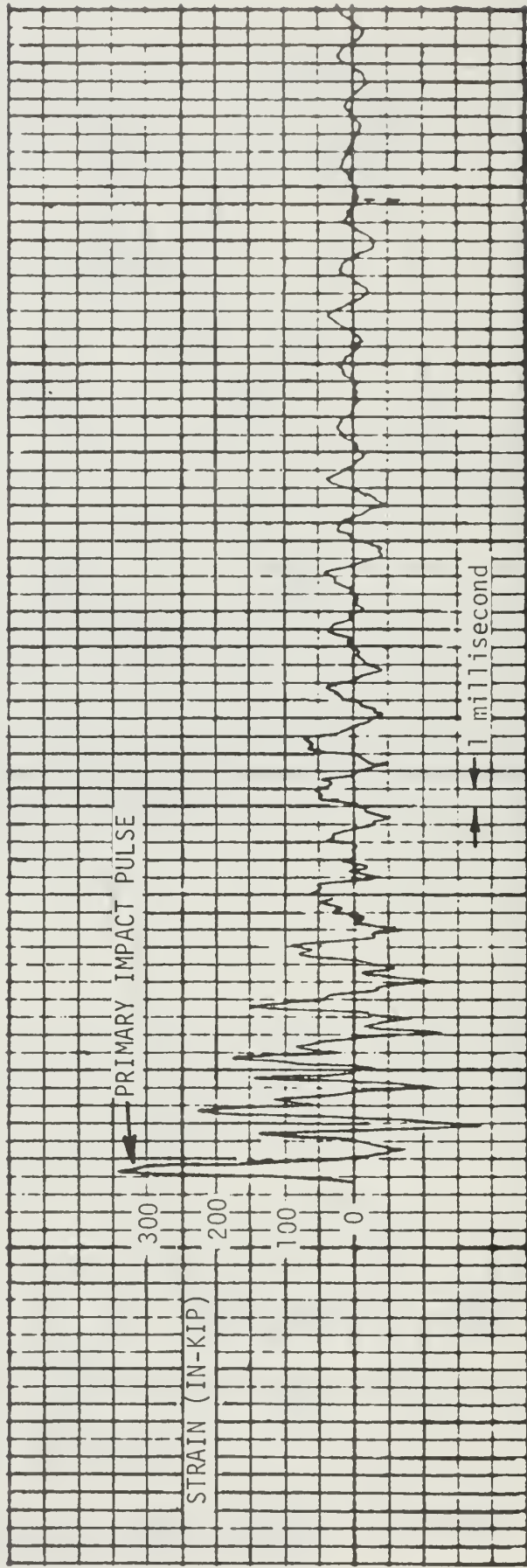


FIGURE 4-3. FREQUENCY SPECTRA OF RAIL SEAT BENDING STRAIN FROM TRACK AND LABORATORY MEASUREMENTS



(a) Track Measurement



(b) Laboratory Measurement

FIGURE 4-4. TYPICAL TIME HISTORIES OF TIE STRAIN FROM TRACK AND LABORATORY MEASUREMENTS

first impact pulse and in the number of oscillations produced either by a train wheel irregularity or by a single blow of the drop hammer. Combined with the frequency comparisons shown previously in Figure 4-3, these records provided evidence that the nature of track impact loading has been successfully reproduced in the laboratory.

- c. Variation in spacing of the tie supports from 15 to 30 inches produced an increase in strain amplitudes of only about 10 percent. Therefore, it was concluded that support spacing was not a critical factor so long as it was maintained constant. A spacing of 15 inches was adopted.

Impact Strain Attenuation vs. Pad Stiffness

Selection of Pads for NEC Field Tests. For the EVA pad and eight potential alternatives, the peak bending strains from low-level (non-crack) drops are shown in Figure 4-5. The left side of the figure shows the results for a cluster of more flexible pads of standard (5-mm) thickness. These results can be compared directly with the curve for EVA #1, the first EVA test pad. The right side of the figure shows similar results for two grooved pads of increased thickness. Their results can be compared directly with the curve for EVA #2, the second EVA test pad. It should be noted that most of the flexible pads were heavily grooved to increase flexibility.

The vertical force-deflection characteristics of each pad were measured statically and at loading/unloading rates up to 9 cycles per second. For each pad, a value of "dynamic stiffness" was determined as the slope of the line connecting 4,000 and 20,000 pounds during the pad compression portion of the dynamic loading cycle. Figure 4-6 shows the dynamic load-deflection results for the three pads which were later selected for field testing. All static and dynamic load-deflection plots are included in Appendix A of [3].

From comparable peak bending moments at each drop height in Figure 4-5, a mean percentage bending moment reduction was calculated for each alternative pad. The static and dynamic values of pad stiffness were obtained from the data illustrated in Figure 4-6. The results are compiled in Table 4-1 along with stiffness values for a number of pads which were not selected for impact testing.

The results show that with two exceptions, bending moment attenuation increases as pad stiffness decreases. However, the rate of attenuation does not reach 20 percent until the dynamic pad stiffness falls below 1 million pounds per inch, which is one-fifth the stiffness of the EVA pad. While a 20 percent bending moment reduction would reduce the probability of crack initiation, the results of the next section indicate that the elimination of cracks would probably require a pad with stiffness less than about 500,000 pounds per inch. This is the value obtained by the 9 mm pad in new condition.

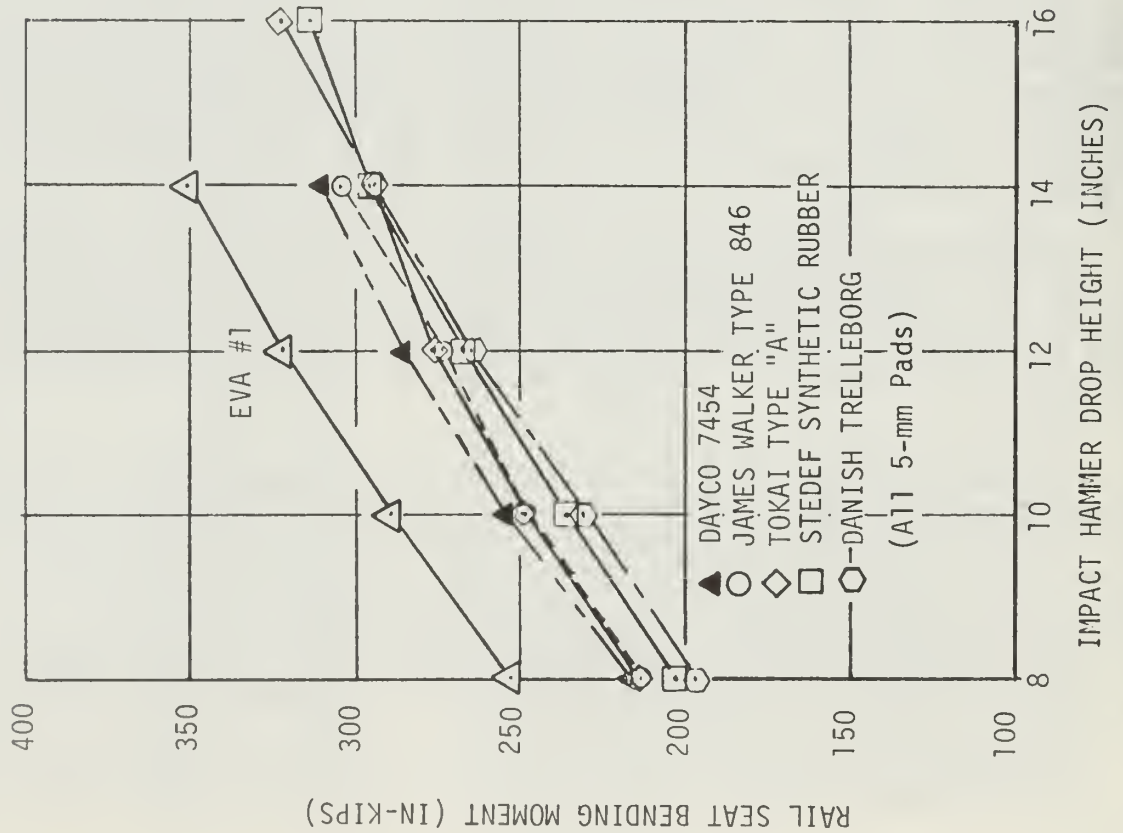
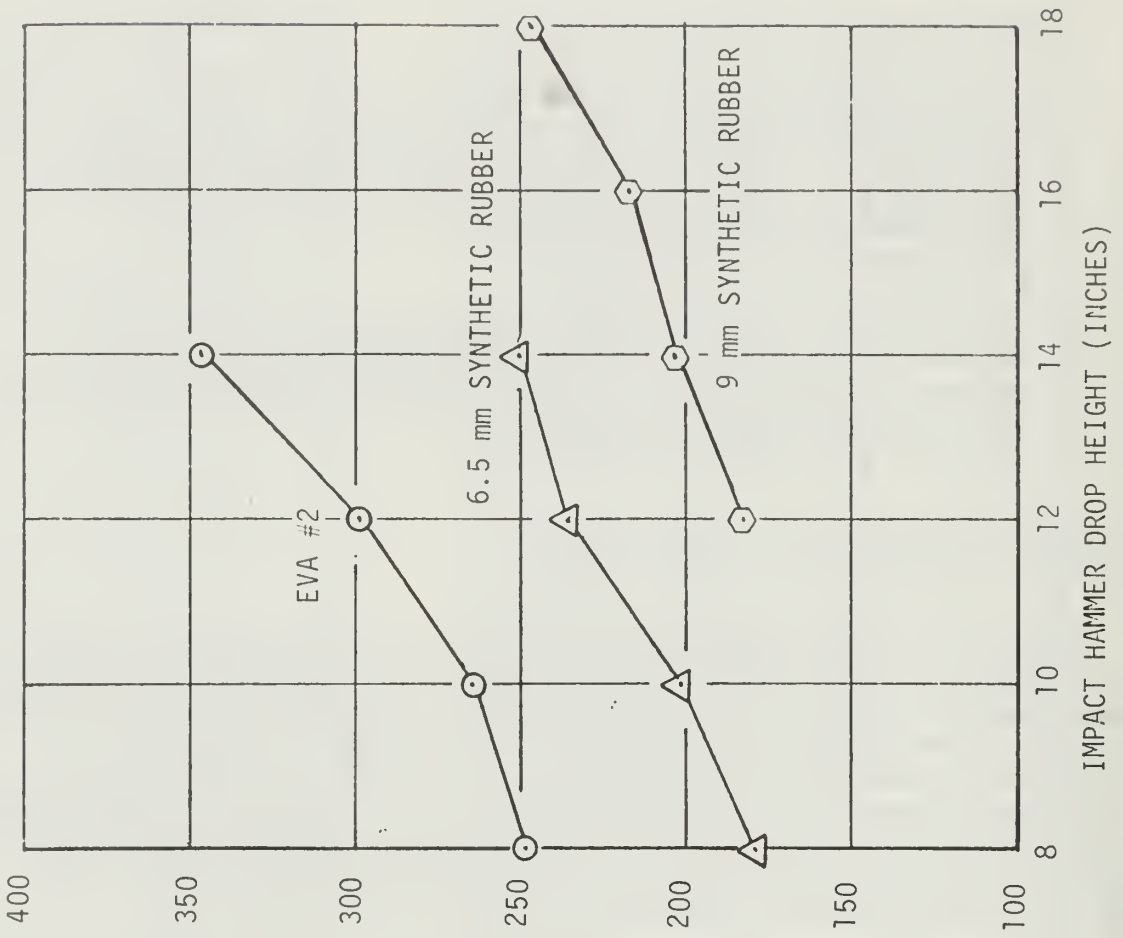


FIGURE 4-5. EFFECT OF TIE PAD SUBSTITUTIONS ON IMPACT STRAIN AT TIE RAIL SEAT

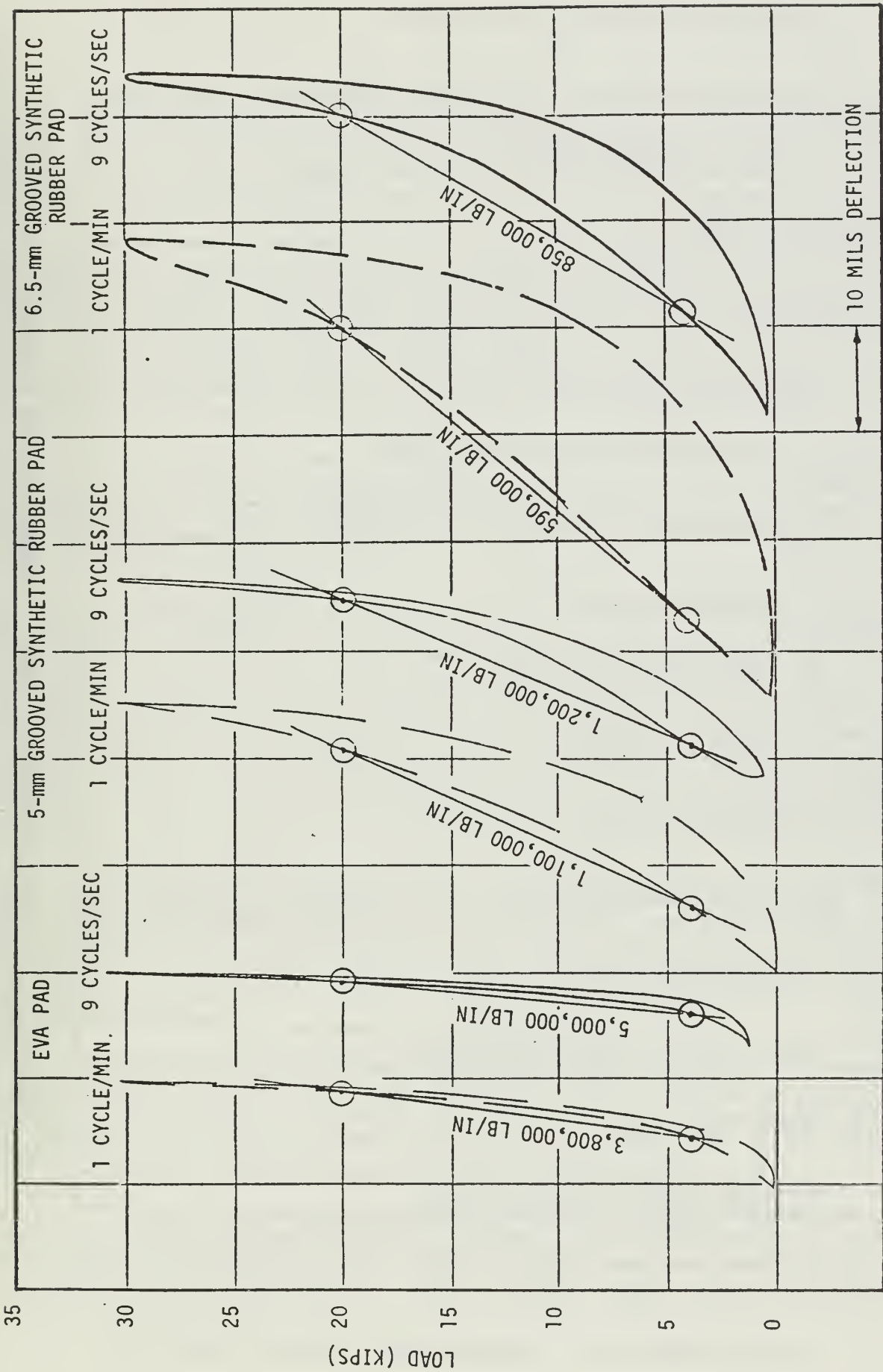


FIGURE 4-6. TYPICAL LOAD-DEFLECTION PLOTS FROM TIE PAD STIFFNESS TESTS

COMPRESSIVE STIFFNESS (MILLION LB/IN)

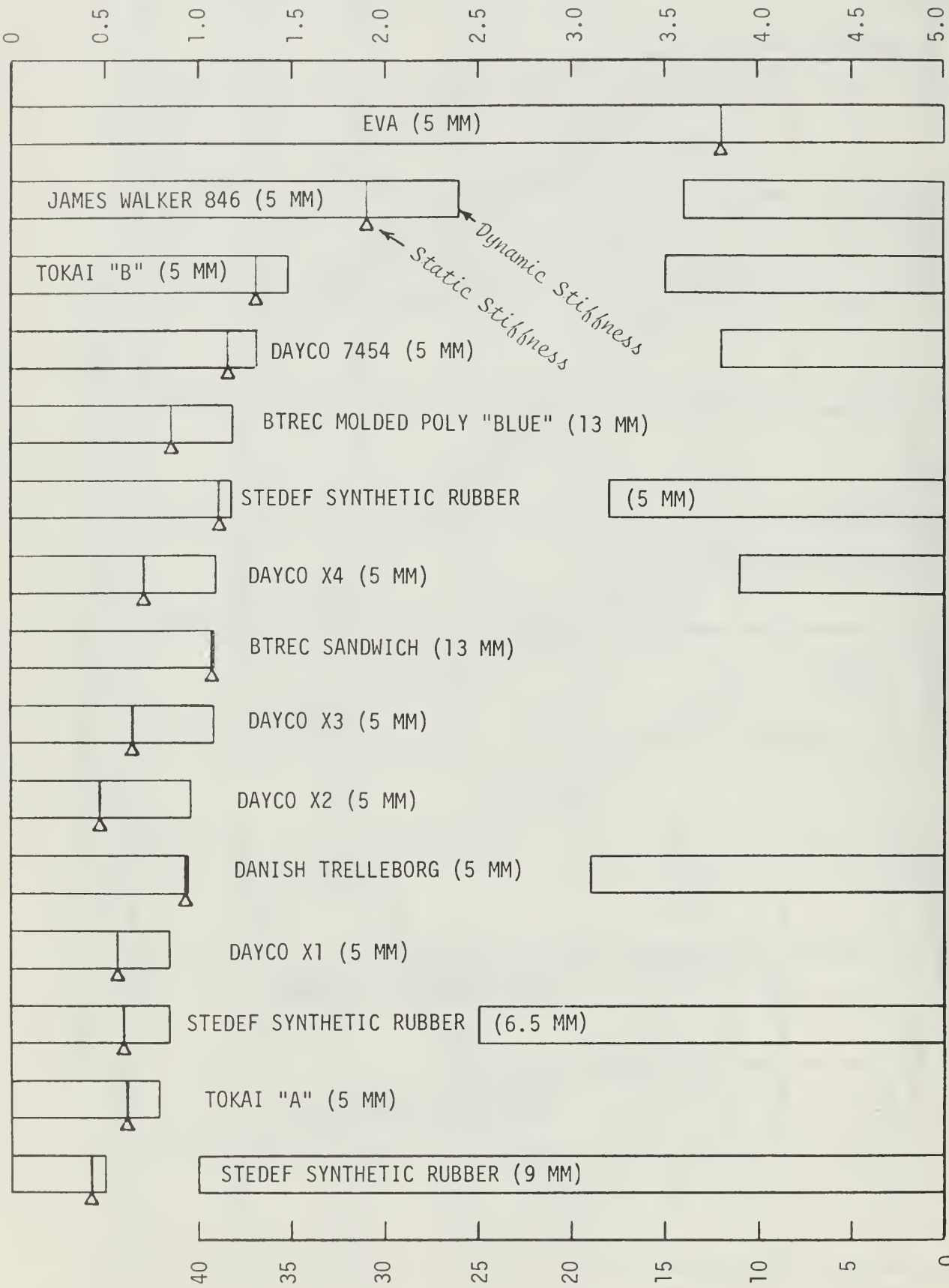


TABLE 4-1. TIE PAD STIFFNESS AND IMPACT ATTENUATION RATES FROM BASIC TESTS

PERCENT ATTENUATION OF BENDING MOMENT RELATIVE TO EVA PAD

Additional Strain Attenuation Tests. Additional strain attenuation tests were sponsored by a pad manufacturer (Dayco Corp.). With the sponsor's permission, the tests are included here because they reveal important facts about the relationship between pad stiffness and strain attenuation. The test procedure was essentially identical to that for the first series of tests.

A summary of dynamic pad stiffness (10-Hz load rate) and strain attenuation is shown in Table 4-2. The previously used EVA Pad #2 was again tested to provide a reference against which the attenuations of the flexible pads were compared. However, the dynamic stiffness measurements revealed that this pad has stiffened substantially as a result of the original laboratory impacts. The original stiffness of approximately 5 million lb/in had increased to 8.4 million lb/in. Although there was no obvious physical damage to the pad, the impacts had apparently produced a permanent set.

To obtain a reference which more closely matched that for the first tests series, a new EVA pad was also subjected to the impact and dynamic stiffness tests. This pad demonstrated strain attenuation of 6 percent relative to the used EVA pad, and its dynamic stiffness was 4.3 million pounds per inch vs. 8.4 for the used pad.

A previously used 6.5-mm SBR pad was also included in the tests. This pad had stiffened from 850,000 lb/in to 1.1 million lb/in but showed an improvement in performance against the original (but now much stiffer) EVA pad, from 25-percent strain attenuation (Table 4-1) to 29-percent (Table 4-2). Relative to the new EVA pad, the SBR pad attenuated strain by 23 percent. A somewhat reduced performance against the new EVA pad could be expected, since the new EVA pad was about 10-percent more flexible than was the original pad in new condition. These results indicated that the strain attenuation capability of the SBR pad was approximately the same as that found in the first series of tests, although its dynamic stiffness had increased by 29 percent.

The results for seven variations of Dayco tie pads are also shown in Table 4-2. Although the dynamic stiffness of these pads varied widely, the most important parameter regarding impact attenuation was pad thickness. The 5.5-mm pad performed poorly relative to the other flexible pads, all of which had 6.5-mm thickness. Relative to the new EVA pad, a maximum strain attenuation rate of 28 percent was found for the pad marked Dayco #2. All of the Dayco pads were new.

The additional tests demonstrate that dynamic stiffness as currently measured provides a very unreliable measure of strain attenuation capability. However, the stiffness measurements are useful as an indicator of the change in condition which may have taken place in a given pad as the result of testing or service.

It should be noted that the stiffness of a new pad can increase significantly over the expected life of the pad. JNR results show an increase of two-thirds in the stiffness of the Tokaido Shinkansen Type A pads over an expected 10-year life (from 90 tons/cm or 500,000 pounds/inch to 150 tons/cm or 840,000 pounds/inch) [7].

COMPRESSIVE STIFFNESS (MILLION LB/IN)

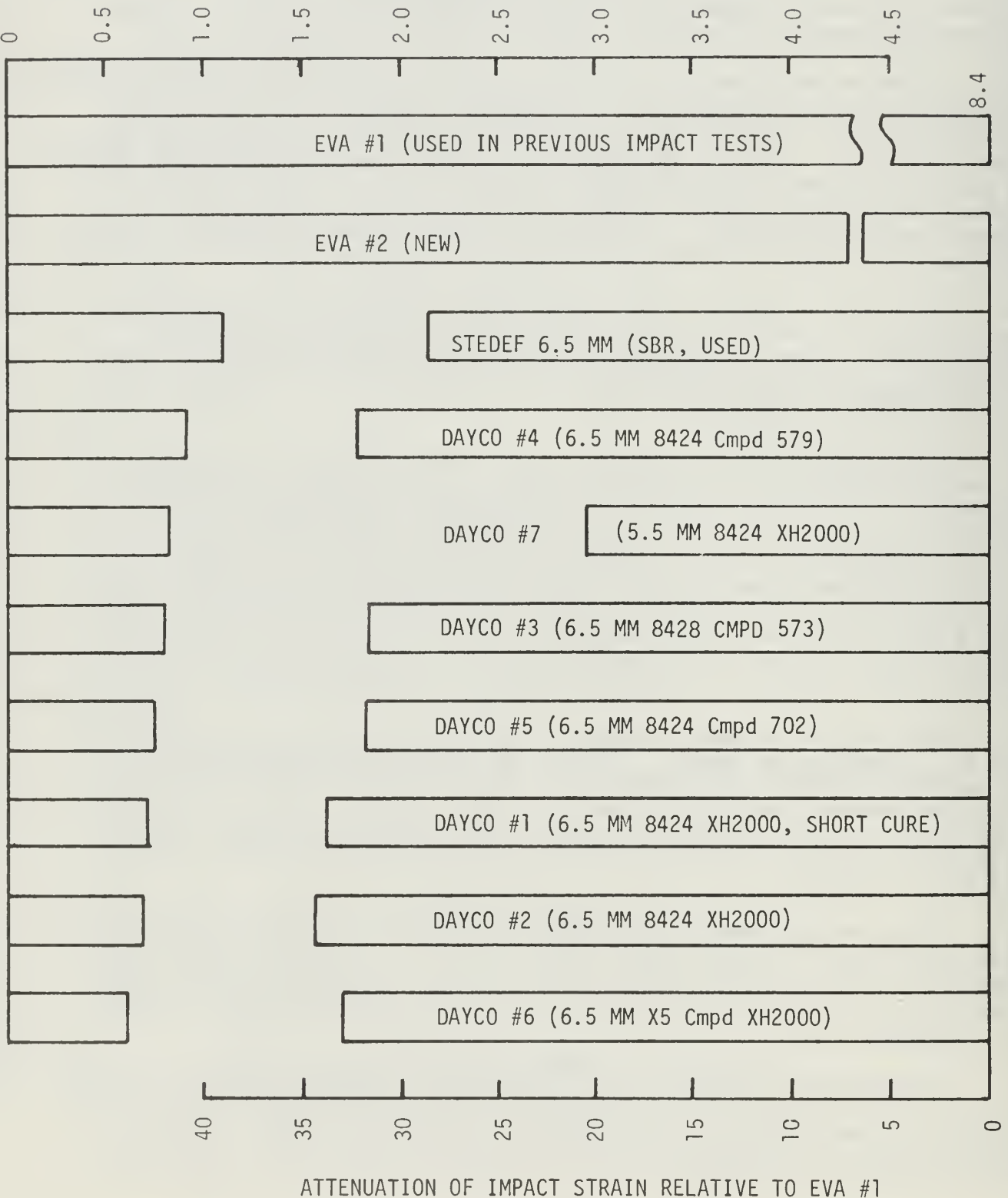


TABLE 4-2. TIE PAD STIFFNESS AND IMPACT ATTENUATION RATES FROM ADDITIONAL TESTS

Tests Under Worst-Case Impacts

The next objective was to determine whether a practical level of pad stiffness could be expected to prevent cracks in a tie subjected to the highest level of impact bending moment (600 inch-kips) measured in track. However, the drop height required to deliver the maximum strain with the EVA pad was not known and could not be determined without cracking the tie and distorting the measurement of bending moment. Therefore, a test series 3 was conducted in the following sequence:

- a. Tests with the EVA #2 pad at drop heights of 8 and 14 inches, to reestablish a baseline after an interim of two weeks
- b. Tests with the 9 mm and 6.5 mm Neoprene pads, respectively, up to about 400 inch-kips of dynamic bending moment (possibly above the crack threshold)
- c. Final tests with the EVA #2 pad at drop heights of from 14 to 20 inches, where the bending moment level exceeded 600 inch-kips.

The data for this test series 3 are shown in Figure 4-7, along with directly comparable data from Figure 4-5 (Test 2).

The results for Tests 2 and 3 differ by a general upward shift in the bending moment level produced with the same pad and drop height. There are two probable causes for this shift:

- a. Pad stiffening. The previously discussed manufacturer's tests demonstrated that the EVA pad stiffened as a result of the impact testing.
- b. Tie cracking. Evidence of cracking consisted of a continuous increase in dynamic strain level for successive drops at the same height, during most Test 3 drops with the EVA pad. Only the dynamic strain component was measured, since the gage bridge was rebalanced after each drop. Scatter increased as the maximum bending moment levels were approached. Examples of the range of bending moments occurring for successive drops at a given height are included in the curve marked "End Test 3."

An additional major increase in comparative dynamic strain levels can be seen in the test series 3 with the EVA #2 pad. Fourteen-inch drops were conducted immediately before and after tests with the flexible pads. The two sets of drops produced an increase in the mean peak bending moment of 65 inch-kips. Such an increase can only be attributed to the development of a crack under the gage coupon. Since the faces of this tie were not Stresscoated, there was no visual identification of a crack during these tests, although the faces were inspected regularly.

Although cracking apparently existed during all series 3 tests and resulted in upward drift of the bending moment levels from equal impacts, several pertinent observations can be made about the data in Figure 4-7:

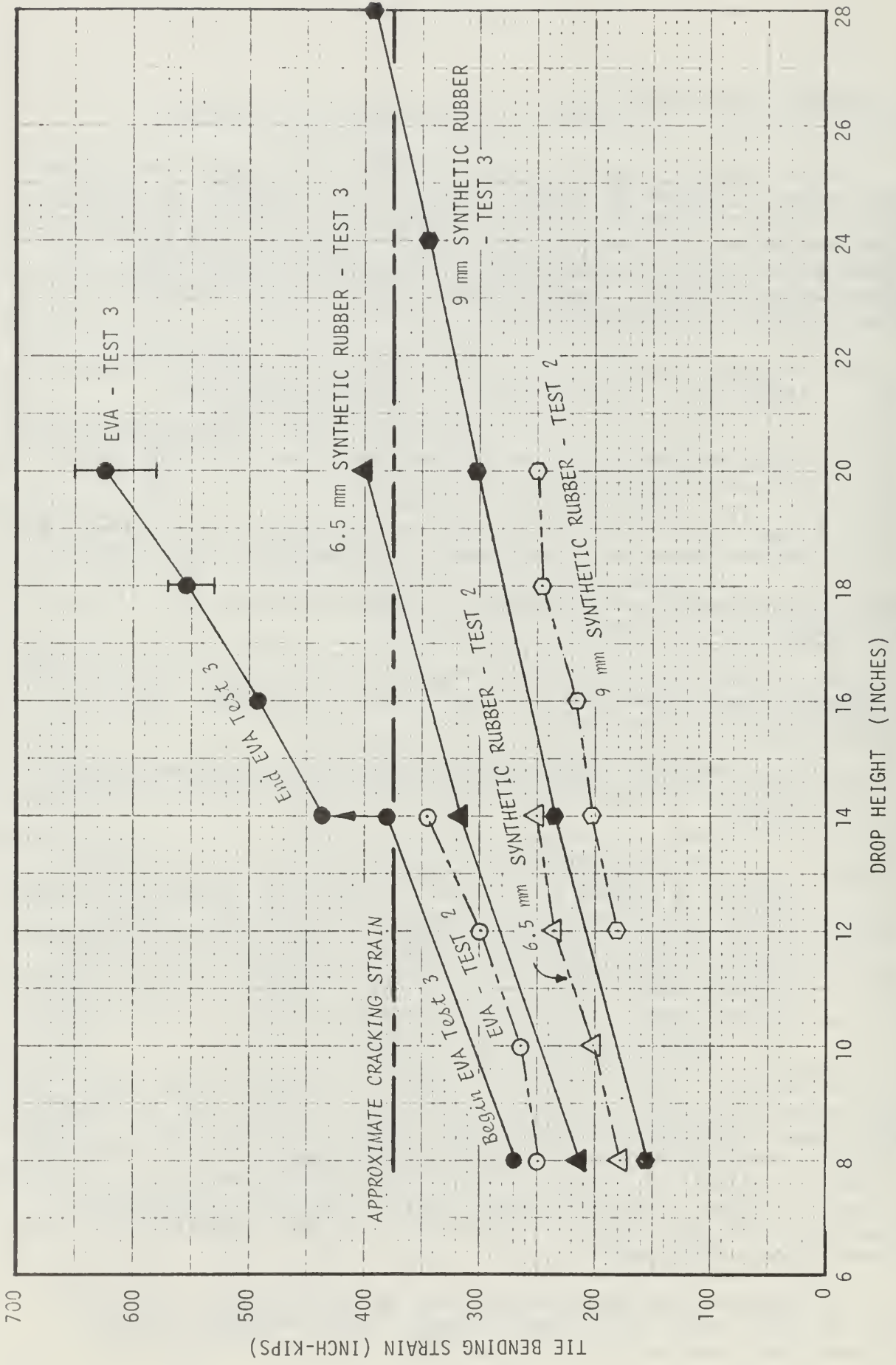


FIGURE 4-7. TIE BENDING VS. DROP HEIGHT FOR TESTS UP TO MAXIMUM SIMULATED TRACK INPUT

- a. The following combinations of pad and drop height produced approximately equivalent levels of mean peak bending moment:
- (1) EVA pad at 14 inches (overall mean = 408 inch-kips)
 - (2) 6.5 mm pad at 20 inches (400 inch-kips)
 - (3) 9 mm pad at 28 inches (392 inch-kips)
- b. A linear projection of the curve marked "EVA - TEST 2" would exceed 600 inch-kips at the 28-inch drop height. Therefore, from the most conservative assessment of the data, it can be projected that the 28-inch height with the EVA pad simulates the worst-case condition measured in track (600 inch-kips). It is possible that the strain magnification, which is evident in the post-crack EVA data, is also present in track measurements. If so, the worst-case tie impact loads could be reproduced by the 20-inch drop height with the EVA pad.
- c. It can be concluded from the data that a pad equivalent to the 9-mm pad in new condition (500,000 lb/in = 90 tons/cm) is the best choice to prevent cracks under all but the most extreme conditions. Also, a pad having the stiffness provided by the 6.5-mm pad (850,000 lb/in = 133 tons/cm) should prevent cracks under all but the most extreme conditions.
- d. The rate at which a pad stiffens over its lifetime depends on the pad material and the environment. These must be considered. The JNR found that the Tokaido Shinkansen Type A pad, with a nominal stiffness of 90 tons/cm (500,000 lb/in) in new condition, deteriorated to 150 tons/cm (840,000 pounds/inch) in the expected 10-year life of the pad [7]. This constitutes a stiffness increase of two-thirds. In addition, some pad materials stiffen as the temperature drops. The stiffness of the pad material should be examined at the lowest temperature expected in the Northeast Corridor environment--about -20° F. These effects make it imperative to use materials which retain their elasticity and to obtain the lowest practical stiffness of the pads in new condition. The stiffness of 90 tons/cm (500,000 lb/in) is the lowest value used by the JNR for pads of 5-mm thickness.

4.4 Destructive Tie Tests

Noninstrumented, destructive impact tests were conducted on three ties to determine the range of drop heights required to produce advanced cracks of the type found in track. While two of the ties were of the type used on the Northeast Corridor, the third was made with concrete modified with a latex polymer. The latex modification permits a smaller cross section for equivalent strength, since the concrete can sustain higher strains without cracking. The rail seat areas of each tie face were Stresscoated. One end of each tie was impacted at heights varying from 14 to 36 inches using 2-inch increments from 14 to 20 inches and 4-inch increments thereafter.

An impact procedure was developed during the tests. In most cases, a detectable crack extension would emerge after 3 to 10 repetitions at a given drop height. Further repetitions at the same drop height would produce relatively little additional extension. Therefore, a procedure was adopted in which 10 drops were made at each height, with inspections after the third and tenth drops.

Crack progression under the impacted rail seats is shown for three ties in Figure 4-8. Cracks were first detected at the drop height of 16 inches on the two NEC ties (and earlier on the RT 7SS tie) and at 18 inches on the latex modified BW-3 tie. Total crack height for the BW-3 tie fell slightly below that of the mean of the two NEC ties. Further tests would be required to determine whether the differences in crack initiation height or total height constituted a statistically significant difference in crack resistance.

After completion of the first test (Tie 0432), it was discovered that cracks had developed at the nonimpacted rail seat as well as at the impacted rail seat. Subsequent tests produced the same result. In each case, total crack height on the nonimpacted end was 70 to 80 percent of the total crack height on the impacted end. Maximum crack heights for the two ends of each tie are compared in the box of Figure 4-8. This result demonstrates that a stress wave propagates across the tie with little attenuation of the initial amplitude and reinforces the assessment that the tie acts as a free-free beam.

It should be pointed out that without the Stresscoat applied to the tie faces, few if any of the laboratory cracks would have been detected. In contrast, cracks on ties in track were visible either with an alcohol spray or with no surface treatment. It can be concluded that service-produced cracks are well-developed before they become visible, and that repeated working under normal service loads causes the cracks to widen.

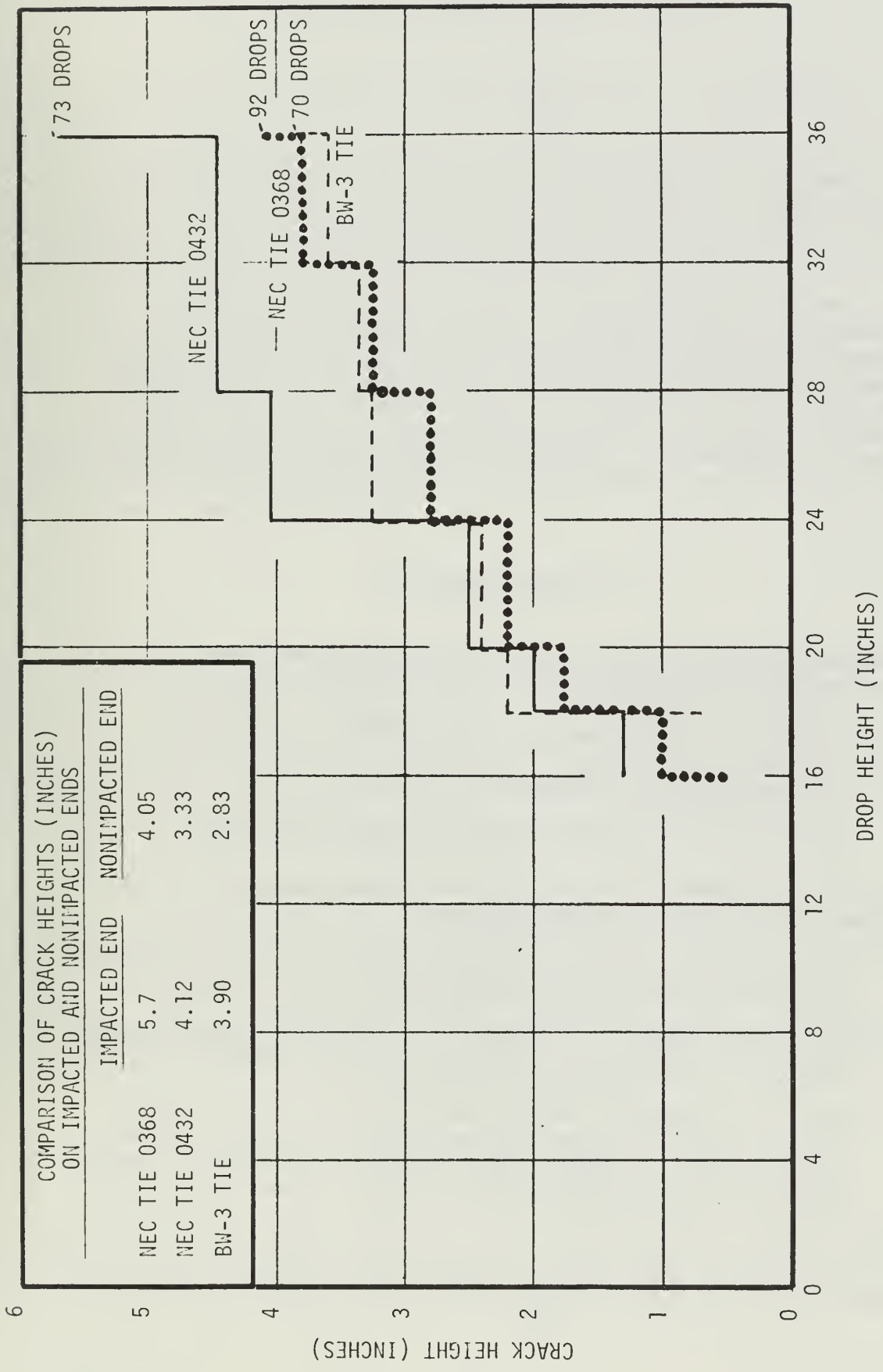


FIGURE 4-8. TIE CRACK DEVELOPMENT VS. IMPACT HAMMER DROP HEIGHT

5.0 TRACK MEASUREMENTS TO VERIFY THE EFFECTS OF PAD STIFFNESS ON IMPACT

5.1 Introduction

The laboratory tests demonstrated that major reductions in pad stiffness could significantly attenuate tie impact bending moment. To verify that the results of the one-tie laboratory test arrangement could be reproduced in track, a field test program was again conducted on the NEC track at Aberdeen, Md. An instrumented zone of 5 ties was established within a segment of 50 ties where pad substitutions were made. Measurements included vertical wheel/rail load, tie bending moment at the rail seats, rail and tie accelerations, and vertical rail/tie deflection. As described in the following sections, the tests verified the results of the laboratory bending moment attenuation tests. The major cause of the worst-case impacts was identified. On the basis of the results, recommendations are made for both a tie pad substitution and a program to eliminate the "worst case wheel" conditions. It is concluded that only this combination can eliminate the further development of cracks.

5.2 Pad Selection

From the laboratory tests, three types of pads were selected for successive substitution in the test zone. These were:

- a. the 6.5-mm grooved synthetic rubber pad
- b. the 5-mm grooved synthetic rubber pad
- c. the 5-mm EVA pad (current NEC track construction pad).

The dynamic stiffness plots for these pads were shown previously in Figure 4-6. Each pad was selected for a specific reason:

- a. The 5-mm EVA pad was required for control, to provide a direct comparison with the effectiveness of the other two pads.
- b. The 5-mm synthetic rubber pad provided the best bending moment attenuation among laboratory test pads of "standard" thickness.
- c. The 6.5-mm synthetic rubber pad provided the most effective strain attenuation among pads which might be used with the current Pandrol fastener clip. A thicker pad was not selected because of the incompatibility with the current Pandrol clips.

5.3 Test Layout

The 5-tie instrumented zone is illustrated in the schematic of Figure 5-1 and in the top photo of Figure 5-2. The location was selected after careful inspection to make certain that all 5 ties were uncracked. It was planned to install the most flexible pad first, followed by the intermediate pad and finally the rigid EVA pad. This would minimize the chance of a crack developing during the test period. Cracks cause a small amount of permanent strain on the strain gages, but do not appreciably change the slope of a load-vs-bending strain calibration curve (below the prestress limit).

Alternate pads were installed in a 50-tie segment surrounding the instrumented zone. The installations were made over 50 ties to minimize the dynamic effects of the transition between the flexible test pads and the current rigid production pads. Since the track carried southbound traffic exclusively, test pads were installed on 40 ties upstream (north) of the instrumented zone and on 5 ties downstream of the zone. Only 40 of the 6.5-mm flexible pads were available--enough for 20 ties. To fill out the upstream portion of the 50-tie segment, the 5.0-mm intermediate pads were used for both the first and second test series.

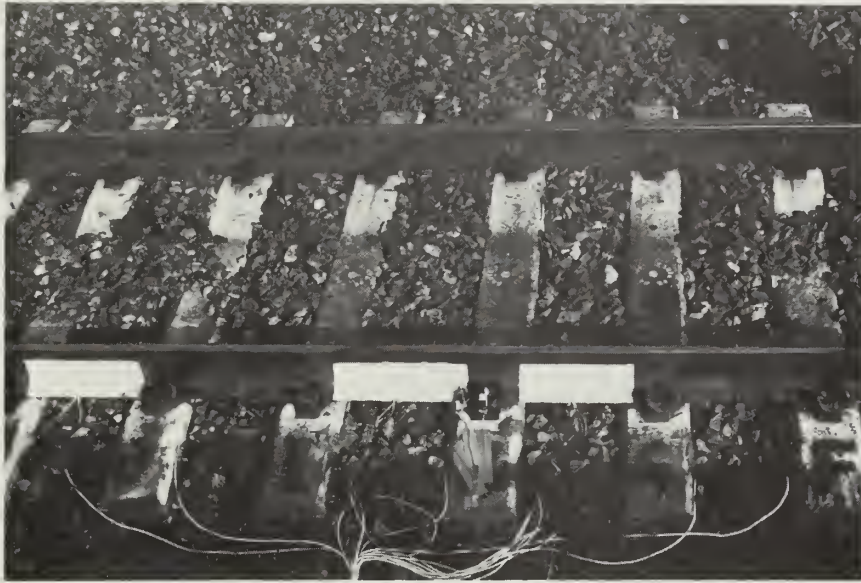
5.4 Test Procedure

The three types of new pads were installed in the 50-tie segment for periods of 5 days each. The most flexible 6.5-mm pad was installed first, followed by the flexible 5-mm pad, and finally by the rigid EVA pad currently used for Northeast Corridor concrete tie construction. For each installation, data were collected from approximately 5000 total axles, of which approximately 50 percent were passenger axles. Most of the passenger traffic passed the site at speeds between 70 and 100 mph, while most of the freight traffic fell within the speed range of 40 to 60 mph.

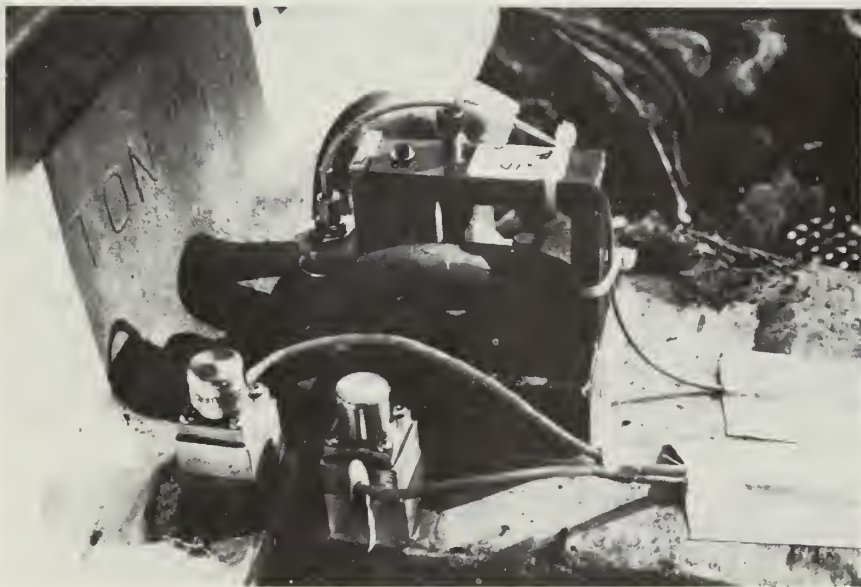
In the instrumentation van, the data were stored on analog tape and processed to identify the peak values of wheel/rail load and tie bending moment produced by the passage of each wheel. Because of the wide band of frequency response required (1200 Hz), analog peak detection was used. The captured peaks were converted to digital values and stored on digital cassettes. Peak values from each train pass were tabulated and printed. After completion of the tests, the data from the digital cassettes were processed at Battelle to produce statistical summaries.

5.5 Instrumentation

Tie bending strain coupons were installed under the west rail on the 5 consecutive ties and under the east rail on the center tie. This provided a zone length slightly greater than a wheel circumference; thus for one rail, all wheel impact conditions would be identified at some point in the zone.



(a) Instrumented Zone



(b) Deflection and Acceleration Transducers

FIGURE 5-2. INSTRUMENTED TRACK ZONE AND TRANSDUCERS

The single gage on the opposite rail provided an indication of the symmetry of impact strains occurring on the one center tie. The strain coupons were calibrated to measure tie bending moment, as described in Appendix A.

Vertical wheel/rail load circuits were installed in three cribs, as shown in Figure 5-1. These circuits were required for two purposes: (1) to serve as wheel detector sensors, and (2) to capture a representative sample of the wheel impact loads occurring in the test zone. Only one rail was instrumented because the 1980 tests had demonstrated that the populations of loads on the two rails were very nearly identical.

Vertical accelerations were measured on the top surface of the tie and on the adjacent rail base as shown in Figure 5-2 (a). The magnitude of the transfer function between the two signals provided an alternate indication of the relative attenuation from each of the test pads. Vertical rail-to-tie deflection measurements were made on the field and gage sides of a single rail seat, as shown in Figure 5-2(b). The location of the acceleration and deflection transducers was varied between the end and center ties of the 5-tie zone. Acceleration and deflection data were collected for a portion of the traffic passing over each type of pad.

Five linear strain gages were installed at intervals of 10 inches along the lower edge of one tie face of the center tie. These gages defined the variation of strain over the length of the tie and the absolute magnitude of strain produced by impact loads.

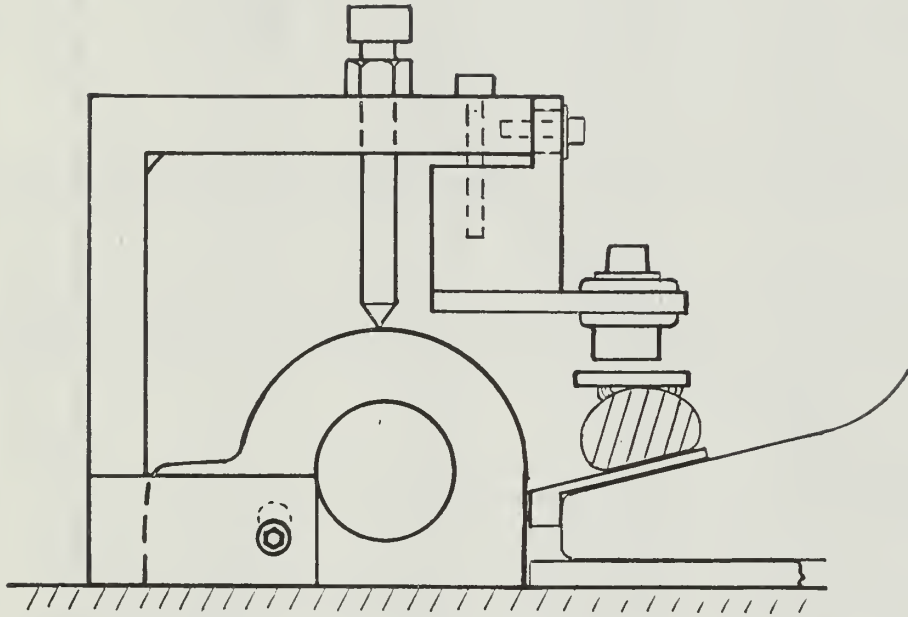
The installation and calibration of transducers and the processing of collected data are described in Appendix A.

5.6 Test Results

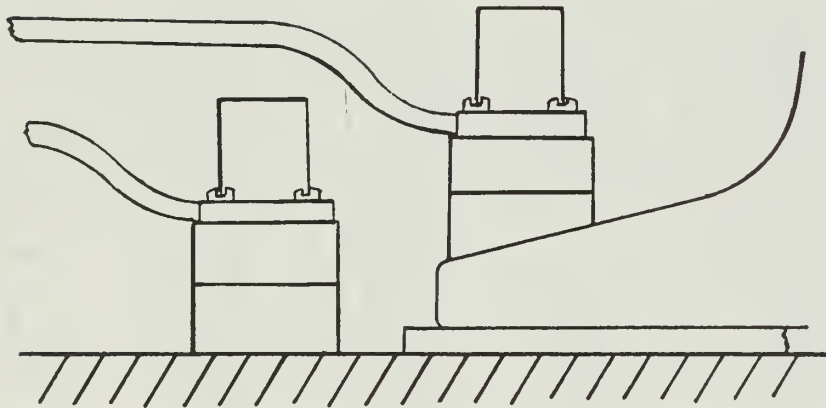
From the 5 days of data collected with each of the three test pad installations, statistical summaries of peak tie bending moments and vertical wheel/rail loads were compiled for an average tie location and an average load measurement site (crib). The data show the influence of tie pad stiffness on impact load conditions for several classifications of traffic and ranges of speed. The essential results of the data compilations are discussed as follows.

The Effects of Pad Substitutions on Tie Bending Moments and Vertical Loads

All Passenger Traffic. The attenuation of bending moments by pad substitutions can be seen in Figure 5-4(a). Bending moments above the "cracking threshold" of 375 inch-kips occurred with the following frequencies:

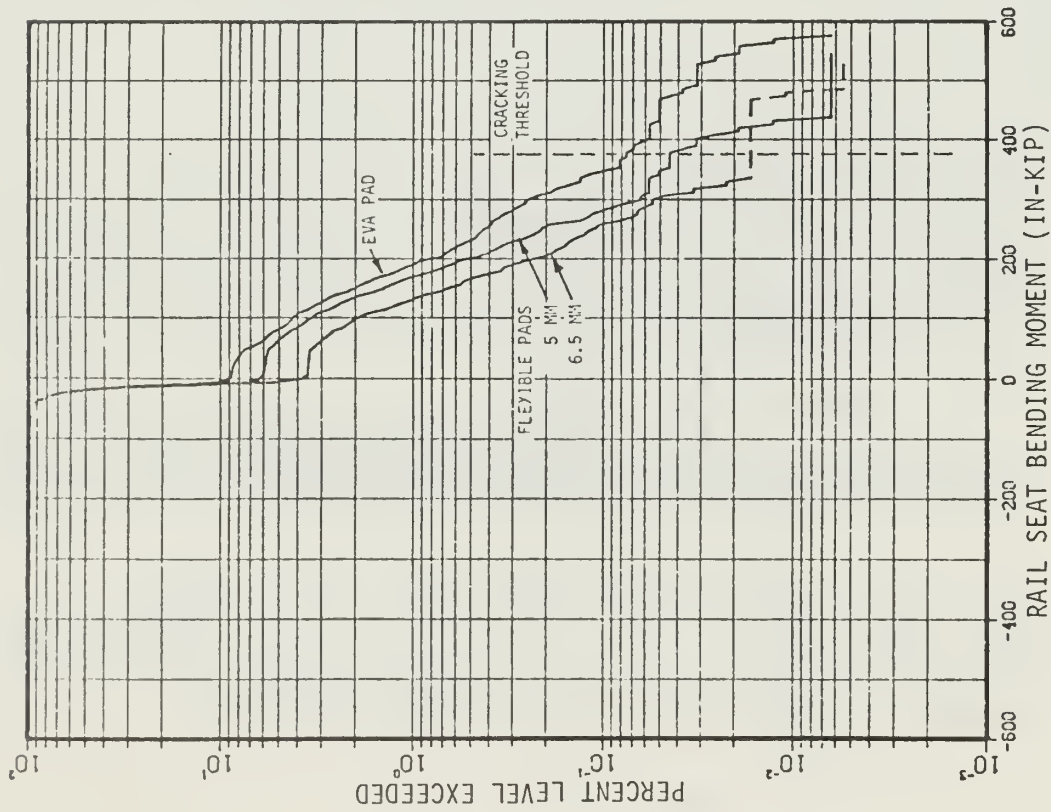


(a) Vertical Rail Clip Deflection

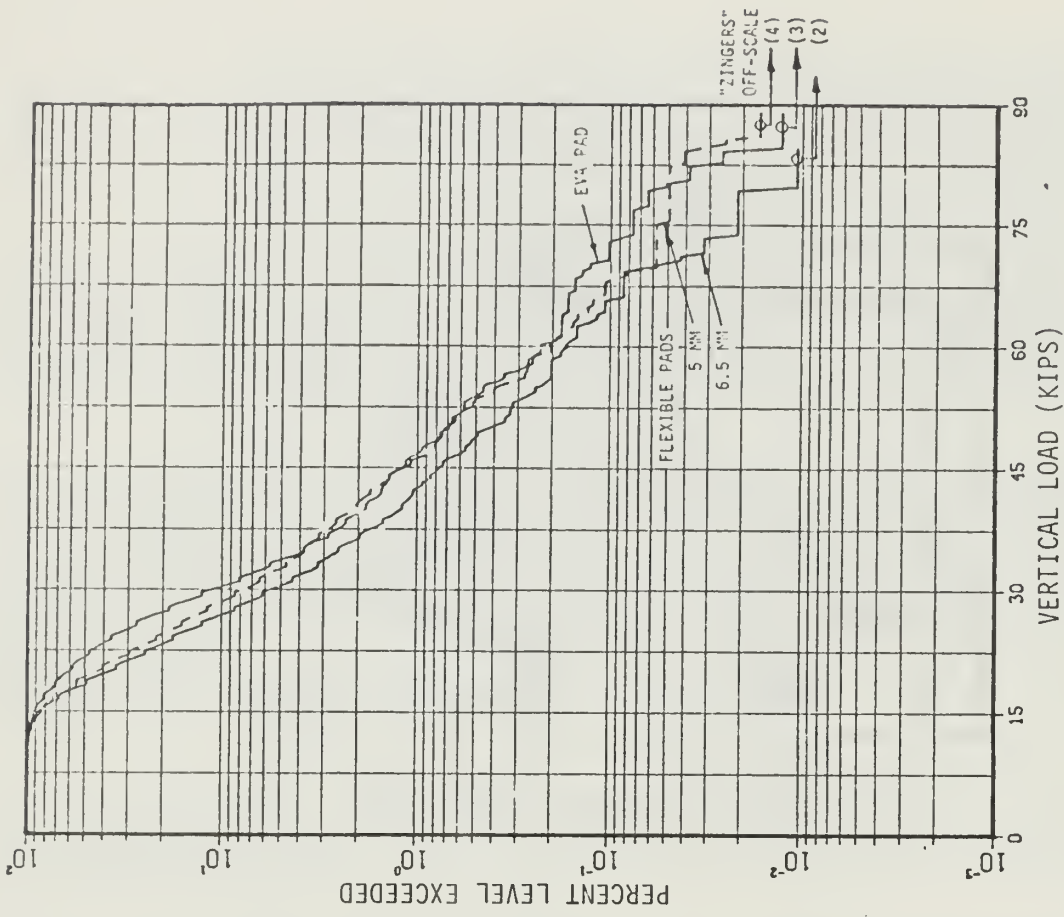


(b) Rail and Tie Accelerations

FIGURE 5-3. PLACEMENT OF DEFLECTION AND ACCELERATION TRANSDUCERS



(a) EXCEEDANCE LEVELS OF TIE BENDING MOMENT



(b) EXCEEDANCE LEVELS OF VERTICAL LOAD

FIGURE 5-4. EXCEEDANCE LEVELS OF TIE BENDING MOMENT AND VERTICAL LOAD FOR NORTHEAST CORRIDOR PASSENGER TRAFFIC ABOVE 70 MPH ON EACH OF THREE TIE PADS

<u>PAD TYPE</u>	<u>EXCEEDANCE FREQUENCY</u>	<u>AVERAGE NO. OF DAYS BETWEEN THRESHOLD EXCEEDANCES</u>
EVA	1/1300	2.6
5-mm Flexible	1/2200	4.4
6.5-mm Flexible	1/14,000	28

The number of days between threshold exceedances stated above are based upon the average number of passenger axles passing over the test site during the test period: approximately 500 axles per day.

While the most flexible pad did not eliminate the occurrence of bending moments above the cracking threshold, these events were reduced significantly. This reduction could minimize both the requirements for improvements in wheel conditions and the damage from normal wheels passing over track defects.

Figure 5-4(b) shows the exceedance levels of vertical wheel/rail loads produced by passenger traffic. While the results for the EVA and 5-mm flexible pads are nearly identical, those for the 6.5-mm pad show a significant reduction in the frequency of occurrence of very high (cracking-producing) loads. By matching exceedance percentages from the cracking threshold of bending moment the cracking threshold of vertical wheel/rail load can be placed at about 80 kips.

It should be noted in Figure 5-4(b) that for each type of pad, a few events produced such high-strain levels that they saturated the data system. It is unlikely that any pad within the practical range of thickness could attenuate such events sufficiently to prevent cracking. These very low-probability events point to the need to an improvement in wheel tread conditions along with the use of a more flexible pad.

All Freight Traffic. Figure 5-5 illustrates the exceedance levels of tie bending moment and vertical wheel/rail load which were produced by freight traffic loading on each type of pad. There were no occurrences of tie bending moments above the cracking threshold. The influence of tie pad stiffness was much less evident than with passenger traffic. The tie bending moment results conformed to the expected trend, showing a slight reduction of maximum values with reduction in tie pad stiffness. However, the trend was reversed in the vertical load results, where the 6.5 mm flexible pad produced the highest levels of loads in the "impact" range (above 45 kips). This may be an artifact of the relatively small population of freight traffic which is typically less consistent from one day or week to the next, especially when compared with the highly regular and repetitive nature of the passenger car population.

Amfleet vs. Conventional Cars. Most of the Northeast Corridor passenger traffic can be separated into two categories according to the ages of the cars. The older Heritage cars, called "conventional" equipment, were inherited by Amtrak when it assumed passenger service from the railroads. The newer Amfleet cars have been built since 1975.

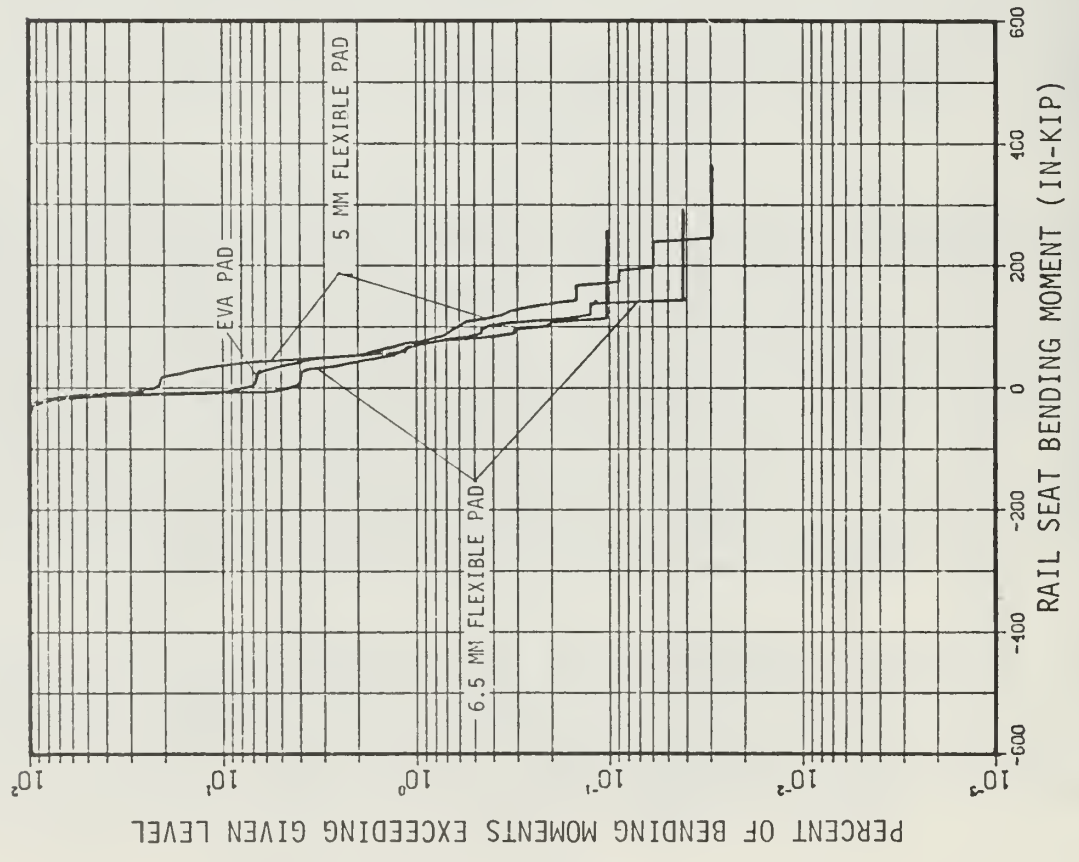
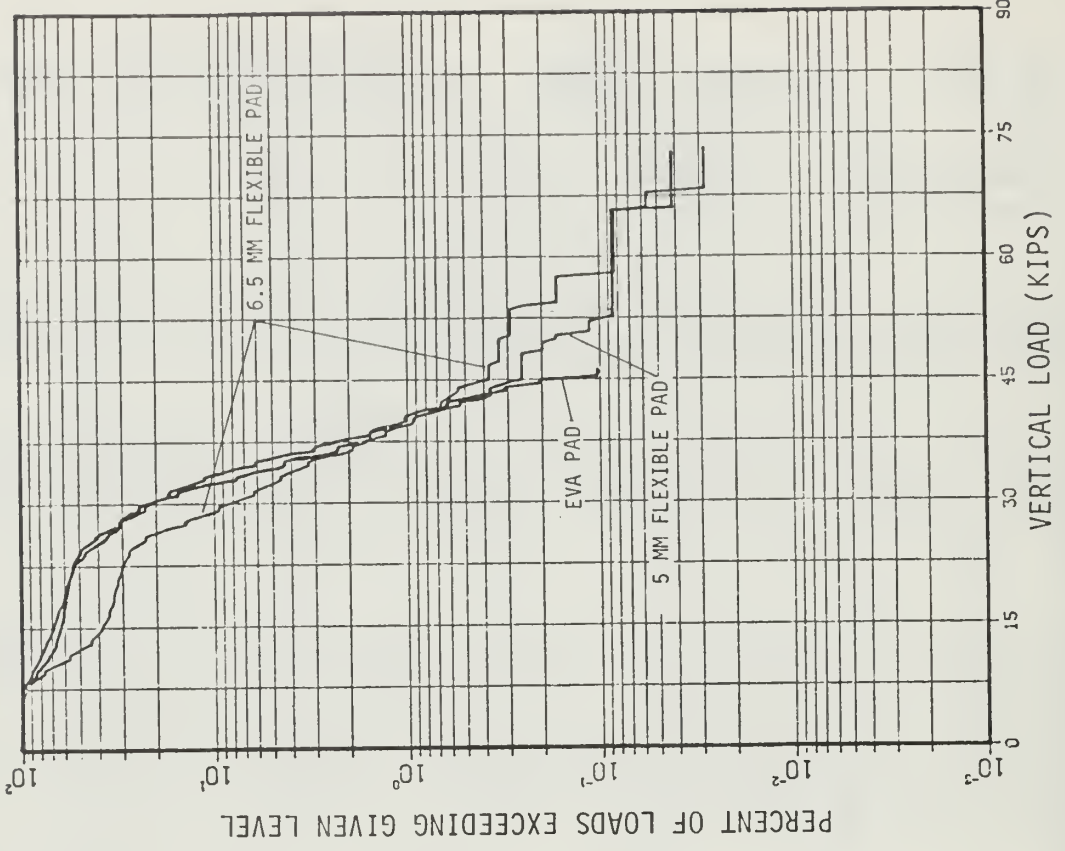


FIGURE 5-5. EFFECT OF TIE PAD STIFFNESS ON RAIL SEAT BENDING MOMENT AND VERTICAL LOAD, ALL FREIGHT TRAFFIC

Although relatively fewer in number, the powered Metroliner cars represent a third classification of passenger cars. Results for these cars were not compiled separately because they did not display serious impact conditions. This can be attributed to the fact that powered Metroliner cars are inspected more often because they are classified as electric locomotives. Wheel conditions comparable to those of the unpowered passenger cars are not allowed to develop. It should also be noted that locomotives pulling the unpowered equipment did not show serious impact conditions, although their average wheel loads were much higher than those of the cars. All compilations of data for passenger cars exclude locomotives.

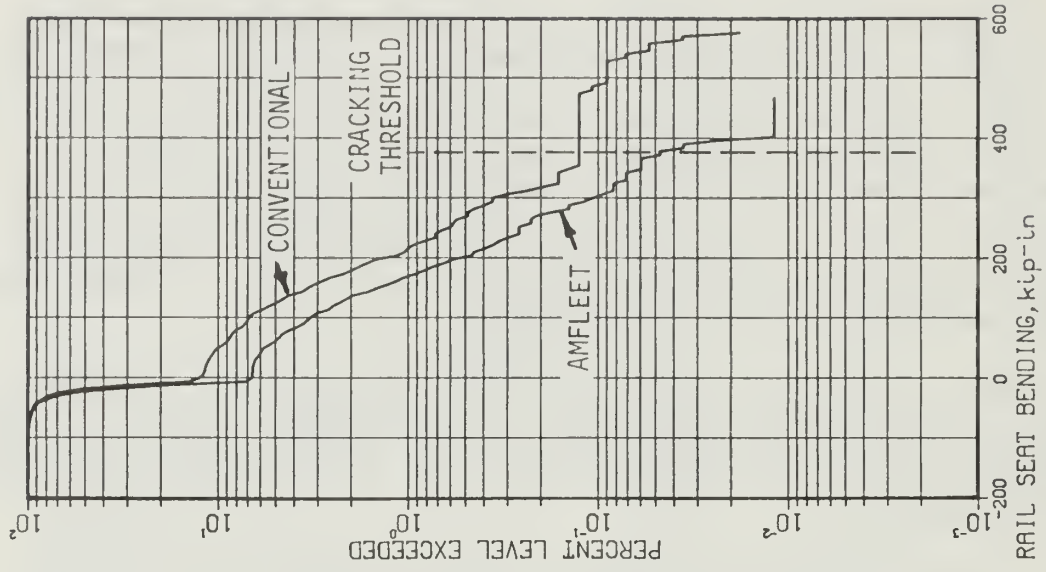
Figure 5-6 compares tie bending moment data collected for Amfleet and conventional passenger cars during each of the three test pad installations. A few extreme values which exceeded 600 inch-kips are not shown because they represent exceptions to the trends defined by the cumulative distributions. The results show that:

- a. For the EVA and 6.5-mm pads, the conventional cars produced consistently higher overall strain levels.
- b. This trend did not occur with the 5-mm flexible pad, where the data for the two car types were nearly identical down to the frequency-of-occurrence level of 0.1 percent. The Amfleet cars produced the highest peak bending moment with the 5-mm pad.

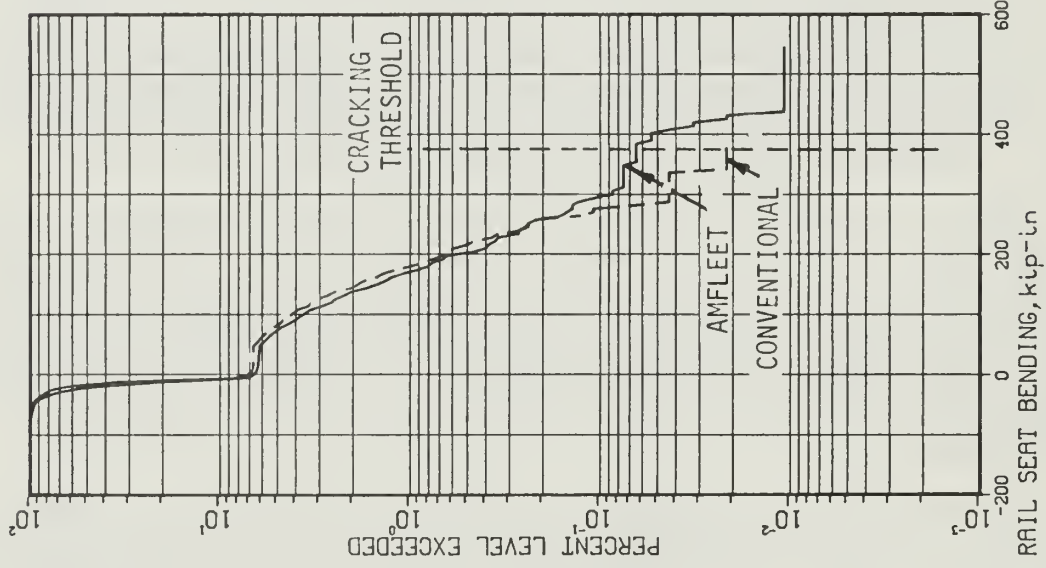
Figure 5-7 repeats the data of Figure 5-6 with arrangement of the data by car type. It can be seen that for the Amfleet cars, the results for the EVA and 5-mm flexible pads were nearly identical, while for the conventional cars, the results for the 5-mm and 6.5-mm flexible pads were nearly identical. This indicates that the dynamic characteristics of the vehicles contribute to the strains produced in the tie, and that only pads with stiffness equal or below that of the 6.5-mm pad can be expected to consistently reduce tie damage.

Figures 5-8 and 5-9 show vertical wheel/rail load data in formats corresponding to those of the preceding two figures. In Figure 5-8 it can be seen that vertical loads from conventional cars were consistently higher than those of Amfleet cars for all 3 pad types. However, Figure 5-9(a) verifies the trend of Figure 5-7(a) in which the 5-mm flexible and EVA pads display approximately equal performance. This emphasizes the necessity to install pads with the lowest practical dynamic stiffness.

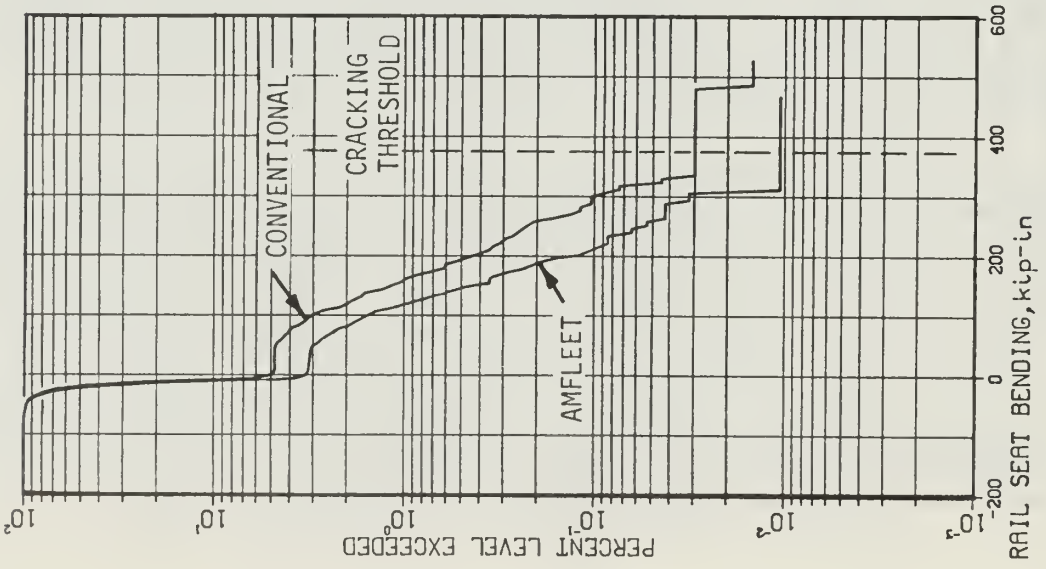
For conventional passenger cars, the vertical loads measured with the EVA and 6.5-mm flexible pads are divided into by 10-mph speed bands in Figure 5-10. These cars consistently experienced maximum responses in the speed band between 80 and 90 mph. Conversely, no clear trend with speed could be identified for Amfleet cars. This difference in response appears to be associated with relative size or wavelength of the tread defects observed on the two types of vehicles. Most defects on the Amfleet wheels were smaller spalls and short "slid flats" which are higher in frequency content and have less energy in any one impact. On the contrary, the conventional cars tended to develop longer wavelength, higher energy impacts which apparently excite more dynamic interactions between the vehicle and the track structure.



(c) EVA Pad

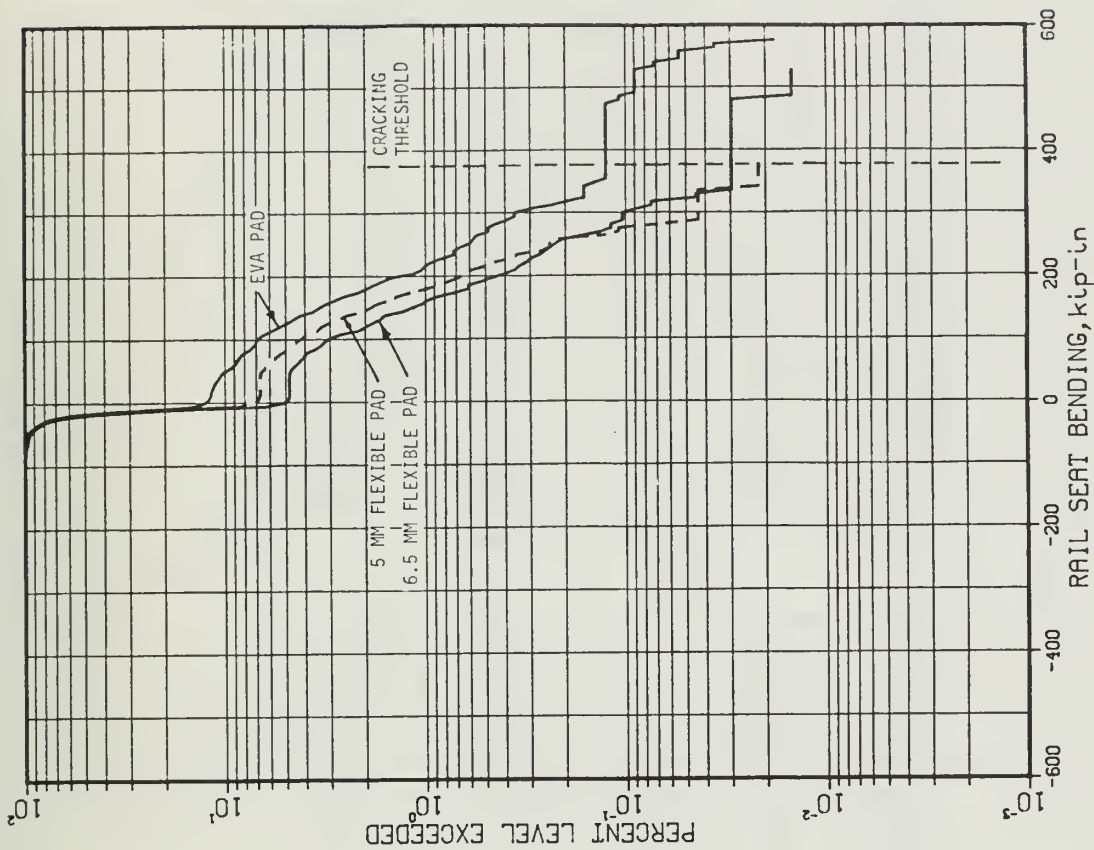


(b) 5 mm Flexible Pad

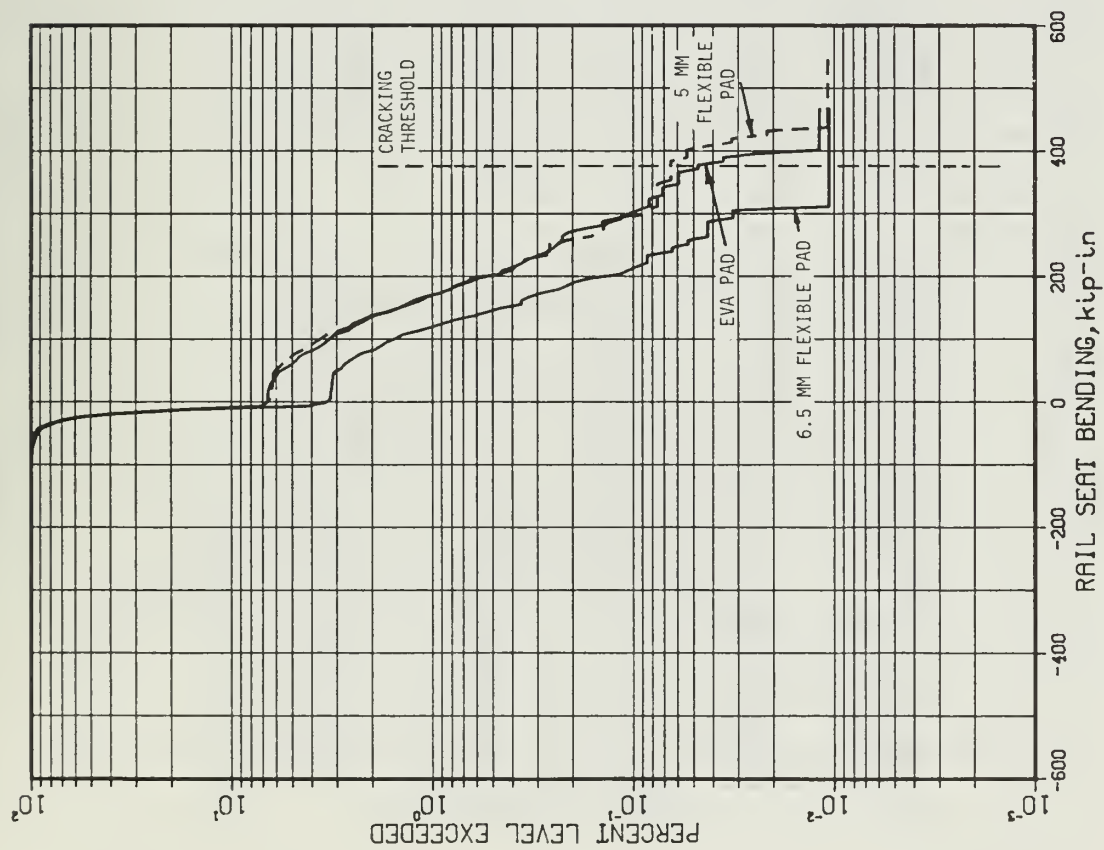


(a) 6.5 mm Flexible Pad

FIGURE 5- 6. TIE BENDING STRAIN DATA FOR AMFLEET AND CONVENTIONAL CARS - ARRANGEMENT BY PAD TYPE

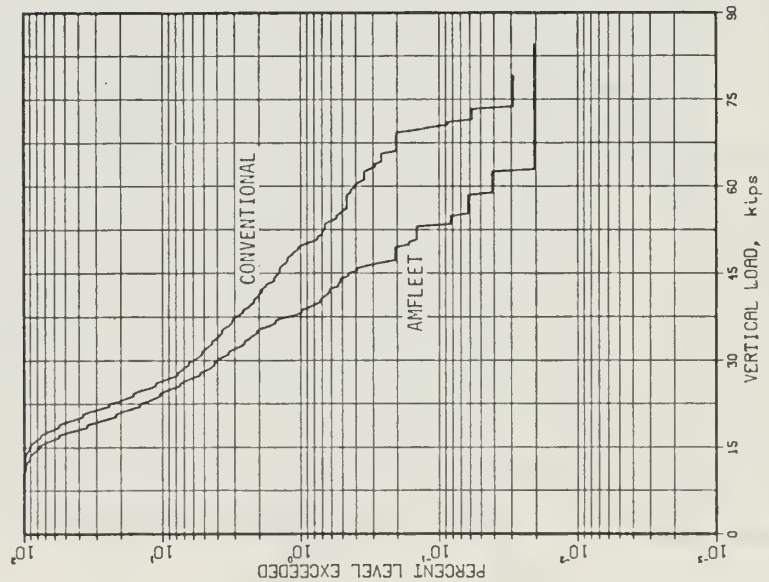


(a) Amfleet Passenger Cars

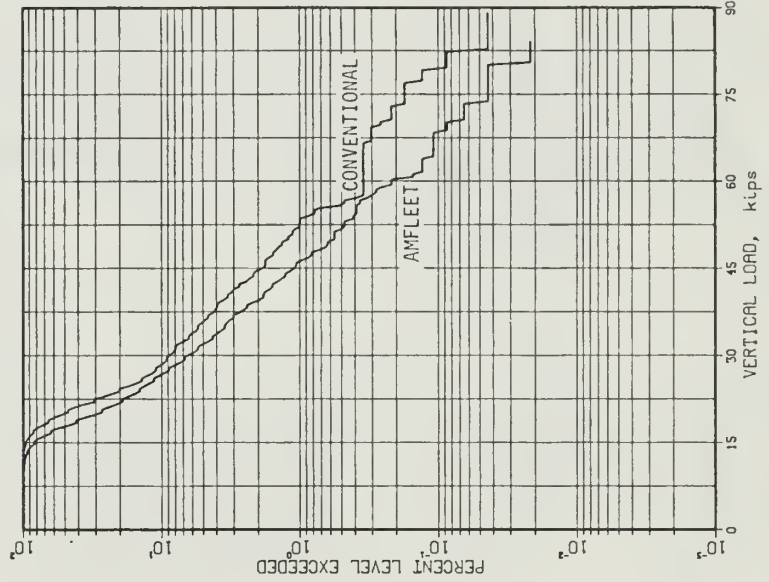


(b) Conventional Passenger Cars

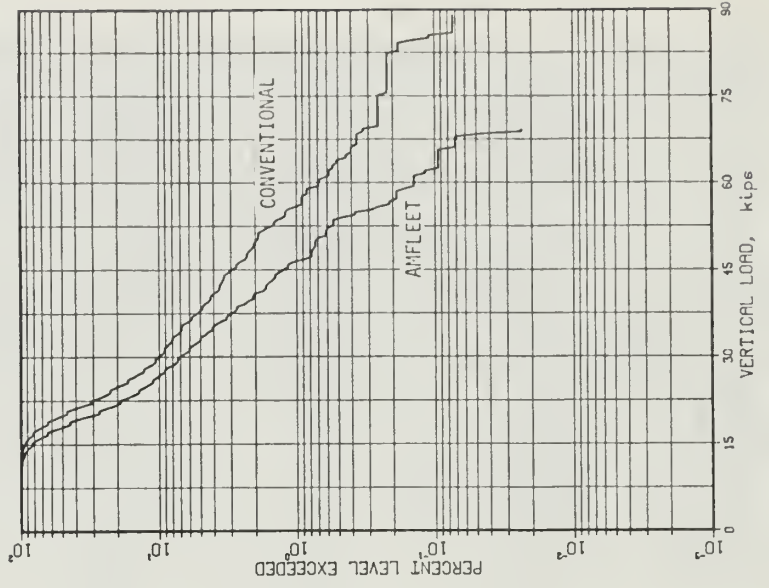
FIGURE 5-7. TIE BENDING STRAIN DATA FOR AMFLEET AND CONVENTIONAL PASSENGER CARS - ARRANGEMENT BY CAR TYPE



(a) 6.5 mm Flexible Pad

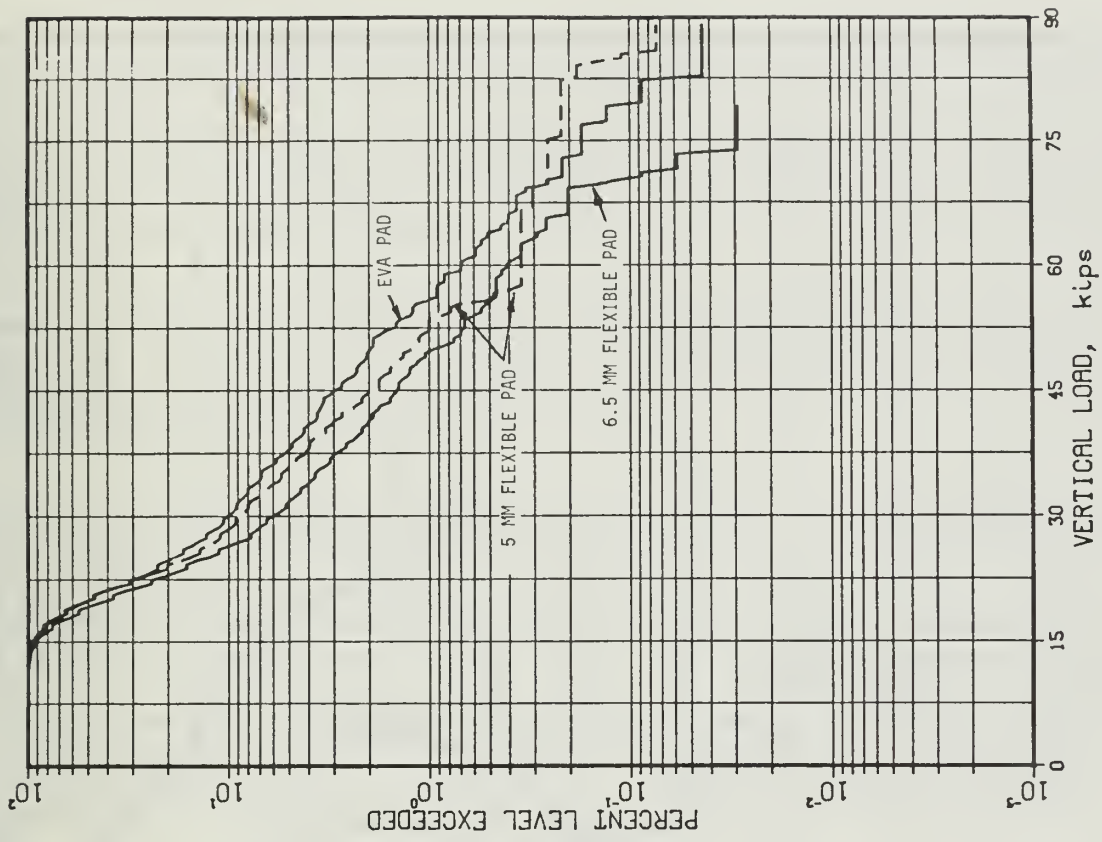


(b) 5 mm Flexible Pad

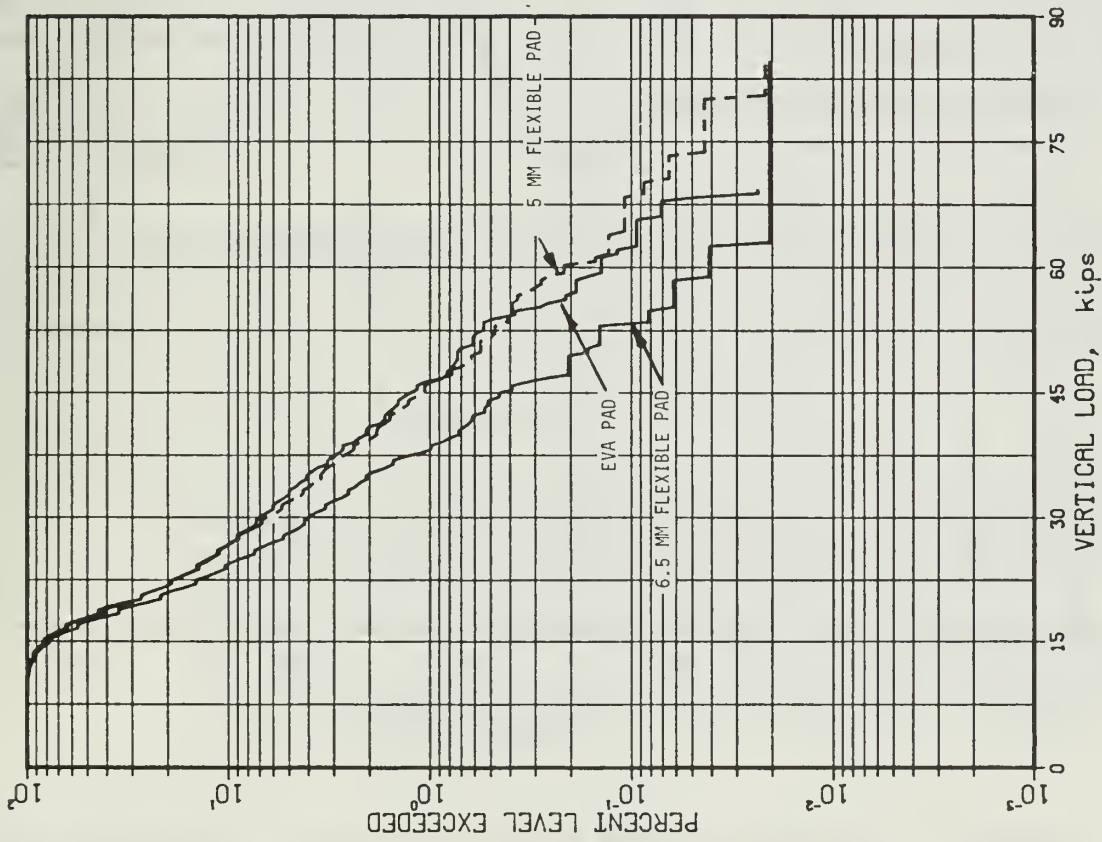


(c) EVA Pad

FIGURE 5-8. VERTICAL WHEEL/RAIL LOADS FOR AMFLEET AND CONVENTIONAL PASSENGER CARS - ARRANGEMENT BY PAD TYPE



(a) Amfleet Passenger Cars



(b) Conventional Passenger Cars

FIGURE 5-9. VERTICAL WHEEL/RAIL LOADS FROM AMFLEET AND CONVENTIONAL PASSENGER CARS - ARRANGEMENT BY CAR TYPE

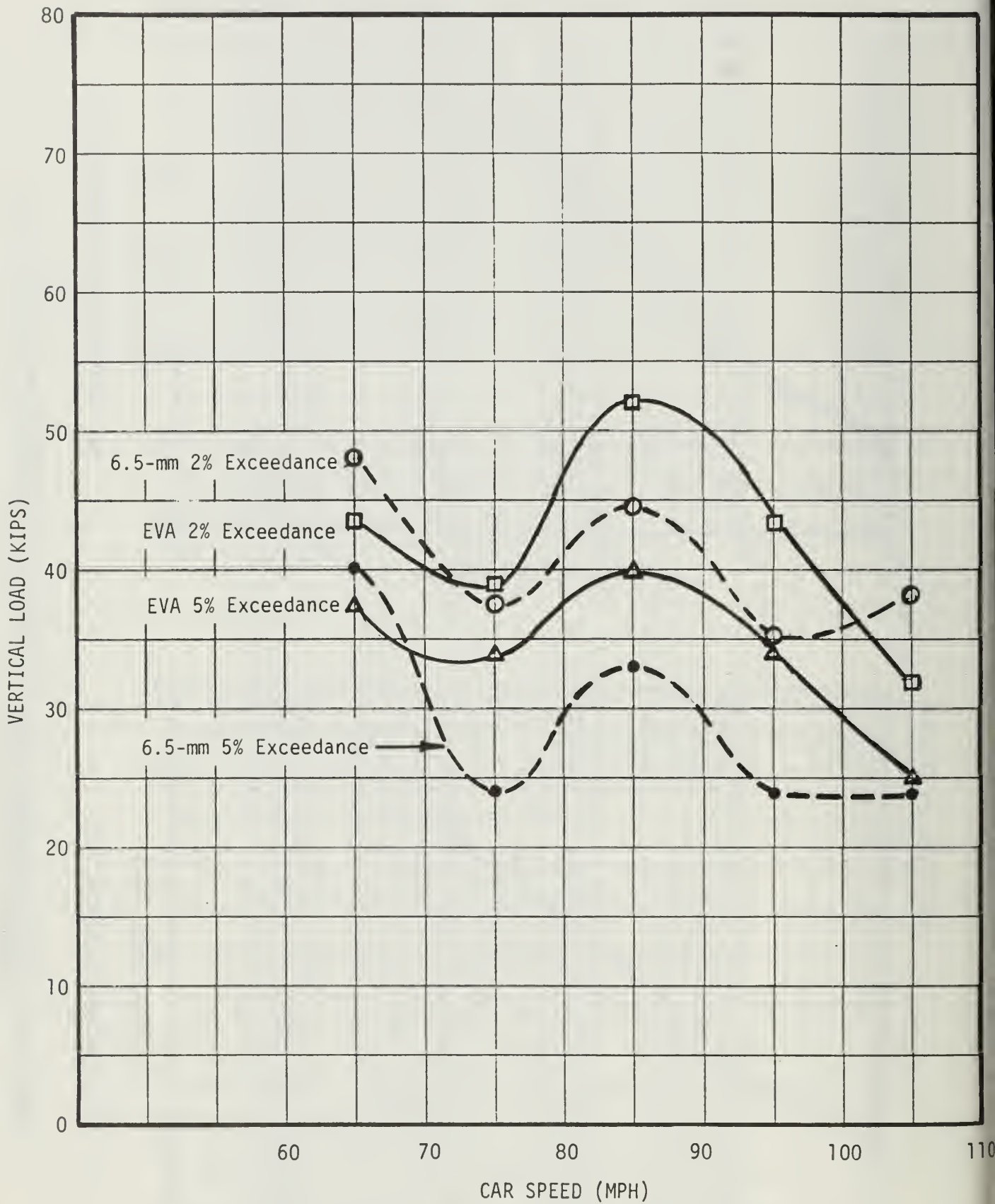


FIGURE 5-10. EFFECT OF SPEED ON VERTICAL LOADS OF CONVENTIONAL CARS

Vertical Rail Clip Deflection. Among the issues involved in a pad conversion is the possibility that a more flexible pad will produce greater rail clip deflections and cause the clips to fail in fatigue. Because the highest deflections occur on curves, deflections were measured on a one-degree curve in Aberdeen where most passenger train speeds were 80 - 100 mph, and most freight train speeds were 40 - 50 mph. The greatest deflections were invariably caused by freight trains.

Rail clip vertical deflections were measured on the field and gage sides of the high rail only. Most of the rail movement has been observed on this rail rather than on the low rail. Pad substitutions were made to permit measurement of deflections on both the current rigid EVA pad and on the 6.5-mm flexible synthetic rubber pad.

Frequency-of-occurrence plots in Figure 5-11 compare the levels of peak-to-peak vertical clip deflections (rail/tie deflections at the clip toe) for measurements on the rigid and flexible pads. The measurements verify a trend which had been indicated in earlier measurements at FAST: peak-to-peak deflections were higher for the rigid pad than for the flexible pad. Much of this imbalance was due to greater uplift deflections which occurred at the gage side of the high rail on the rigid pad. In addition, the rail tended to rotate about the field-side corner of the rail base with the rigid pad, while a more balanced rotation occurred with the flexible pad. These results indicate that there may be no detriment to clip fatigue life when the flexible pad is substituted.

An earlier study [8] identified a fatigue limit of the NEC clips at about 35 mils of vertical rail clip deflection. The deflection measurements indicate that this limit will probably not be approached on tangent track regardless of pad stiffness, because the mean deflections are relatively low. Further, the data indicate that the fatigue limit will be reached on curved track only with the current rigid pad. Thus, it is possible that continued use of the rigid pad would eventually cause some clip fatigue failures on curved track.

Transfer Function of Rail/Tie Acceleration. Figure 5-12 displays the amplitude of the transfer function of rail and tie acceleration for each of the three pad types. Data were collected over a representative train pass in each case. The effect of the decrease in pad stiffness is demonstrated by:

- a. reduction in amplitude with reductions in stiffness, over the frequency range from 200 to 800 Hz
- b. reductions in frequency at the point of 3 dB attenuation (a commonly used reference level) with reduction in pad stiffness. The fundamental bending frequency of the NEC concrete tie is about 125 Hz. At this frequency, there is a reversal of trend in that the amplitude increases with decrease in stiffness. The softer pads have effectively less damping at this frequency. However, most energy from impact loading conditions is produced at higher frequencies (350 - 650 Hz), where attenuation is available from the more flexible pads.

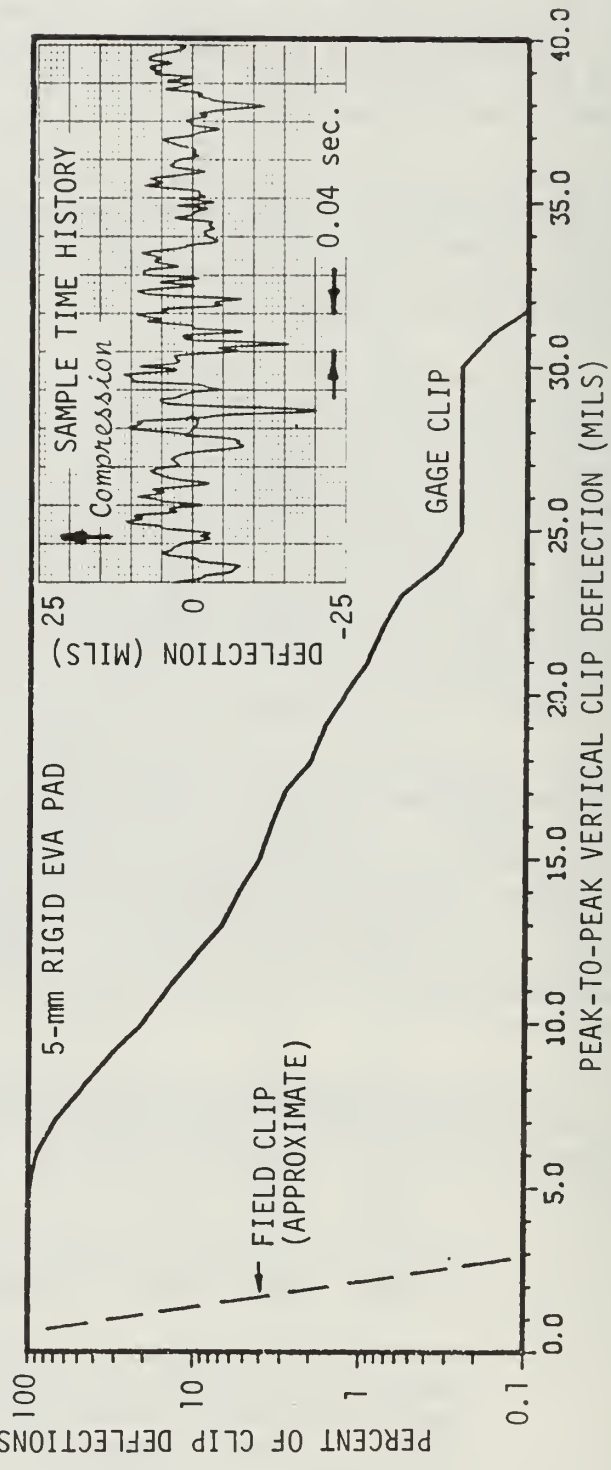
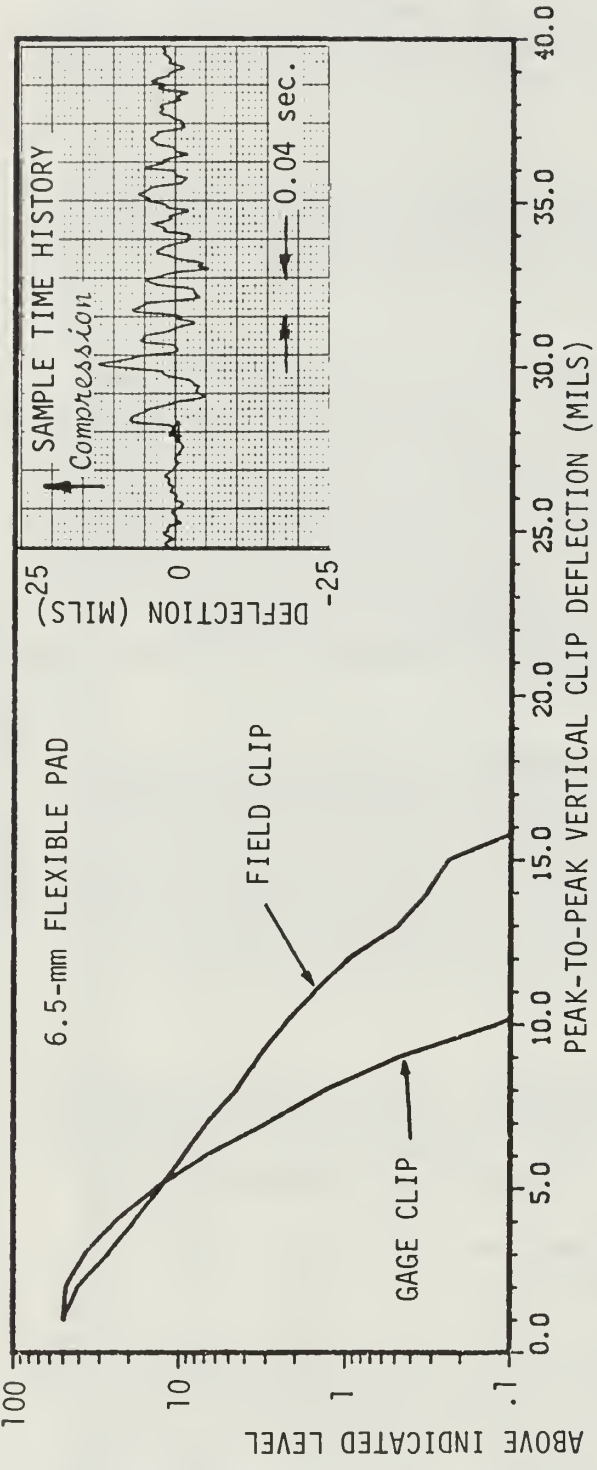


FIGURE 5-11. MEASUREMENTS OF "PEAK-TO-PEAK" VERTICAL CLIP DEFLECTIONS ON A HIGH-SPEED, ONE-DEGREE CURVE OF THE NORTHEAST CORRIDOR TRACK AT ABERDEEN, MD.

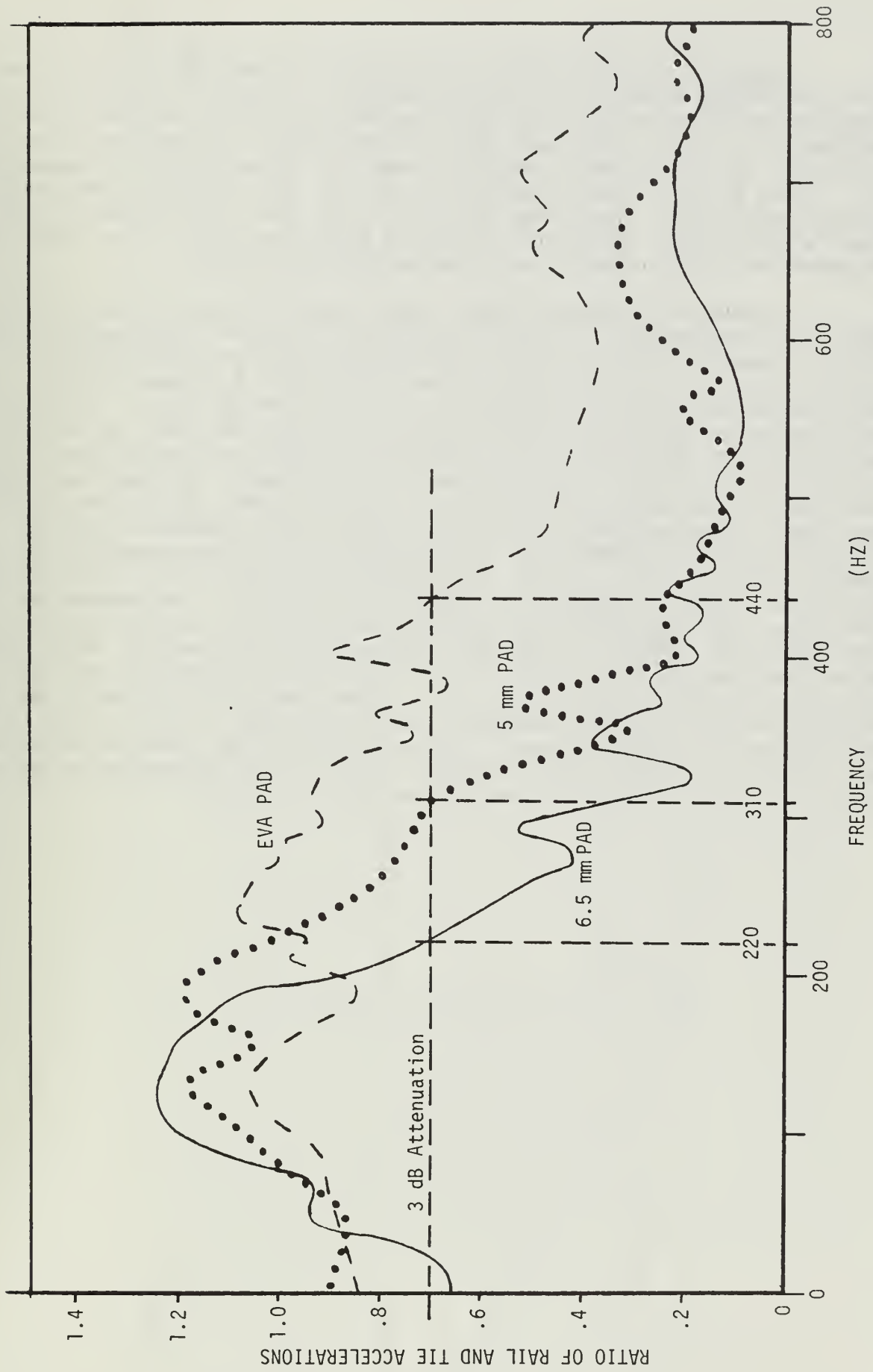


FIGURE 5-12. RAIL-TO-TIE ACCELERATION TRANSFER FUNCTIONS FOR THE THREE TEST PADS

Worst Case Event. Figure 5-13 illustrates the plot of tie bending strain (expressed as equivalent bending moment) vs. time for the single worst-case event which occurred during the three weeks of data collection. The true amplitude of strain is not known since the data system saturates at about 900 inch-kips. This event was produced by a wheel of a conventional passenger car. Figure 5-14 provides a time history of the train consist which produced the worst case event. While magnitudes of strain and vertical load at the impact are off-scale, the normal wheel load magnitudes can be identified, and the permanent strain offset due to the impact can be seen.

A number of additional wheel impact conditions were traced and the wheels were photographed. Typical spalled conditions are illustrated in Figure 5-15(a). However, the worst impacts were produced by the long-wavelength (12-18 inches) irregularities of the type illustrated in Figure 5-15(b). This particular wheel produced a measured vertical load of 85.8 kips. The wheel irregularity consisted of a flattening or chording of the wheel circumference over a length of about 12 inches. The area contained very little spalling of the type which is usually associated with "flat" wheels. The wheel was placed on a wheel truing machine which permitted the measurement of the radial distance from a fixed reference, across the wheel tread, at several selected stations across the chorded area. The results of these measurements are plotted in Figure 5-16. Each of the tread profiles shown can be compared with the dotted line which represents a new 1:40 tread taper. The measured profiles show radial deviations from the original profile up to 0.16 inches. Of more importance, however, is the fact that the deviations vary by about 0.09 inches from the edge to the center of the chorded area (from left or right edge to the middle of Figure 5-16). This wheel condition illustrates the type of condition which must be eliminated from NEC passenger traffic if the ties are not to sustain further damage. These long-wavelength irregularities are more difficult to identify than are wheel spalls. This emphasizes the necessity for a regular program of wheel inspection and truing.

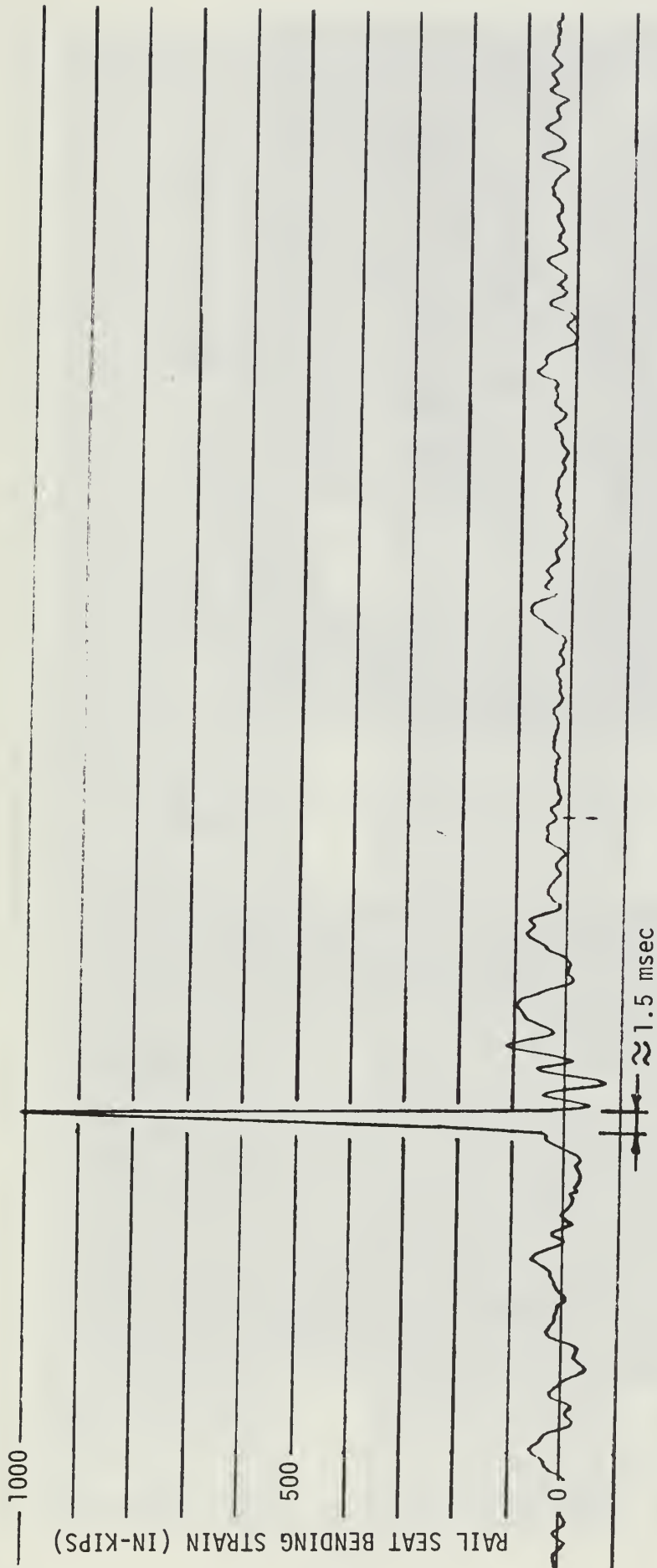


FIGURE 5-13. RAIL SEAT BENDING STRAIN FROM CRACK-PRODUCING IMPACT, CONVENTIONAL PASSENGER TRAIN, 5 - mm FLEXIBLE PAD, TIE NO. 5

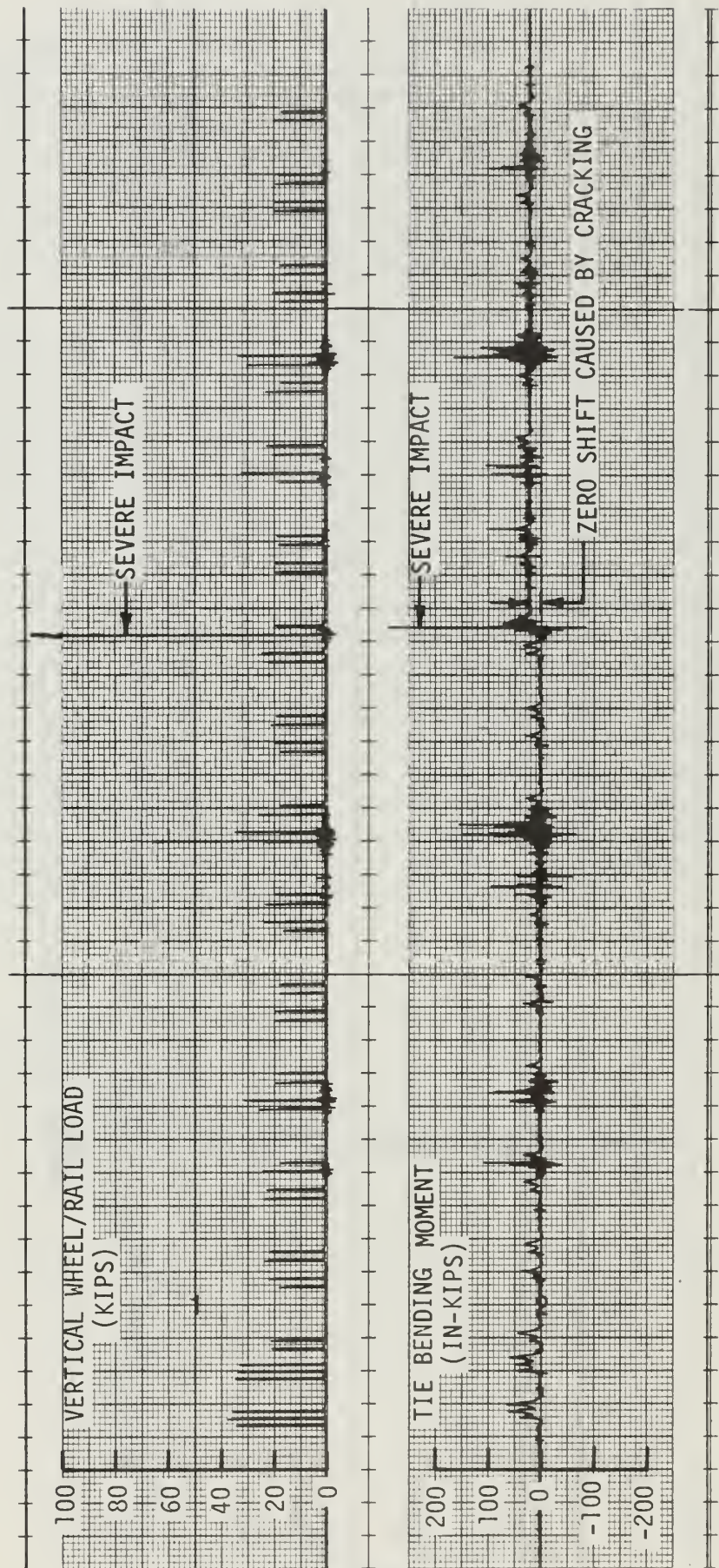


FIGURE 5-14. EXAMPLES OF VERTICAL LOAD AND TIE BENDING MOMENT RECORDS FOR A CONVENTIONAL PASSENGER TRAIN



(a) Typical Spalled Wheel Tread



(b) Worst-Case Flattened Wheel Condition

FIGURE 5-15. WHEEL CONDITIONS IDENTIFIED BY TRACK LOADING MEASUREMENTS

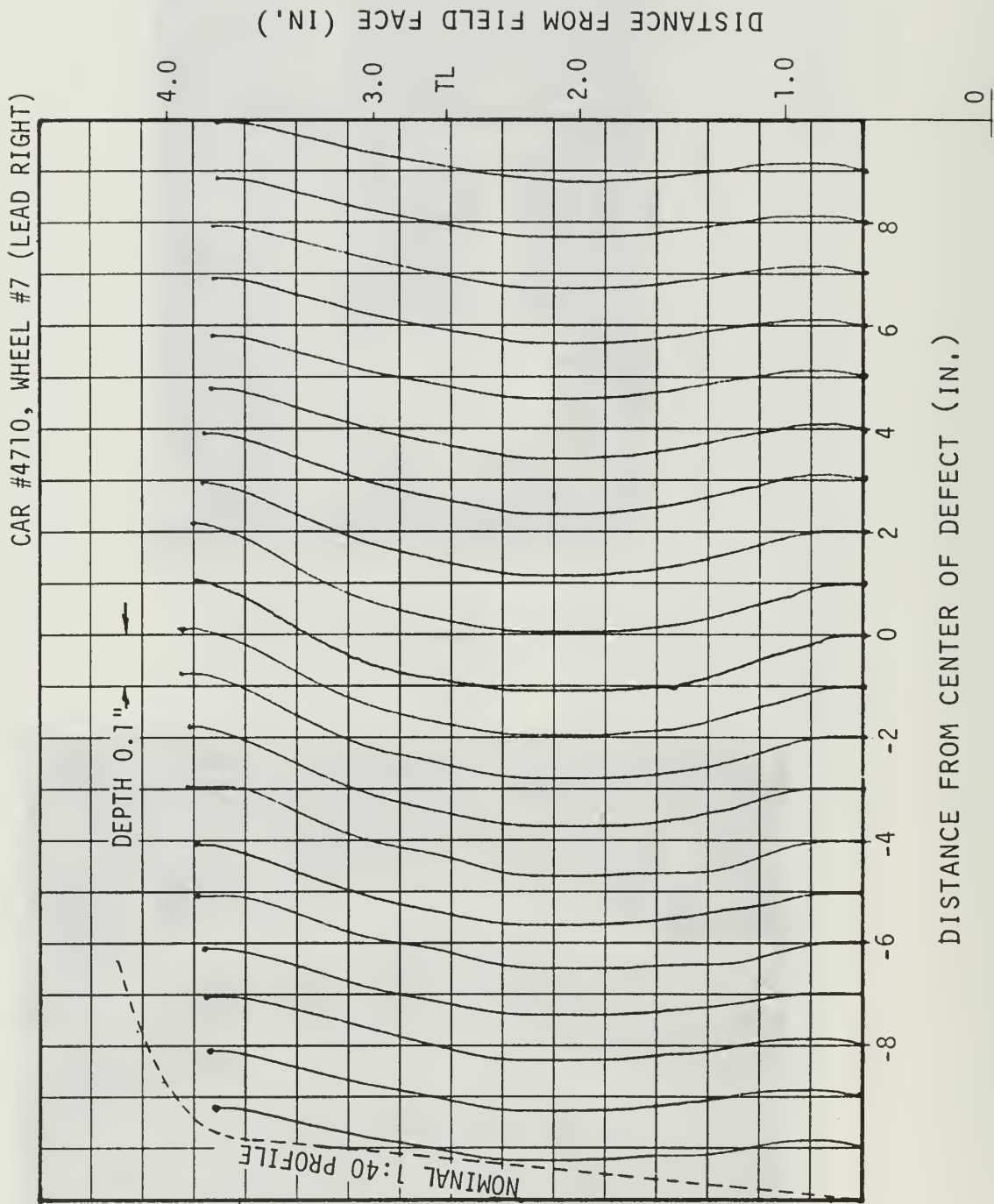


FIGURE 5-16. MEASUREMENT OF WHEEL TREAD PROFILE AND RADIAL ECCENTRICITY

6.0 SUMMARY OF RESULTS

6.1 Background

- a. Between June and September 1980, hairline rail seat bending cracks were found in several inspection zones of the Northeast Corridor concrete tie track. While the cracks did not constitute failure of the ties, they were a cause for concern because the ties had been designed to the latest strength specifications of the AREA and Amtrak and were expected to sustain traffic loading without cracking.
- b. Static bending tests were conducted on ties removed from track. While minor cracks had no apparent effect on the ultimate bending strength of the ties, cracks extending beyond the upper level of prestress tendons reduced ultimate bending strength by an average of 16 percent.
- c. In a special test zone of 60 new ties, 30 ties were fitted with a grooved, flexible pad and 30 were fitted with the standard, rigid, EVA pad. Over the next nine months, the rate of cracking in the flexible pad zone first lagged, then exceeded the rate of cracking in the rigid pad zone. Later inspection of the flexible pads revealed damage due to compression and fraying, but it appeared that the flexible pads had provided some reduction in cracking during the initial period before the damage.
- d. The tie inspections and strength tests clearly indicated a need for an investigation to determine the cause of the cracking and to recommend corrective action.

6.2 Evaluation of June 1980 Test Data

- a. Wheel/rail load and tie bending moment data originally collected in June 1980 were re-processed to permit the detection of peak responses occurring at frequencies higher than the original limit of 300 Hz. It was found that the frequency bandwidth of 0 to 1200 Hz represented an optimum choice, in that it produced over 90 percent of the unfiltered response amplitudes while minimizing system noise.
- b. The reevaluation indicated that tie bending moments sufficient to cause rail seat bending cracks were produced by about 0.1 percent of the passenger train wheels passing the measurement site. With this rate of occurrence, an average tie site could experience a bending moment with the potential to crack a tie about once every 1.8 days, for traffic densities equal to those at the test site. However, subsequent laboratory tests indicated that multiple

impacts, on the order of 5 to 10, of this magnitude are required to initiate and propagate a crack of sufficient length and width to be detected during a field inspection of ties in track.

6.3 Laboratory Tests of the Effects of Tie Pad Stiffness on Impact Attenuation

- a. Laboratory impact loading tests were conducted using a single-tie test arrangement. The range of amplitudes and the approximate frequency content of impact bending moments measured in track were successfully reproduced by single blows of the impact fixture drop hammer.
- b. A "cracking threshold" for impact loading was identified at a level of strain equivalent to 375 inch-kips of static bending moment. This was very nearly equal to the mean cracking strength found in earlier static strength tests.
- c. In tests with the standard, rigid, EVA pad, cracks were consistently initiated by impacts from a drop height of 16 inches with the 115-pound impact hammer. With increased drop heights, the rail seat bending cracks continued to propagate upward from the tie bottom and to develop a pattern often found in service: a "Y" which begins at the top prestress strands.
- d. Nondestructive instrumented drop tests were conducted with the EVA pad and with eight pads of lower stiffness. The compressive load-deflection characteristics of each pad were measured both statically and at a load rate of 9 Hz over a load range of 0-30,000 pounds. These tests demonstrated that major decreases in tie pad stiffness could significantly reduce the tie bending moments occurring at given drop heights. The following table indicates the degree of bending moment attenuation obtained with some of the pads:

<u>PAD TYPE</u>	<u>NOMINAL DYNAMIC STIFFNESS (LB/IN) FOR LOADS BETWEEN 4,000 and 20,000 POUNDS</u>	<u>PERCENT PEAK STRAIN ATTENUATION</u>
EVA	5,000,000	0
5-mm GROOVED SYNTHETIC RUBBER	1,200,000	18
6.5-mm GROOVED SYNTHETIC RUBBER	850,000	25
9-mm GROOVED SYNTHETIC RUBBER	500,000	40

- e. For the field tests, the 5-mm and 6.5-mm grooved synthetic rubber pads were selected to be compared with the EVA pad. The 9-mm pad, which produced the greatest attenuation, was not considered because its adoption for track use would require replacement of the fastener clips.

6.4 Field Tests to Determine the Effects of Tie Pad Stiffness on Impact Attenuation

- a. A zone of 5 consecutive ties was instrumented to measure rail seat bending strain, vertical wheel/rail load, rail and tie accelerations, and fastener clip deflections. Data was collected for 5 days with each of three pad types installed in the zone: (1) the 6.5-mm flexible synthetic rubber pad, (2) the 5-mm flexible synthetic rubber pad, and the 5-mm rigid EVA pad, in the order indicated.
- b. While both flexible pads were effective in reducing the rate of occurrence of tie bending moments above the "cracking threshold," neither eliminated this occurrence under passenger traffic loads. With approximately 500 passenger axles per day, the measured rates at which the cracking threshold was exceeded for each pad were converted to an interval in days between threshold exceedances at an average tie site:

<u>PAD TYPE</u>	<u>AVERAGE NO. OF DAYS BETWEEN THRESHOLD EXCEEDANCE UNDER PASSENGER TRAFFIC</u>
EVA	2.6
5-mm Flexible	4.4
6.5-mm Flexible	28

- c. Freight traffic produced no tie bending moment above the cracking threshold during the 15 days of data collection, and the quantity of data available was not sufficient to permit projections of exceedance rates. However, since freight equipment is not inspected as frequently as passenger equipment, it must be assumed that major wheel defects (those large enough to cause cracks) can occur.
- d. Most of the Northeast Corridor passenger traffic consists either of the older, conventional Heritage cars or of Amfleet cars which have been built since 1975. Of these two classes, the conventional equipment produced consistently higher overall bending moment and load levels.
- e. It should be noted that the Metroliner cars did not produce tie bending strains above the cracking threshold. Because Metroliner cars are considered electric locomotives, they are inspected much more frequently than are passenger cars.

- f. Many of the wheels causing serious impact conditions were traced and photographed. In a few cases, the radial divergence of the wheel irregularity was measured. The worst case impacts were produced by relatively long wavelength (12-18 inches) chorded areas which were not necessarily accompanied by the spalls commonly identified as "flat wheel" conditions. These long-wavelength irregularities are more difficult to identify than are wheel spalls. The regular occurrence of wheel irregularities of both types emphasizes the necessity for the timely inspection of wheels and removal of serious defects.

7.0 CONCLUSIONS AND RECOMMENDATIONS

- a. Cracks at the rail seats of Northeast Corridor concrete ties are caused by the impacts resulting from wheel irregularities on a very small percentage of passenger car wheels.
- b. The substitution of a more flexible pad can definitely reduce the rate of occurrence of impacts with the potential to cause tie cracks. The pad should have an approximately linear load-deflection characteristic up to about 30,000 pounds of compressive load and should have a dynamic stiffness of about 850,000 pounds per inch or lower. Other required properties include high tensile strength and resistance to compressive set, age hardening, and abrasion.
- c. The long-term durability of flexible pads should be evaluated through track and laboratory tests. Japanese National Railways' service histories to date indicate a life expectancy of 10 years with an increase in spring rate over that period of two-thirds.
- d. A plan should be developed for an on-line wheel impact detector, connected to an existing communications system, which will permit the detection and identification of wheels which produce serious impact conditions.
- e. Evaluations of tie pads for service under impact loading conditions should include tests of the type outlined in Appendix B.

REFERENCES

- [1] "Manual for Railway Engineering," American Railway Engineering Association, Chicago, Illinois, Chapter 10 (Revised 1981).
- [2] Tuten, J.M., "Analysis of Dynamic Loads and Concrete Tie Strain from the Northeast Corridor Track," technical memo by Battelle's Columbus Laboratories to the Federal Railroad Administration, Improved Track Structures Research Division, Contract DOT-FR-9162, May 1981.
- [3] Dean, F.E. and Harrison, H. D., "Laboratory Study to Determine the Effects of Tie Pad Stiffness on the Attenuation of Impact Strain in Concrete Ties," report by Battelle's Columbus Laboratories to the Federal Railroad Administration, Improved Track Structures Research Division, Contract DOT-FR-9162, May 1981.
- [4] Harrison, H. D., Progress Report for March 1981 on Contract No. DOT-FR-8164, "Tie and Fastener Performance and Correlation Analysis," by Battelle's Columbus Laboratories to the Federal Railroad Administration, Improved Track Structures Research Division.
- [5] "Static Tests at Littleton, Mass.," National Railroad Passenger Corporation memo from D.L. Jerman to D.C. Wilcox, December 16, 1980.
- [6] Dean, F.E., "Tests to Determine the Effects of Service Loading on the Bending Strength of Concrete Ties," Transportation Test Center FAST Report No. 81/11, December, 1981.
- [7] Watanabe, K., "Engineering of Rail Fastening," Japanese Railway Engineering, Vol. 19, No. 4, 1980.
- [8] Dean, F.E., "Measurements of Rail/Tie Deflections and Fastener Clip Strains at the Facility for Accelerated Service Testing," Transportation Test Center, FAST Report No. 81/03, December 1981.

APPENDIX A

INSTRUMENTATION AND DATA PROCESSING

TRANSDUCERS: Description, Installation, and Calibration

The track measurements made in the two field measurement programs consisted of vertical and lateral wheel/rail loads, tie bending moment, vertical rail and tie accelerations, and vertical rail-to-tie deflection. For each of these measurements, a typical transducer and the methods used to install and calibrate it are briefly described as follows.

Wheel/Rail Loads

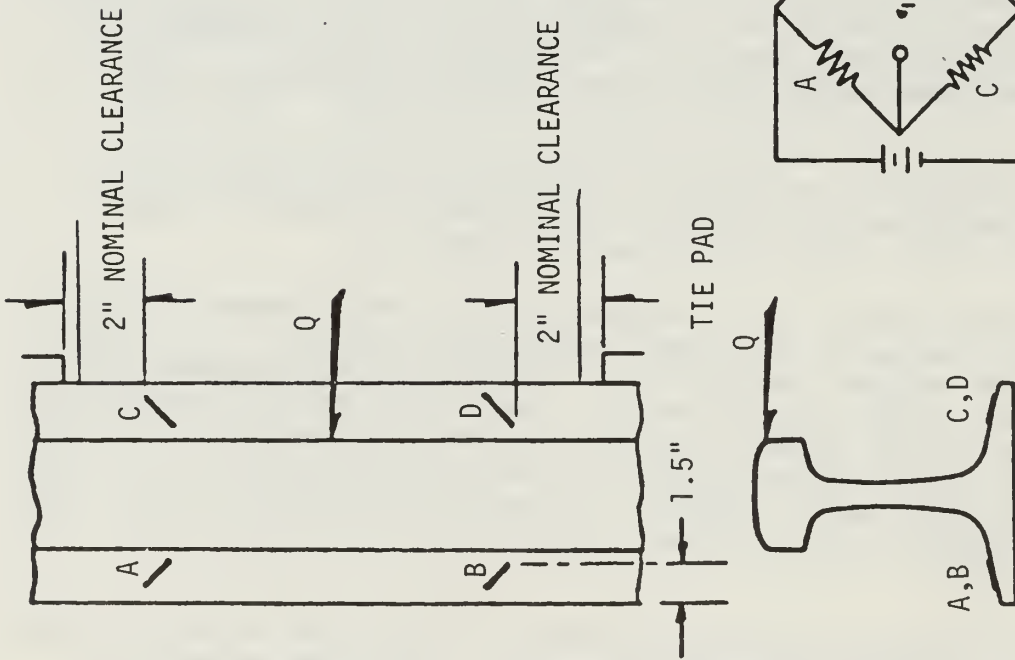
Strain gage patterns measuring principal strains in the rail web were used to measure vertical wheel/rail loads during both the June 1980 tests and the July 1981 tests. Gages mounted on the rail base were also used during the June 1980 tests to measure lateral wheel/rail load. The two load measurement circuits are shown schematically in Figure A-1.

Weldable strain gages were used for the load circuits. A rough grinder removed all mill scale and pits from the gaged areas of the rail. A small die grinder was then used to finish the area directly under and surrounding the gages and strain relief straps. The dimensional correspondence of one gage and its counterpart on the opposite side of the rail was carefully maintained with a pre-formed template. The gages and strain relief straps which support the leads were installed with a capacitive-discharge spot welder.

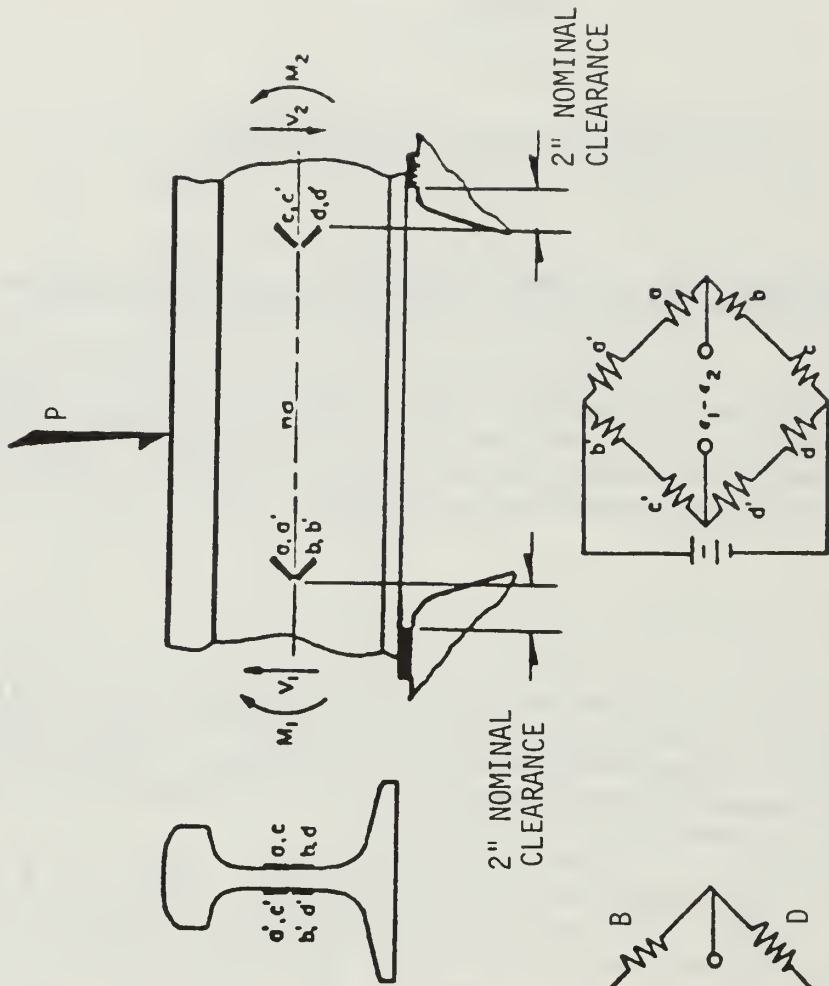
After attachment, each gage was checked for continuity (350 Ohm resistance) and isolation from the rail (> 20 M-Ohm from shield to rail) before termination into one of the bridges of Figure A-1.

A physical, end-to-end calibration was performed between each load transducer and the output of its signal conditioning amplifier. Calibration loads were applied through a special track loading fixture suspended under a loaded hopper car, as shown in Figure A-2. The fixture applies vertical and lateral loads to the rail through laboratory-calibrated load cells. As loads are applied, the outputs of the appropriate load cell and bridge circuit are plotted. The vertical load is generally cycled from 0 to 30 kips to 0. The lateral load is cycled from 0 to 20 kips to 0 while the vertical load is held constant at 30 kips.

A typical plot of vertical calibration load vs. the output of a vertical load bridge circuit is shown in Figure A-3. The slope of the plot



(a) LATERAL LOAD-MEASURING CIRCUIT



(b) VERTICAL LOAD-MEASURING CIRCUIT

FIGURE A-1. STRAIN GAGE CIRCUITS TO MEASURE LATERAL AND VERTICAL WHEEL/RAIL LOADS

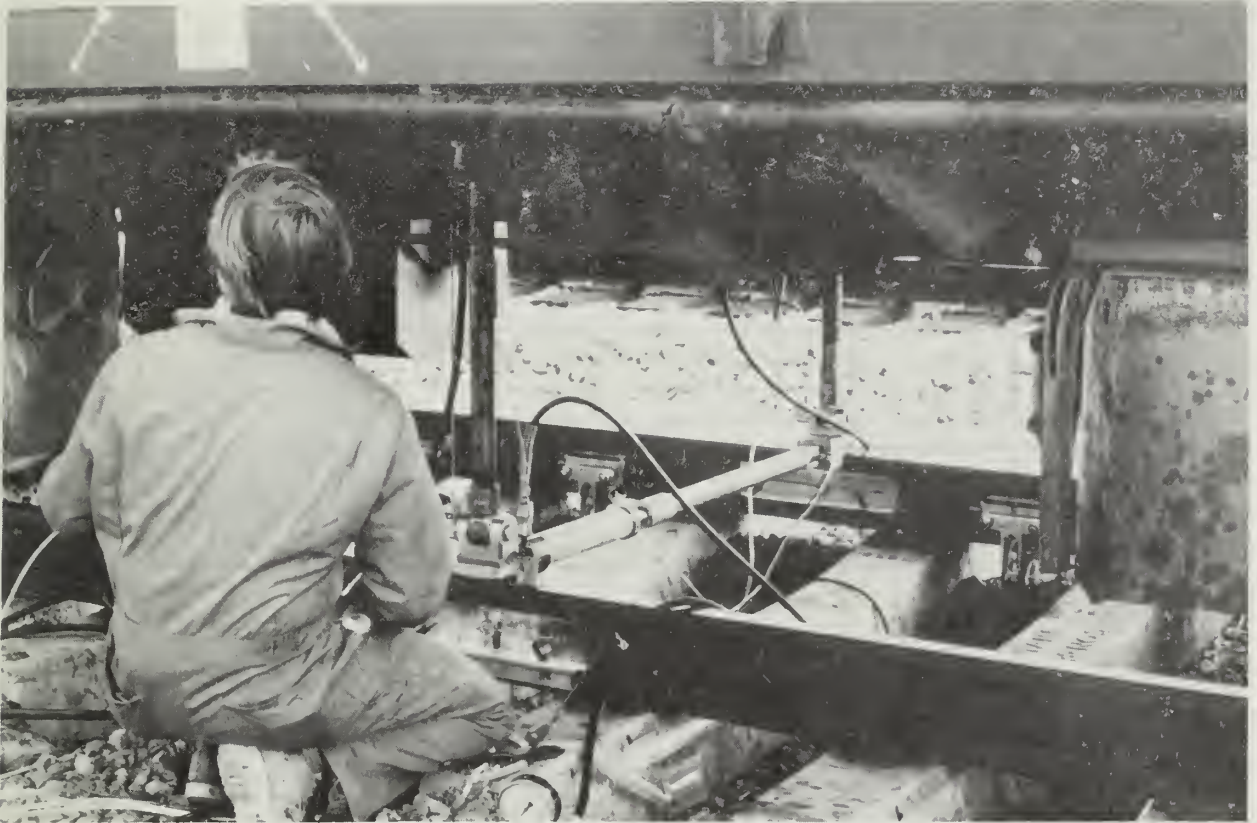


FIGURE A-2. RAIL LOADING FIXTURE USED FOR MODULUS TESTS AND RAIL CIRCUIT CALIBRATION

V176L

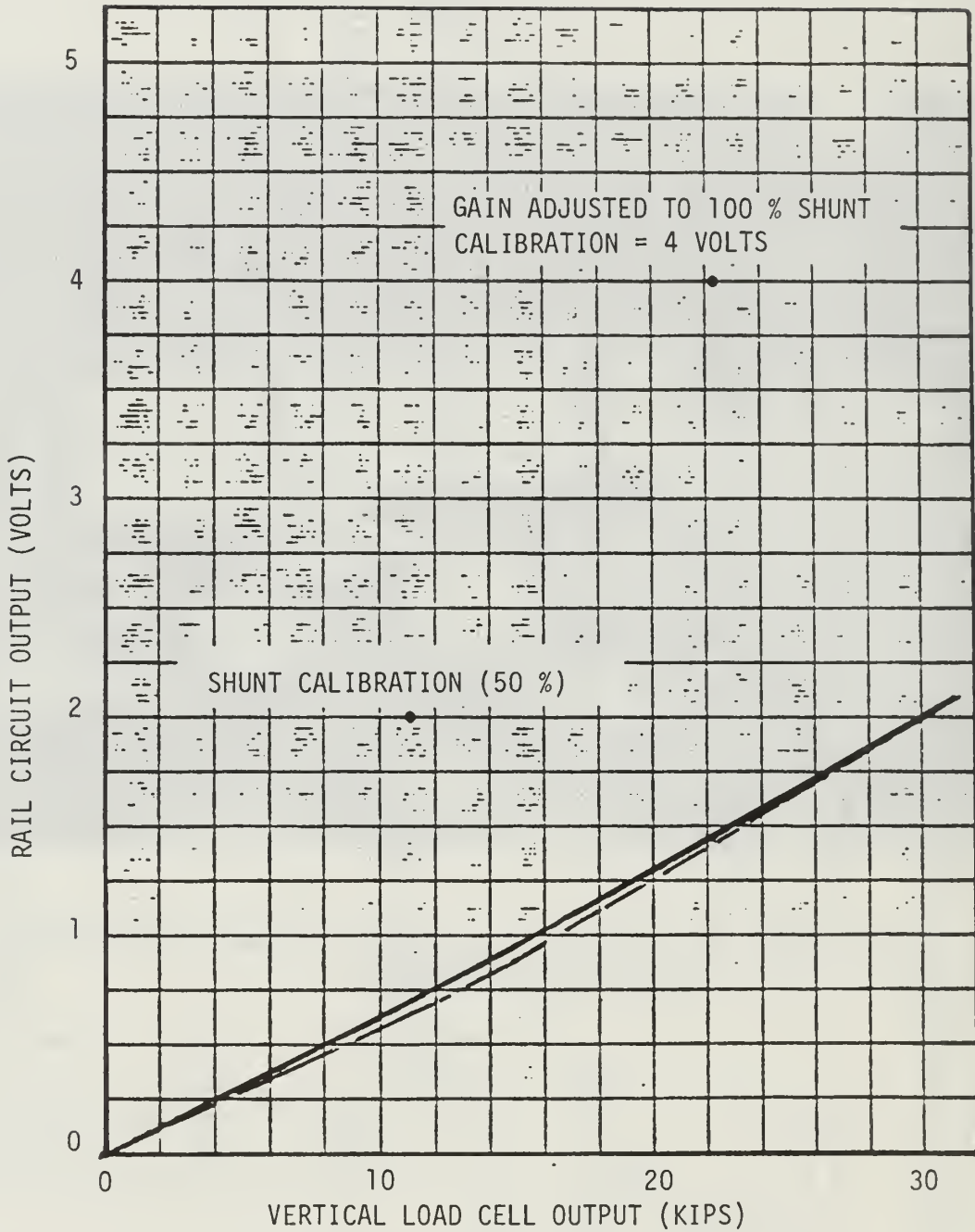


FIGURE A-3. VERTICAL WHEEL/RAIL LOAD CIRCUIT CALIBRATION

provides the load-voltage relationship (kips/volt) for the single amplifier setting used during the calibration. To define the load vs. voltage relationship independently of the state of amplification, bridge shunt calibrations are required. The offset voltages produced by two shunt calibrations are shown on the plot of Figure A-3. Each shunt was obtained from precision resistors placed across two opposite arms of the bridge. The values of the shunt resistance were:

- a. 1 M-Ohm to produce a "50 percent" calibration
- b. 500 K-Ohm (two 1M-Ohm in parallel) to produce a "100 percent" calibration.

From Figure A-3, the shunt resistances were determined to be equivalent to the following loads:

- a. "50 percent" calibration: 30.0 kips
- b. "100 percent" calibration: 60.0 kips.

This equivalence of load to shunting is independent of the state of the amplifier. The offset voltages produced by these shunts are not important so long as the "100 percent" shunt does not exceed the "full-scale" range of the amplifier. Battelle uses 5 volts as the definition of full-scale output. This "full-scale" limit is established by the input sensitivity set on the FM tape recorder.

For convenience in digitizing the analog data, the amplifiers of all vertical load channels were then adjusted so that the "full-scale" output (5 volts) was equivalent to 76.2 kips vertical load. In the example of Figure A-3, the change was accomplished by adjusting the amplifier so that the "100 percent" shunt (equivalent to 60.0 kips) produced 5.08 volts output instead of the original 4.0 volts. The "zero" could be offset negatively to produce a greater dynamic range than the 76.2 kips. Final processing was performed with a 90 kips range.

The calibration of lateral load (for the 1980 tests only) was performed in a similar manner. For each load circuit, shunts of one and then two 750 K-Ohm resistors were applied across each of two opposite arms of the gage bridge. The amplifier gain was set so that the shunts produced 2 and 4 volts, respectively. With the track loading fixture, a vertical load of 30 kips was applied and lateral load was cycled from 0 to 20 kips 0. Typical calibration results are shown in Figure A-4. After the calibration, the amplifier gain was adjusted so that the "full-scale" output of 5 volts was produced by 25.4 kips lateral load.

Tie Bending Moments

Longitudinally mounted strain gage coupons were used to measure tie strain, which was calibrated in terms of bending moments applied to the ties in-track. Measurements were made under the rail seats and at tie centers

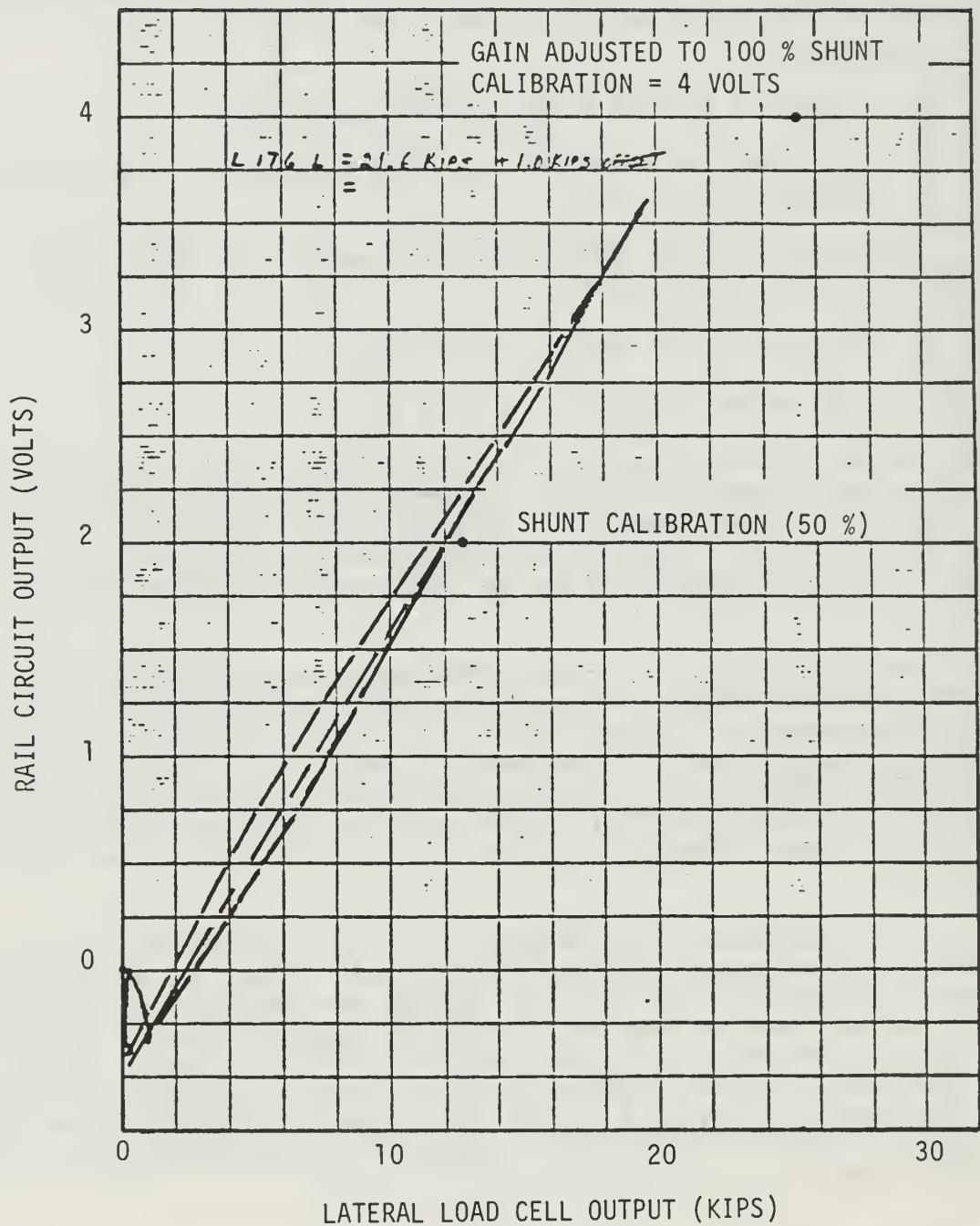


FIGURE A-4. LATERAL WHEEL/RAIL LOAD CIRCUIT CALIBRATION

during the 1980 tests at Aberdeen. During the 1981 tests, only rail seat bending moments were measured because it had been determined that the levels of interest occurred only at the rail seats of tangent track on the Northeast Corridor.

Each coupon consists of two longitudinally mounted active gages and two laterally mounted, floating temperature compensation gages, as shown in Figure A-5. The four gages form a complete bridge circuit.

The "strain" is measured in terms of the bending moment required to produce an output of the bridge circuit in the linearly elastic range. During the laboratory impact tests, it was learned that the relationship between coupon output and applied impact load (and thus moment) remains approximately linear through the high-impact range, although cracks cause a small offset of the zero or balance position of the circuit.

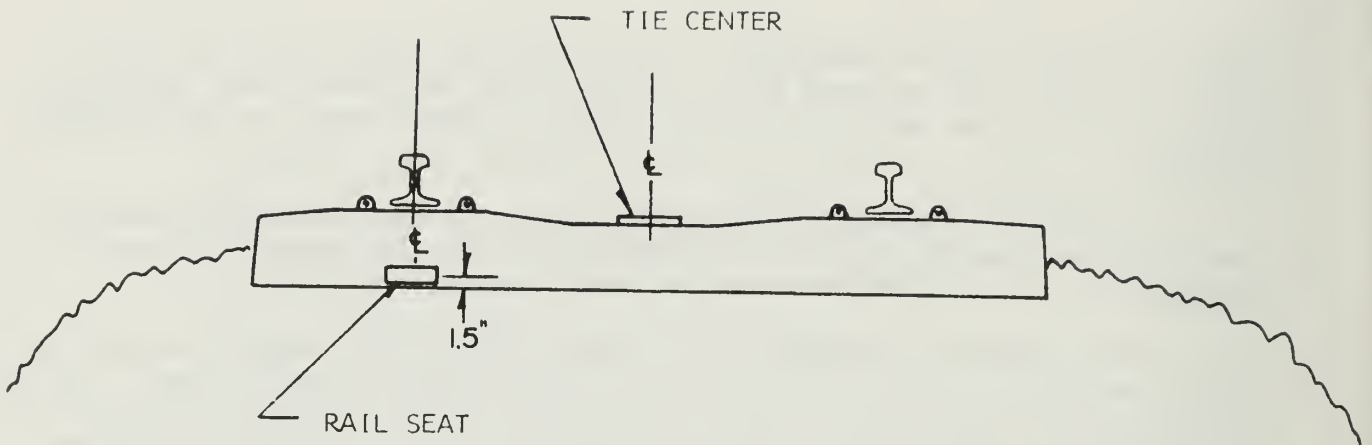
Figure A-6 illustrates the application of bending moment to a tie in track. The applied load P is converted to bending moment by assuming that the pad distributes the load in the form of two concentrated loads $P/2$, as shown in the figure. The effective separation of the loads $P/2$ was established in an earlier laboratory test program [A-1].

Calibration of the strain coupons is similar to that of the load circuits. The amplifier is adjusted to provide certain offset voltages from "50 percent" and "100 percent" two-arm shunts. The values of the shunt resistances were 1 M-Ohm and 500 K-Ohm, respectively. After the equivalence of bending moment and the shunt resistance was established, the amplifier was adjusted so that the "full-scale" amplifier output of 5 volts was equivalent to 635 kip-in. Because of the consistency of strain sensitivity observed in the 1980 tests and the lab tests, it was decided to forego physical calibration of the five instrumented ties in the 1981 tests, particularly since all data were comparative between the three sets of pads. A mean value sensitivity of 165 kips-in. for the 100 percent cal step was used for all rail seat circuits.

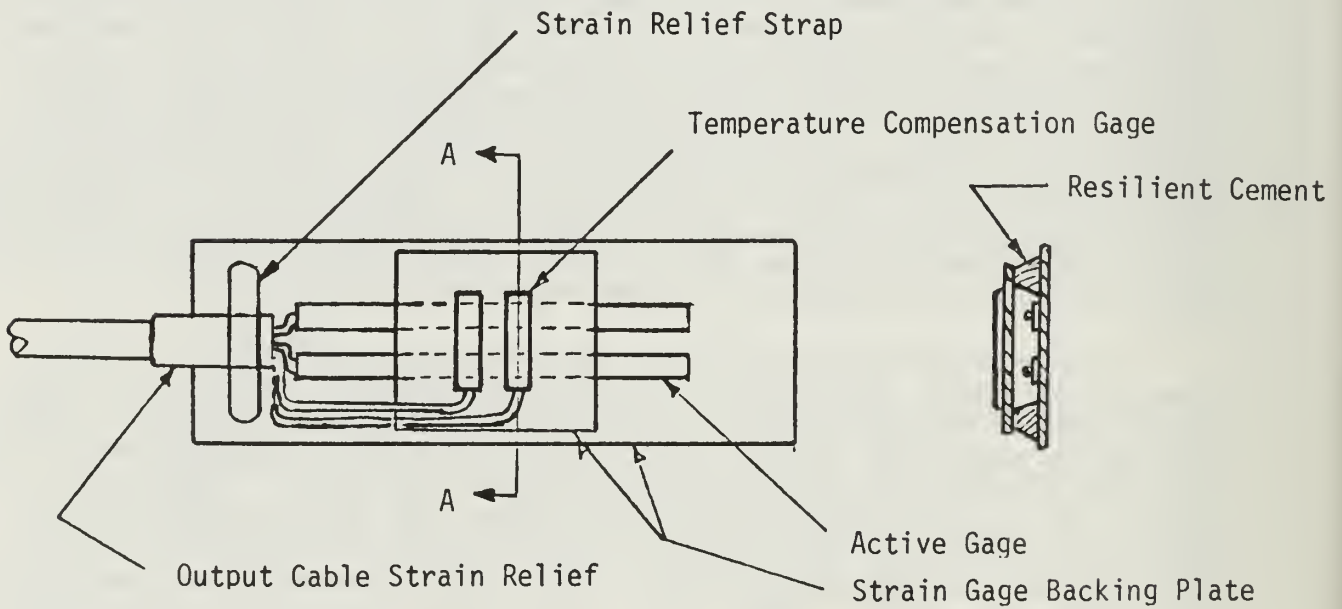
In addition to the rail seat bending strains measured on 5 ties, linear strain gages were placed at 5 positions along one face of the center tie in the instrumented zone. Gage placement is illustrated in Figure A-7(a). The 120-Ohm gages have a gage factor of 2.0. Each gage requires three 120-Ohm precision resistors to complete a 4-arm bridge. Using two, 1 M-Ohm shunt resistors across each of two arms of the bridge, the shunt calibration was equivalent to 240 microinches/inch of linear strain. This equivalence was used to adjust the amplifiers so that 5 volts full-scale output was equivalent to 440 microinches/inch. These strain signals were collected intermittently on channels 11 to 14 of the data system. The same channels were shared for measurement of accelerations and rail/tie deflections.

Rail and Tie Accelerations

The accelerometers shown schematically in Figure A-7(b) were used to simultaneously measure the acceleration of the top surface of one tie and of

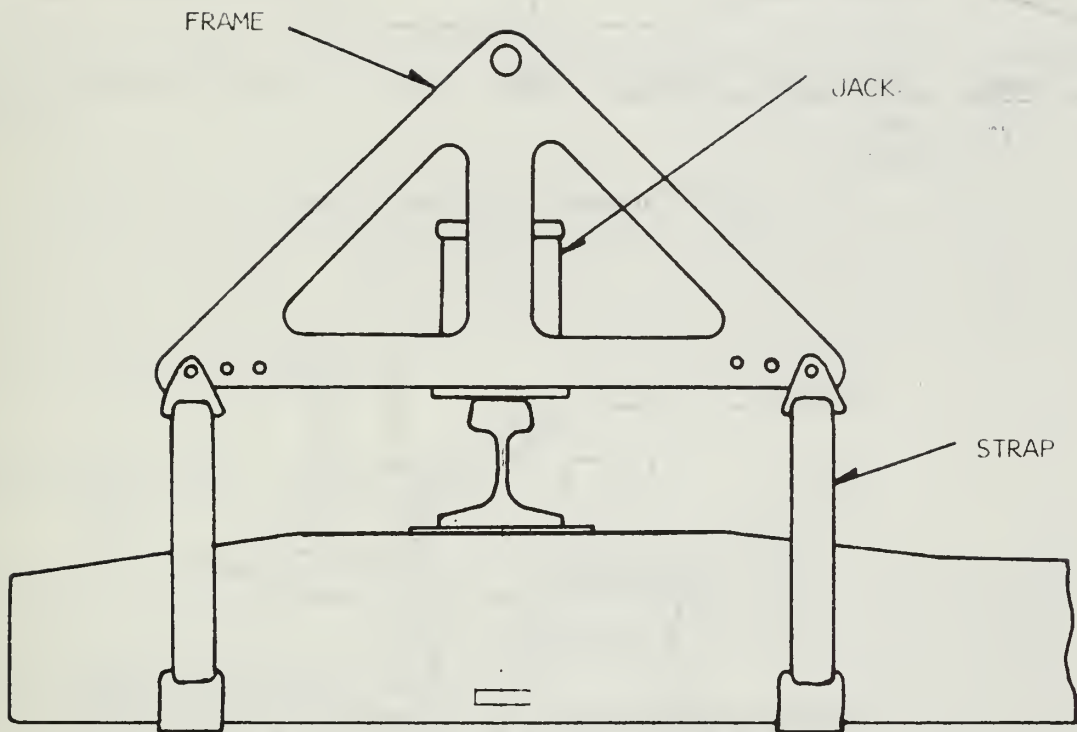


(a) Strain Coupon Installation

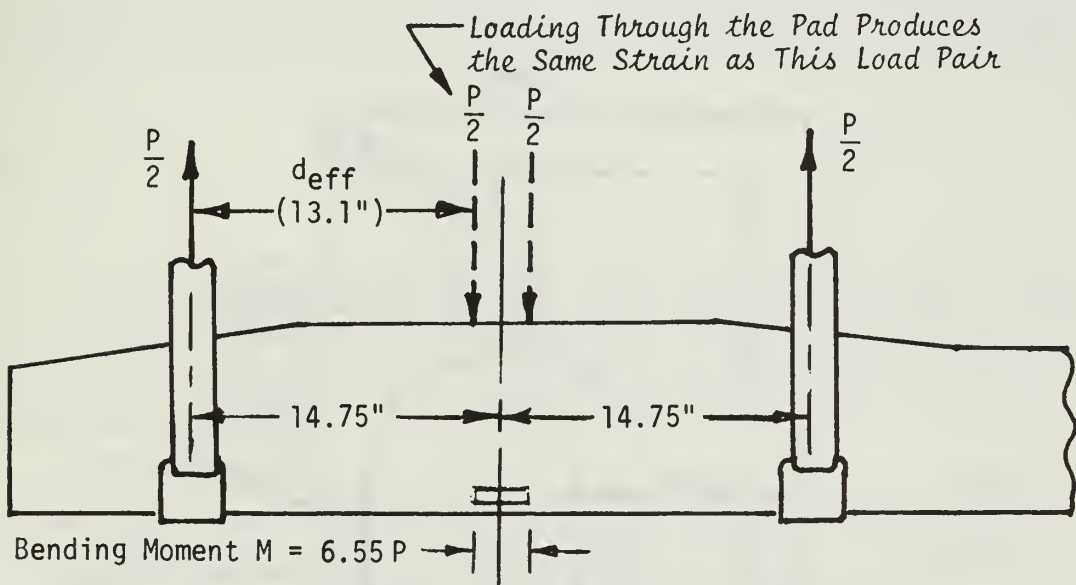


(b) Coupon Construction

FIGURE A-5. STRAIN GAGE COUPON FOR INSTALLATION ON CONCRETE TIES

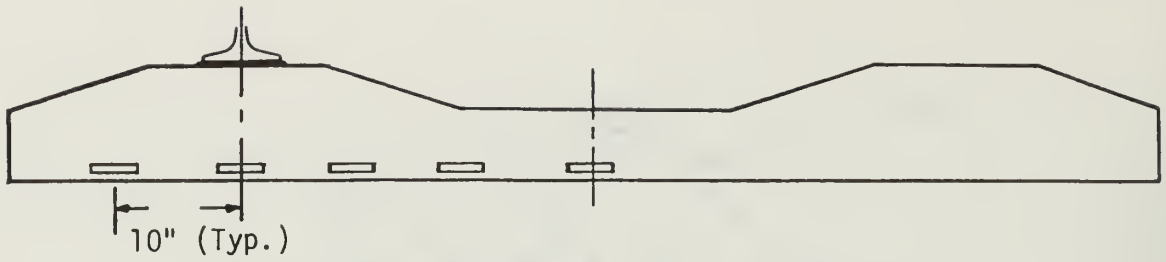


(a) Rail Seat Loading Arrangement

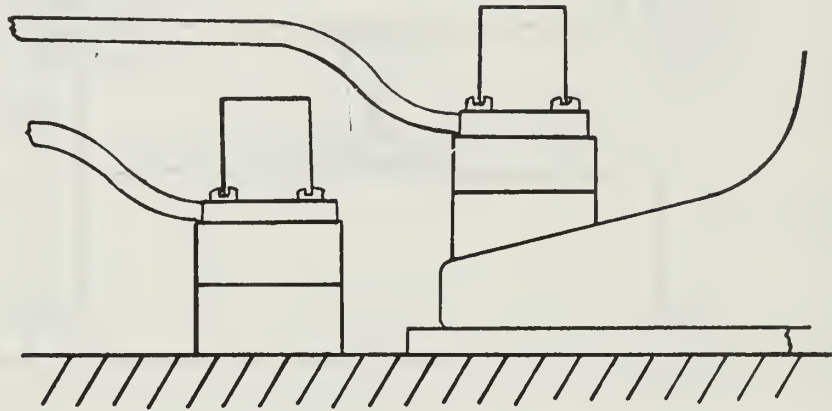


(b) Loading Schematic

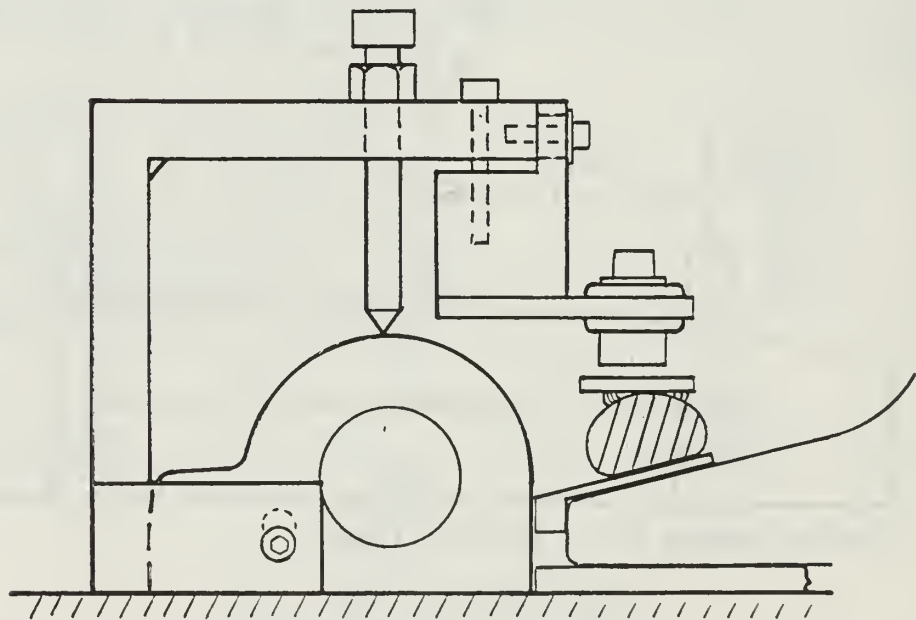
FIGURE A-6. FIXTURE FOR IN-SITU CALIBRATION OF TIE BENDING STRAIN



(a) Placement of Linear Gages



(b) Rail and Tie Accelerations



(c) Rail Clip Vertical Deflections

FIGURE A-7. PLACEMENTS OF STRAIN GAGES, ACCELEROMETERS AND DISPLACEMENT TRANSDUCERS

the adjacent rail base. The transfer function obtained by spectral analysis of the acceleration signals provides a measure of the attenuation offered by the tie pad.

The electronics of the accelerometers resemble a 4-arm strain gage bridge. Excitation power (5v) was supplied, shunt calibrations were performed, and the signals were amplified by the SCA units in a manner similar to that for the load circuits. The accelerometers were constructed so that a 10 K-Ohm, single-arm shunt was equivalent to an acceleration of 75 g. This equivalence was used to adjust amplifier gain so that the full-scale output of 5 volts was produced by 600 g.

Rail-to-Tie Deflection

Vertical rail-to-tie deflection was measured on the field and gage sides of one rail seat by the arrangement shown schematically in Figure A-7(c). Special transducer mounting brackets were anchored to the fastener shoulders. The sensor was fastened to the bracket and a round metal disc target was glued to the fastener clip at the clip toe. The sensor operates on the eddy-current principle to measure the gap between the sensor face and the target. The manufacturer's signal conditioning electronics unit supplied both excitation power and signal amplification.

Calibration involves an interactive adjustment of the gap between the sensor and the target, until the output signal measures zero volts at minimum gap and the desired voltage at maximum gap. Three full turns of a 40-pitch machine thread were used to create a full-range displacement of 0.075 inches between minimum and maximum gaps.

Data Acquisition

A block diagram of the wayside data acquisition system used in the field tests is shown in Figure A-8. In its normal (non-multiplexed) configuration, the system can accommodate 14 analog data channels in "real time" from the transducer through the entire signal path until the data are stored as processed engineering values in microcomputer memory. A schematic of the signal path is shown in Figure A-9.

To accommodate the more than 14 channels needed during the 1980 tests, the signal-conditioned analog signals are frequency-modulated using voltage-controlled oscillators (VCO) and summed together in groups of 14 channels which can then be recorded on a single track of the 14-track recorder. This was avoided on this program to improve the system performance at the wide data bandwidths required. In addition to the 14 data channels, the edge track is reserved for voice annotation.

After initial storage on analog tape, the load and tie bending moment signals were processed to detect the peak values resulting from each wheel

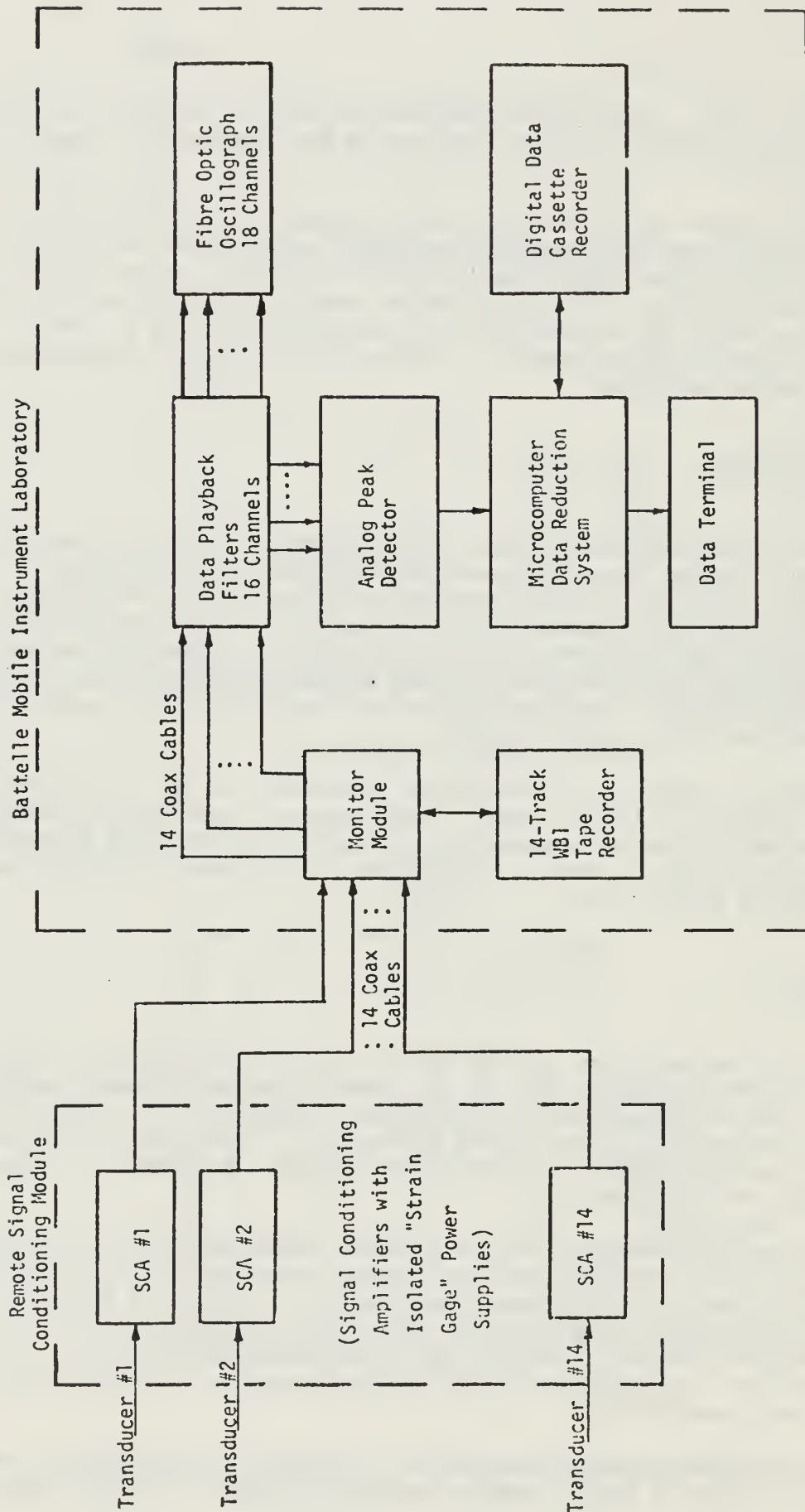


FIGURE A-8. SCHEMATIC OF WAYSIDE DATA ACQUISITION SYSTEM

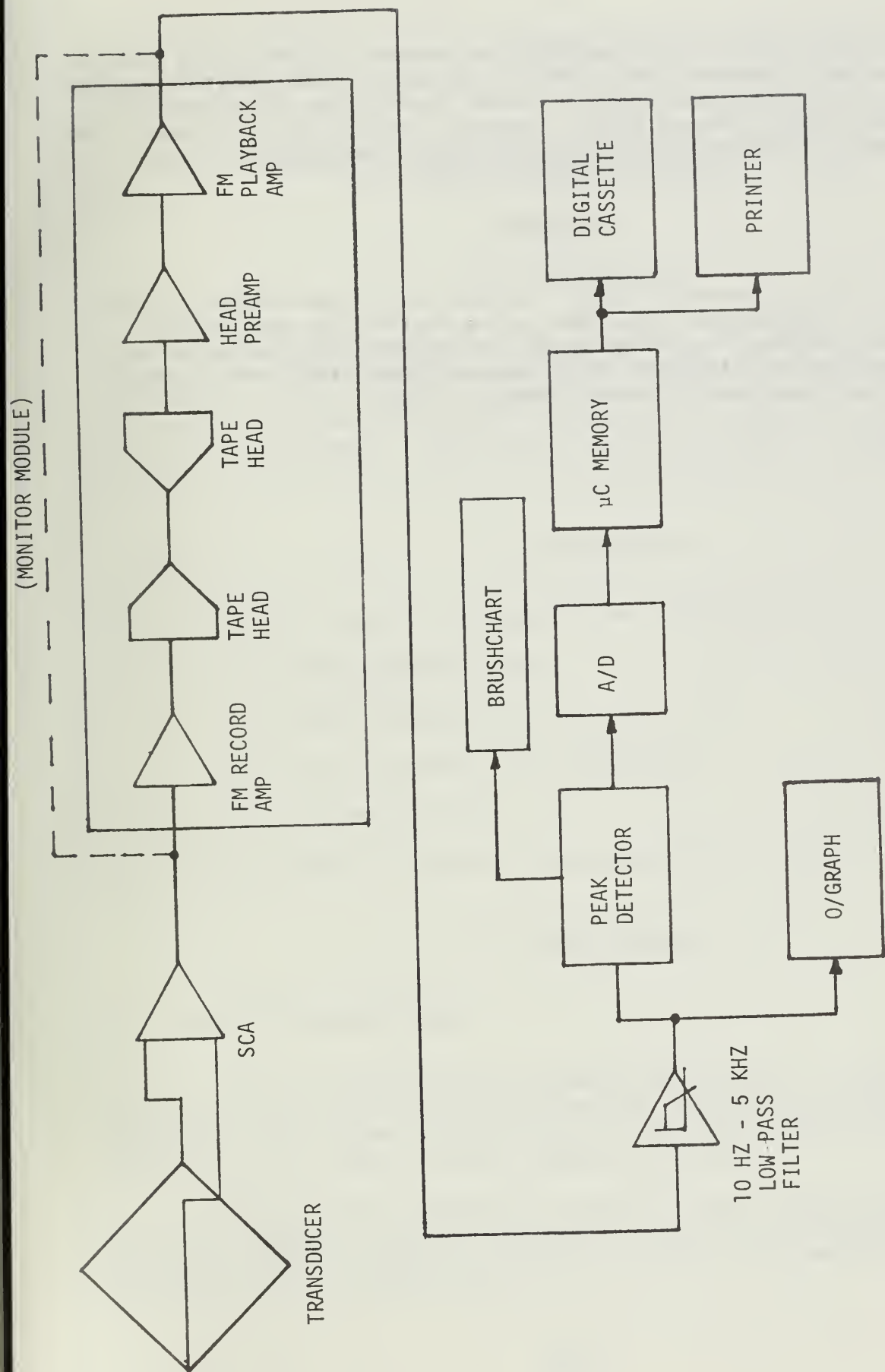


FIGURE A-9. SCHEMATIC OF SIGNAL PATH FROM TRANSDUCER TO DIGITAL STORAGE AND PRINTOUT

pass. The analog detector makes possible the capture of signal peaks containing high-frequency components which might be missed by normal digital sampling techniques. An on-board microcomputer system converts the analog peaks to digital values, stores them on digital cassettes for statistical processing at Battelle, and tabulates and prints the peak values from each train pass.

Reference

- [A-1] Dean, F.E. and Harrison, H.D., "Concrete Tie Instrumentation for the Phase II Tie/Fastener Experiment at the Facility for Accelerated Service Testing," report by Battelle's Columbus Laboratories to the Federal Railroad Administration, Improved Track Structures Research Division, Contract DOT-FR-9162, December 1979.

APPENDIX B

RECOMMENDATIONS FOR PERFORMANCE AND CHARACTERISTIC TESTS OF CONCRETE TIE PADS

B.1 Introduction

During this investigation and an earlier study [B-1], several tests were developed which assess the ability of a tie pad to attenuate impact loads and to survive under many years of service loading. These tests are recommended for inclusion in any set of qualification tests of pads intended for service under impact loading and/or heavy axle loads. A recommended sequence of these tests and the test procedures are described as follows.

B.2 Test Sequence

The test should be conducted in the following order:

- (1) Impact attenuation test
- (2) Dynamic stiffness at room temperature
- (3) Dynamic stiffness at low temperature
- (4) Repeated loads test
- (5) Dynamic stiffness at room temperature

B.3 Test Procedures

B.3.1 Impact Attenuation Test

This test was developed to measure the ability of flexible pads to attenuate impact strains produced by the EVA pad which was originally installed on the Northeast Corridor track. The test is described briefly in Chapter 4 of this report and more completely in [B-2].

The test is not limited to a specific impact loading fixture or to the use of a specific reference tie pad. However, it should be noted that any deviation from the procedure of [B-2] would require the completion of several preliminary steps. These include:

- a. Development of a system which provides an essentially friction-free drop of an impact hammer onto a rail segment fastened to a test tie. The fixture must assure repeatable drop heights over the range that includes the height which is expected to initiate cracks.
- b. Definition of the drop height which initiates cracks when the reference pad is installed on the test tie. This requires the use of a crack-revealing coating and the destructive testing of at least three rail seats.
- c. Adjustment of the duration of the first impact pulse to match that measured in track. This is approximately 1.5 m/sec for the high-speed impacts measured on the Northeast Corridor track. The adjustment was accomplished by trial-and-error selection of a shim to separate the impact hammer head from the remainder of the hammer.
- d. Use of a data processing system which captures peak strains without attenuation over a frequency range of 0 to 1200 Hz.

Because of these fixture-related variables, it should be understood that the range of drop heights used in the following procedures apply only to the fixture described in Reference [B-2] and illustrated in Figure 4-1 of this report. However, these procedures will serve as a general outline for the conduct of impact attenuation tests.

The test is conducted in the following steps:

- (1) Precondition the reference pad with 10 drops from a height of 14 inches.
- (2) Make three additional drops from a height of 14 inches with the reference pad installed. Record the peak voltage output of the strain gage bridge for each drop. The mean of response peaks shall be assigned the value of 350 inch-kips of bending moment, to establish an approximate equivalence between impact strain response level and the strain produced by static bending strength tests. However, this level should be considered arbitrary in that it is used as a reference only.
- (3) With the reference pad still installed, make three drops at each of the following heights: 8 inches, 10 inches, and 12 inches. Record each peak bending moment and take the mean of the peaks at each drop height. The mean peak response at each height defines the reference level against which the bending moments produced by any other pad will be compared.
- (4) For all other candidate pads, repeat steps (1) to (3), recording the peak bending moment for three drops at each height from 8 to 14 inches in 2-inch increments. In addition, continue the test of each pad at drop height increments of 2 inches until the peak bending moment level approaches 90 percent of that recorded for the reference pad at 14 inches.

- (5) Upon completion of the tests of candidate pads, the reference pad can be tested at heights above its cracking threshold. Although a crack may develop, its effect is to cause a small permanent strain. The bias due to the permanent strain can be removed by rezeroing the strain gage bridge after each drop. This optional step will complete the useful life of the test rail seat.
- (6) Candidate pads should demonstrate the ability to attenuate bending moment relative to that produced by the reference pad. This will be measured as the ratio:

$$\frac{\text{REFERENCE BENDING MOMENT} - \text{CANDIDATE PAD BENDING MOMENT}}{\text{REFERENCE BENDING MOMENT}}$$

for each corresponding drop height. The final attenuation value shall be the mean of those obtained at each drop height.

B.3.2 Dynamic Stiffness at Room Temperature

This test is conducted twice, before and after the repeated loads test. Its purpose is to determine the degree of change of pad condition which takes place as the result of the repeated loads test and as the result of the reduction of temperature in Test (3).

The test shall be conducted using a loading machine or actuator capable of providing compressive load to the pad at a rate of 10 cycles per second over the range between 0 and 30,000 pounds. The pad must be supported by a plane surface of load-machine quality. A loading plate placed over the pad shall have dimensions of 1" x 6" x 8" and shall have milled upper and lower surfaces.

The test shall be conducted as follows:

- (1) Place the pad on the support surface and place the loading plate over the pad.
- (2) Mount a displacement device so that it measures the vertical displacement of the loading plate along an axis which lies within a radius of 2 inches of the loading axis.
- (3) Apply a cyclic vertical load to the loading plate with the loading axis over the center of the pad. The loading rod shall have a squared, milled-finish end with a cross-sectional area of at least 8 inches². Positive centering of the plate under the centerline of the load axis shall be provided by scribed lines or guide blocks.

- (4) Apply the cyclic load for at least one minute. For several load cycles, record load and deflection simultaneously using a recording device which permits no filtering of cyclic responses over the frequency range between 0 and 30 Hz.
- (5) Plot the recorded cycles of load vs. deflection on an x-y plotter. The dynamic spring rate of the pad shall be determined as the slope of the line connecting points on the compressive load portion of the cycle at 4,000 and 20,000 pounds.
- (6) The temperature at which these tests are conducted shall be 70 ± 5 °F.

B.3.3 Dynamic Stiffness at Low Temperature

Dynamic stiffness at low temperature shall be measured as follows:

- (1) A thermocouple shall be embedded in a hole drilled at least 1/2 inch into the pad from one of its edges.
- (2) The pad shall be placed between two loading plates as described in B.3.1. The plates and pad shall be placed in an insulated box which is cooled by liquid nitrogen to a temperature of about -20 °F. The temperature shall be verified by measurement with the embedded thermocouple.
- (3) The pad and surrounding plates shall be placed in the loading machine as described in B.3.1. Cyclic loads between 0 and 30,000 pounds shall be applied at the rate of 10 Hz.
- (4) The temperature shall be monitored by the thermocouple. When the temperature reaches -10 °F, several load cycles shall be recorded.
- (5) The dynamic stiffness shall be determined as described in B.3.1.

No definite criteria has been established for the maximum allowable percent change in stiffness between room temperature and -10 °F. The performance goal of a stiffness change not exceeding 10 percent is recommended.

B.3.4 Repeated Loads Test

Procedures for the conduct of fastener repeated loads tests are described in Chapter 10 of the AREA Manual for Railway Engineering and in specifications developed by Amtrak [B-3]. In several cases the repeated loads tests conducted by either of these methods have not adequately predicted fastener performance in track. There was no direct relationship between the service-loading environment encountered by the fastener and the loads applied in the tests.

Simulation of the fastener-loading environment require methods to measure the environment in track and to monitor its application in the laboratory. The most direct approach to this objective is through rail-to-tie deflection measurements. The most important deflection components are:

- a. vertical deflection at the clip toe on field and gage sides
- b. lateral rail head deflection.

It is recommended that this process of track measurement and monitoring of deflections during the repeated loads tests be incorporated into all future specifications. This will require the adjustment of the load levels (vertical uplift and compression, lateral inward and outward) to recreate the deflection levels measured in track at an appropriate occurrence frequency.

B.3.5 Final Stiffness Test

The test of dynamic stiffness at room temperature should be run after the repeated loads test. The change in stiffness between the first and second tests should be determined. This change should be limited to an appropriate maximum between 10 and 20 percent. Additional tests will have to be conducted to determine a level of stiffness change which can be met by materials of high performance and acceptable cost.

References

- [B-1] Dean, F.E., "Investigation of Rail Fastener Performance Requirements," report by Battelle's Columbus Laboratories to the Federal Railroad Administration, Improved Track Structures Research Division, Contract DOT-FR-9162, June 1981.
- [B-2] Dean, F.E. and Harrison, H.D., "Laboratory Study to Determine the Effects of Tie Pad Stiffness on the Attenuation of Impact Strain in Concrete Ties," report by Battelle's Columbus Laboratories to the Federal Railroad Administration, Improved Track Structures Research Division, Contract DOT-FR-9162, June 1981.
- [B-3] "Concrete Tie Technical Provisions," Section II, The National Railroad Passenger Corporation, November 8, 1977.

